Modeling and Control of Formation Flying Satellites in 6 DOF

Esten Ingar Grøtli

NTNU

Norwegian University of Science and Technology

NTNU
Norges teknisk-naturvitenskapelige universitet

Fakultet for informasjonsteknologi, matematikk og elektroteknikk
Institutt for teknisk kybernetikk

MASTEROPPGAVE

Kandidatens navn: Esten Ingar Grøtli

Fag: Teknisk Kybernetikk

Oppgavens tittel (norsk): Modellering og regulering av formasjoner av satelitter i 6 DOF

Oppgavens tittel (engelsk): Modeling and control of formation flying satellites in 6 DOF

Oppgavens tekst:
Relative positioning of satellites in formations is an important control problem within the field of satellite formation flight. Dependent on the formation mission, various degrees of position accuracy is needed, and feedback control is necessary to achieve this. This work focus on modeling and control of the relative distances and attitude in a satellite formation.

Oppgaver:
1. Perform a literature-study on modeling and control of position of a formation of satellites
2. Derive a dynamic model of the relative position and attitude of a formation of satellites. Include J2-pertubations in the model.
3. Design state-feedback control laws for relative position.
4. Assume that velocity is not available for feedback, and design an observer for use with the position controllers.
5. Based on techniques developed for synchronization of AUVs, propose a controller for synchronization of two satellites.
6. Based on the achieved results, write and submit abstracts to
   a. Space Technology Education Conference, Aalborg, Denmark, 6-8 April 2005
   b. SIMS2005 - Scandinavian Conference on Simulation and Modeling, Trondheim, October 13-14, 2005

Oppgaven gitt: 18/1-05

Besvarelsen leveres: 15/6-05

Besvarelsen levert:

Utført ved Institutt for teknisk kybernetikk

Veiledere: Åge Skullestad, Kongsberg Defence & Aerospace,
Raymond Kristiansen, Høgskolen i Narvik

Trondheim, den

Jan Tommy Gravdahl

Jan Tommy Gravdahl
Faglærer

Preface

I would like to acknowledge the support from my supervisor Associate Professor Jan Tommy Gravdahl. Thanks also to my advisor Raymond Kristiansen for valuable inputs and to Åge Skullestad for showing such interest in my work. I am also grateful to Jennifer MacGregor for her assistance with the figures and with the English language.

Trondheim, June 16, 2005

Esten Ingar Grøtli

Abstract

In this thesis, two different strategies for describing a formation of satellites are proposed. Both rely on a Leader/Follower architecture, i.e. a hierarchical structure where the Follower satellite is controlled so as to maintain a predefined relative position and attitude to the Leader.
The first strategy is to derive the equations of motion for the Follower satellite relative to the Leader, where as the second strategy is to model both satellites as rigid bodies and then use synchronization theory to control their motion relative to each other. Relevant disturbances are modeled and incorporated in both strategies.
The Hill-Clohessy-Wiltshire equations are presented and used for deriving fuel efficient paths, appropriate for formation flying satellites.
By using methods from nonlinear control theory, and taking advantage of results already achieved on formations of other mechanical agents, controllers and estimators are developed. The theoretical results are supported by simulations, using MATLAB® and Simulink®

Contents

List of Figures

Chapter 1

Introduction

The major reason for formations of satellites, is the desire to distribute the functionality of large satellites. The ability of small satellites to fly in precise formation will make a wide array of new applications possible, including a next-generation Internet, space-based radar and ultra-powerful space telescopes.
There is also an economic aspect to this; often it is more expensive to place one big satellite with all the functions built-in, into orbit than several smaller ones of the same collective weight. Therefore as the number of missions that use spacecraft flying in formation, proposed or under development, still increases, one can imagine assembly lines of standardized spacecraft, thus lowering the cost of building them drastically. These standardized spacecraft will of course be fully equipped with the proper instruments for their mission.
A formation is in Folta, Newman & Gardner (1996) defined as "*two or more spacecraft that use an active control scheme to maintain the relative positions of the spacecraft*". In particular, from Scharf, Hadaegh & Ploen (2003), at least one member of the set of satellites must

1. track a desired state profile relative to another member, and
2. the associated tracking control law must at the minimum depend upon the state of this other member

As opposed, is a constellation "*two or more spacecraft in similar orbits with no active control by either to maintain a relative position*". The concept of satellites as a part of a formation have been subject to a lot of scientific research in the last decade. A great overview on this research is found in Scharf et al. (2003) and Scharf, Hadaegh & Ploen (2004).

1.1 Formation flying guidance

Formation flying guidance is defined in Scharf et al. (2003) as "*the generation of any reference trajectories used as an input for a formation member's relative state tracking control law*". The literature can be divided in two main categories, based on the ambient dynamic environment,

1. Planetary Orbital Environments, and
2. Deep Space

where both consider optimal formation reconfiguration. The Planetary Orbital Environments are subject to significant orbital dynamics and the literature is therefore mainly focused on the development of periodic, thrust-free relative spacecraft trajectories, so-called passive relative orbits. Such an orbit must be accurate, since if this orbit is the solution of a disturbance-free

design model, the periodicity may be ruined when the Earth's oblateness is included. As a result, extra fuel is consumed to artificially maintain such an orbit.
In Deep Space the formation flying guidance is simplified by the fact that arbitrary rigid formations can be maintained with no fuel penalty. On the other hand, the fuel consumption has to be balanced across the formation. For example, the life-time of the outermost spacecraft will be shorter by reconfiguration through rotation. The reader may look up Beard & F. Hadaegh (1999) for more information on the subject, but it will not be treated further in this thesis.

1.2 Formation flying control

Formation flying control "*encompasses design techniques and stability results for the coupled-state laws*", according to Scharf et al. (2004). The literature on the subject is divided into five architectures

1. Multiple-Input Multiple-Output (MIMO), in which the formation is treated as a single multiple-input, multiple-output plant.
2. Leader/Follower, in which individual spacecraft controllers are connected hierarchically.
3. Virtual Structures, in which spacecraft are treated as rigid bodies embedded in an overall virtual rigid body.
4. Cyclic, in which individual spacecraft controllers are connected non-hierarchically.
5. Behavioral, in which multiple controllers for achieving different (and possibly competing) objectives are combined.

In the MIMO architecture, formation controllers are designed using a dynamical model of the entire formation, i.e. the formation is treated as a multiple-input, multiple-output plant.
The most studied architecture is undoubtedly the Leader/Follower architecture, which is also often referred to as Chief/Deputy, Master/Slave or even Target/Chase, the traditional terminology from two-spacecraft rendezvous. The Leader/Follower architecture uses a hierarchical arrangement for individual spacecraft controllers that reduces formation control to individual tracking problems. Examples of both linear and nonlinear control strategies are given in Naasz, Karlgaard & Hall (2002), based on the equation of motion attained in Karlsgaard & Lutze (2001).
In the Virtual Structure architecture, the spacecraft behaves as rigid bodies embedded in a larger, virtual body. Reference trajectories are generated from the overall motion of the virtual structure and the spacecrafts specified motion and orientation within it. The overall motion include rigid body motions and contractions/expansions.
Cyclic architecture is formed connecting individual spacecraft controllers, and is in that sense similar to the Leader/Follower architecture. However, the cyclic architecture is not hierarchical, and each spacecraft controls itself with respect to a neighboring spacecraft.
The last architecture, the Behavioral, combines the outputs of multiple controllers to achieve different and possibly competing behaviours.

Chapter 2

Reference Frames

The following reference frames, see Fossen (2002), are convenient when describing satellites in 6 DOF. The first two reference frames are Earth-Centered, where as the last two are body centered.

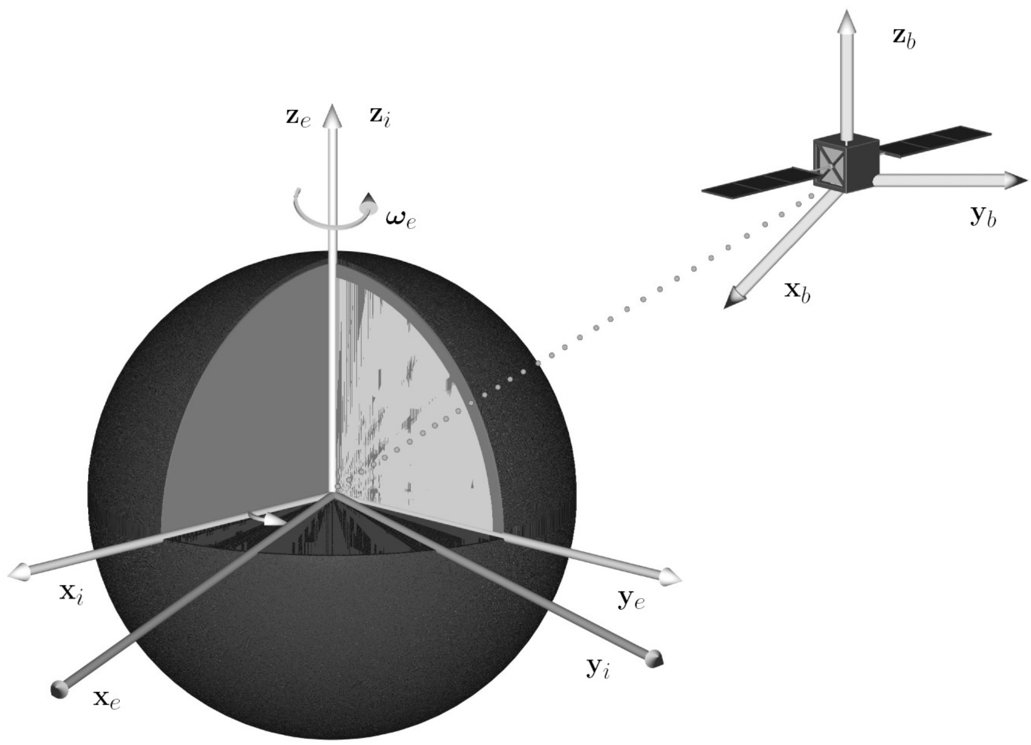

Figure 2.1: The Earth-centered Earth-fixed frame $x_e y_e z_e$ rotates with an angular rate ω_e relative to the Earth-centered inertial frame $x_i y_i z_i$

2.1 Earth-Centered Inertial Frame

The Earth-centered inertial frame, $x_i y_i z_i$, is a non-accelerating reference frame, with frame axis z_i, directed along the axis of rotation toward the celestial north pole. The frame axis x_i is in the *vernal equinox* direction, found by drawing a line from Earth to the Sun on the first day of Spring. The last axis if directed so as to complete a right hand orthogonal frame.

2.2 Earth-Centered Earth-Fixed Frame

The Earth-centered Earth-fixed reference frame, $x_e y_e z_e$, has also its origin fixed to the center of Earth, but rotates about the frame axis $z_e = z_i$ relative to the inertial frame ECI.

2.3 Body Frame

The body reference frame, $x_b y_b z_b$ has its origin located at the center of mass of the satellite. The body axes, x_b, y_b and z_b, are chosen to coincide with the *principal axes of inertia*. Rotation about the x_b, y_b and z_b will be denoted *roll*, *pitch* and *yaw*, respectively.

2.4 Orbital Frame

The orbital reference frame, $x_o y_o z_o$, has its origin located at the center of mass of the satellite. The frame axis x_o is directed away from Earth, along the line connecting the center of Earth with the center of the satellite. The z_o axis points along the orbital angular momentum vector of the spacecraft, and the y_o-axis is directed so as to complete a right hand orthogonal frame. For a circular orbit the y_o axis will point in the velocity direction.

Chapter 3

Notation and Mathematical Background

This chapter introduces the basic mathematics and explains the notation used throughout this thesis. The material is mainly taken from Egeland & Gravdahl (2002), Hughes (1986) and Fossen (2002).

3.1 Vectors

A vector, which description does not rely on the definition of any coordinate frame, will be denoted $\vec{v}$. These vectors are called *coordinate-free*. Vectors described in a certain coordinate frame will be denoted with a bold font and superscript to indicate its coordinate frame, e.g. $\mathbf{v}^b$. They are said to be on *coordinate form*. Angular velocity vectors on coordinate form are denoted in a similar manner, but with additional subscripts to state which frame has the angular velocity and relative to what frame. For instance, will the vector $\boldsymbol{\omega}_{ib}^b$ describe the angular velocity of the body frame relative to the inertial frame expressed in the body frame.

3.2 Vectrices

The basis vectors characterizing a reference frame $\mathfrak{F}_a$, can easily be manipulated using a *vectrix*

$$\boldsymbol{\mathfrak{F}}_a = \begin{bmatrix} \vec{a}_1 \\ \vec{a}_2 \\ \vec{a}_3 \end{bmatrix} \tag{3.1}$$

Once a reference frame has been defined, a coordinate-free vector, $\vec{v}$, can be transformed in a coordinate vector form

$$\vec{v} = (\mathbf{v}^a)^T \boldsymbol{\mathfrak{F}}_a = \boldsymbol{\mathfrak{F}}_a^T \mathbf{v}^a \tag{3.2}$$

The dot product of two vectrices is defined as

$$\boldsymbol{\mathfrak{F}}_a \cdot \boldsymbol{\mathfrak{F}}_b^T = \begin{bmatrix} \vec{a}_1 \cdot \vec{b}_1 & \vec{a}_1 \cdot \vec{b}_2 & \vec{a}_1 \cdot \vec{b}_3 \\ \vec{a}_2 \cdot \vec{b}_1 & \vec{a}_2 \cdot \vec{b}_2 & \vec{a}_2 \cdot \vec{b}_3 \\ \vec{a}_3 \cdot \vec{b}_1 & \vec{a}_3 \cdot \vec{b}_2 & \vec{a}_3 \cdot \vec{b}_3 \end{bmatrix} \tag{3.3}$$

which for

$$\boldsymbol{\mathfrak{F}}_a \cdot \boldsymbol{\mathfrak{F}}_a^T = \mathbf{1} \tag{3.4}$$

This leads to the expression for the relationship between $\mathbf{v}$ and $\vec{v}$

$$\mathbf{v}^a = \boldsymbol{\mathfrak{F}}_a \cdot \boldsymbol{\mathfrak{F}}_a^T \mathbf{v}^a = \boldsymbol{\mathfrak{F}}_a \cdot \vec{v} = \vec{v} \cdot \boldsymbol{\mathfrak{F}}_a \tag{3.5}$$

$$(\mathbf{v}^a)^T = (\mathbf{v}^a)^T \boldsymbol{\mathfrak{F}}_a \cdot \boldsymbol{\mathfrak{F}}_a^T = \vec{v} \cdot \boldsymbol{\mathfrak{F}}_a^T = \boldsymbol{\mathfrak{F}}_a^T \cdot \vec{v} \tag{3.6}$$

Now, let $\boldsymbol{\mathfrak{F}}_a$ and $\boldsymbol{\mathfrak{F}}_b$ be the vectrices corresponding to frame $\mathfrak{F}_a$ and $\mathfrak{F}_b$. By using the above notation, $\mathbf{v}^a = \boldsymbol{\mathfrak{F}}_a \cdot \vec{v}$ and $\vec{v} = \boldsymbol{\mathfrak{F}}_b^T \mathbf{v}^b$, such that

$$\mathbf{v}^a = \boldsymbol{\mathfrak{F}}_a \cdot \boldsymbol{\mathfrak{F}}_b^T \mathbf{v}^b \tag{3.7}$$

$$= \mathbf{R}_b^a \mathbf{v}^b \tag{3.8}$$

i.e.

$$\mathbf{R}_b^a = \boldsymbol{\mathfrak{F}}_a \cdot \boldsymbol{\mathfrak{F}}_b^T \tag{3.9}$$

where $\mathbf{R}_b^a$ is the *rotation matrix.* The transformation between two vectrices is

$$\boldsymbol{\mathfrak{F}}_a = \mathbf{R}_b^a \boldsymbol{\mathfrak{F}}_b \tag{3.10}$$

which can be verified by postmultiplication of $\cdot \boldsymbol{\mathfrak{F}}_b^T$.

3.3 Rotation Matrices

The rotation matrix $\mathbf{R}_b^a$ from reference frame $\mathfrak{F}_a$ to $\mathfrak{F}_b$ has three interpretations, according to Kyrkjebø (2000). It transform vectors represented in frame $\mathfrak{F}_a$ to $\mathfrak{F}_b$ while preserving the length of the vectors. It also rotates a vector within a reference frame. Finally, a rotation matrix describes the mutual orientation between two coordinate frames, where the column vectors are cosines of the angle between the two frames. Using (3.9) and the dot product of two vectrices, the rotation matrix can be written as

$$\mathbf{R}_b^a = \begin{bmatrix} \vec{a}_1 \cdot \vec{b}_1 & \vec{a}_1 \cdot \vec{b}_2 & \vec{a}_1 \cdot \vec{b}_3 \\ \vec{a}_2 \cdot \vec{b}_1 & \vec{a}_2 \cdot \vec{b}_2 & \vec{a}_2 \cdot \vec{b}_3 \\ \vec{a}_3 \cdot \vec{b}_1 & \vec{a}_3 \cdot \vec{b}_2 & \vec{a}_3 \cdot \vec{b}_3 \end{bmatrix} = \begin{bmatrix} \mathbf{c}_1 & \mathbf{c}_2 & \mathbf{c}_3 \end{bmatrix} \tag{3.11}$$

where the vectors $\mathbf{c}_i$ are called *direction cosines.* Notice that $(\mathbf{R}_b^a)^T = \mathbf{R}_a^b$, where $\mathbf{R}_a^b$ is equivalent to the opposite rotation of $\mathbf{R}_b^a$. By using (3.10) and the fact that $\boldsymbol{\mathfrak{F}}_b \cdot \boldsymbol{\mathfrak{F}}_b^T = \mathbf{1}$ a convenient property of the rotation matrices can be deduced, namely orthonormality

$$\begin{aligned} \mathbf{R}_b^a \mathbf{R}_a^b &= \mathbf{R}_b^a (\boldsymbol{\mathfrak{F}}_b \cdot \boldsymbol{\mathfrak{F}}_b^T) \mathbf{R}_a^b \\ &= \mathbf{R}_b^a \boldsymbol{\mathfrak{F}}_b \cdot (\mathbf{R}_b^a \boldsymbol{\mathfrak{F}}_b)^T \\ &= \boldsymbol{\mathfrak{F}}_a \cdot \boldsymbol{\mathfrak{F}}_a^T \\ &= \mathbf{1} \end{aligned} \tag{3.12}$$

Differentiating this equation with respect to time yields

$$\frac{\mathrm{d}}{\mathrm{d}t}(\mathbf{R}_b^a \mathbf{R}_a^b) = \dot{\mathbf{R}}_b^a \mathbf{R}_a^b + \mathbf{R}_b^a \dot{\mathbf{R}}_a^b = \mathbf{0} \tag{3.13}$$

By defining

$$\mathbf{S} = \dot{\mathbf{R}}_b^a \mathbf{R}_a^b \tag{3.14}$$

the above equation becomes $\mathbf{S} + \mathbf{S}^T = \mathbf{0}$ which suggest that the matrix $\mathbf{S} = -\mathbf{S}^T$ is *skew symmetric*. This skew symmetric matrix can be seen as the skew symmetric form of the angular velocity vector, $\boldsymbol{\omega}_{ab}^a$,

$$\mathbf{S}(\boldsymbol{\omega}_{ab}^a) = (\boldsymbol{\omega}_{ab}^a)^\times = \begin{bmatrix} 0 & -\omega_z & \omega_y \\ \omega_z & 0 & -\omega_x \\ -\omega_y & \omega_x & 0 \end{bmatrix} \tag{3.15}$$

Notice that the kinematic differential equation of the rotation matrix can be given on two alternative forms

$$\dot{\mathbf{R}}_b^a = \mathbf{S}(\boldsymbol{\omega}_{ab}^a)\mathbf{R}_b^a \tag{3.16}$$

$$\dot{\mathbf{R}}_b^a = \mathbf{R}_b^a\mathbf{S}(\boldsymbol{\omega}_{ab}^b) \tag{3.17}$$

where the first is obtained by post-multiplication of (3.14) with $\mathbf{R}_b^a$ and the second by using the coordinate transformation rule $\mathbf{S}(\boldsymbol{\omega}_{ab}^a) = \mathbf{R}_b^a\mathbf{S}(\boldsymbol{\omega}_{ab}^b)\mathbf{R}_a^b$. Furthermore, the rotation matrix of a composite rotation, is given by the product of the rotation matrices

$$\mathbf{R}_c^a = \mathbf{R}_b^a\mathbf{R}_c^b \tag{3.18}$$

Two important properties of the indexed angular velocity representation is

$$\boldsymbol{\omega}_{ab}^a = -\boldsymbol{\omega}_{ba}^a \tag{3.19}$$

and

$$\boldsymbol{\omega}_{ac}^a = \boldsymbol{\omega}_{ab}^a + \boldsymbol{\omega}_{bc}^a \tag{3.20}$$

3.4 Unit Quaternions

The *unit quaternions* or *Euler parameters* is a four-parameter representation of attitude, which, unlike the *Euler angles*, avoid singularities. A quaternion

$$\mathbf{q} = \begin{bmatrix} \eta \\ \boldsymbol{\varepsilon} \end{bmatrix} \tag{3.21}$$

consist of a scalar number η and a complex vector $\boldsymbol{\varepsilon}$, defined as

$$\eta = \cos\frac{\beta}{2} \tag{3.22}$$

$$\boldsymbol{\varepsilon} = [\varepsilon_1, \varepsilon_2, \varepsilon_3]^T = \boldsymbol{\lambda}\sin\frac{\beta}{2} \tag{3.23}$$

where the angle β is the rotation about the axis given by the unit vector $\boldsymbol{\lambda}$. A unit quaternion satisfy $\mathbf{q}^T\mathbf{q} = 1$. According to Hughes (1986), the coordinate transformation matrix for the unit quaternions is

$$\mathbf{R}(\mathbf{q}) = \mathbf{R}_{\eta,\boldsymbol{\varepsilon}} = \mathbf{I}_{3\times3} + 2\eta\mathbf{S}(\boldsymbol{\varepsilon}) + 2\mathbf{S}^2(\boldsymbol{\varepsilon}) \tag{3.24}$$

From this equation it follows that $\mathbf{q}$ and $-\mathbf{q}$ represents the same orientation. Furthermore, the inverse rotation matrix can be written

$$\mathbf{R}^{-1}(\mathbf{q}) = \mathbf{R}^T(\mathbf{q}) = \mathbf{R}(\mathbf{q}^*) \tag{3.25}$$

where $\mathbf{q}^*$ is the complex conjugate of $\mathbf{q}$, defined as

$$\mathbf{q}^* = \begin{bmatrix} \eta \\ -\boldsymbol{\varepsilon} \end{bmatrix} \tag{3.26}$$

The quaternion product between two quaternion vectors $\mathbf{q}_1 = [\eta_1 \quad \boldsymbol{\varepsilon}_1^T]^T$ and $\mathbf{q}_2 = [\eta_2 \quad \boldsymbol{\varepsilon}_2^T]^T$ is defined, see Egeland & Gravdahl (2002), as

$$\mathbf{q}_1 \otimes \mathbf{q}_2 = \begin{bmatrix} \eta_1\eta_2 - \boldsymbol{\varepsilon}_1^T\boldsymbol{\varepsilon}_2 \\ \eta_1\boldsymbol{\varepsilon}_2 + \eta_2\boldsymbol{\varepsilon}_1 + \mathbf{S}(\boldsymbol{\varepsilon}_1)\boldsymbol{\varepsilon}_2 \end{bmatrix} \tag{3.27}$$

The matrix

$$\mathbf{F}(\mathbf{q}) = \begin{bmatrix} \eta & -\boldsymbol{\varepsilon}^T \\ \boldsymbol{\varepsilon} & \eta\mathbf{1} + \mathbf{S}(\boldsymbol{\varepsilon}) \end{bmatrix} \tag{3.28}$$

represents quaternion pre-multiplication with $\mathbf{q}$ in the sense that

$$\mathbf{q} \otimes \mathbf{u} = \mathbf{F}(\mathbf{q})\mathbf{u} \tag{3.29}$$

while

$$\mathbf{E}(\mathbf{q}) = \begin{bmatrix} \eta & -\boldsymbol{\varepsilon}^T \\ \boldsymbol{\varepsilon} & \eta\mathbf{1} - \mathbf{S}(\boldsymbol{\varepsilon}) \end{bmatrix} \tag{3.30}$$

represents quaternion post-multiplication with $\mathbf{q}$ in the sense that

$$\mathbf{u} \otimes \mathbf{q} = \mathbf{E}(\mathbf{q})\mathbf{u} \tag{3.31}$$

for any $\mathbf{u} \epsilon \mathbb{R}^4$.
The kinematic differential equations can be written in vector form as

$$\dot{\mathbf{q}} = \frac{1}{2}\begin{bmatrix} -\boldsymbol{\varepsilon}^T \\ \eta\mathbf{1}_{3\times 3} + \mathbf{S}(\boldsymbol{\varepsilon}) \end{bmatrix}\boldsymbol{\omega}_{ab}^b \tag{3.32}$$

or alternatively

$$\dot{\mathbf{q}} = \frac{1}{2}\begin{bmatrix} -\boldsymbol{\varepsilon}^T \\ \eta\mathbf{1}_{3\times 3} - \mathbf{S}(\boldsymbol{\varepsilon}) \end{bmatrix}\boldsymbol{\omega}_{ab}^a \tag{3.33}$$

where $\dot{\mathbf{q}} = [\dot{\eta} \quad \dot{\boldsymbol{\varepsilon}}^T]^T$.

Chapter 4

The HCW's Equations

Satellite formations can of course not be chosen arbitrary, but are constrained by the laws of physics. Since the amount of fuel is a scarce resource, the satellites have to be placed in force-free orbits. Satellites can neither be placed side by side forever or above each other and be expected to be at the same pace. Their orbits will cross.
One of the big challenges is to find appropriate paths for all the satellites in a formation, so that the desired functionalities are achieved, both with a view to fuel efficiency and to fulfill the predefined mission.
The most common linear passive relative orbits, are solutions to the Hill-Clohessy-Wiltshire Equations. The original deduction of these equations are to be found in Hill (1878), and were used to describe the motion of the Moon relative to the Earth. A linearized form of these equations was introduced in Clohessy & Wiltshire (1960), for describing the orbital rendezvous problem.
In this chapter these equations are attained under the assumptions that the Leader satellite is in a circular orbit, the Earth is spherically symmetric, and the nonlinear terms in the relative motion variable can be neglected. The trajectories are in particular useful for formations of earth pointing instruments. Non-circular orbits are treated in, among others, Inalhan, Tillerson & How (2002), and J_2 perturbations are considered in Serrani (2003).

4.1 The Hill-Clohessy-Wiltshire equations

The following deduction is mainly from Schwartz (2004). Starting point is the two-body problem with the assumptions that:

1. The equations of motion are expressed in a non-inertial reference frame and the origin of that frame coincides with the center of mass of the central body
2. The central body and satellite are both homogenous spheres or points of equivalent mass
3. The inverse-square gravitational force between the two bodies are the only force in action

Under these assumptions, the governing equation is

$$\ddot{\vec{r}}_i = -\frac{G(M+m)}{r_i^3}\vec{r}_i \tag{4.1}$$

where G is the gravitational constant, M is the mass of the central body, m_i is the mass of the satellite in question, and $\vec{r}_i$ is the vector from the center of mass of the central body to the satellite. Let the subscript $i = l, f$ denote the Leader and Follower satellite respectively. The position of the Follower, with respect to the Leader is given by

$$\vec{\rho} = \vec{r}_f - \vec{r}_l \tag{4.2}$$

For convenience the relative motion equations are expressed in a circular reference frame, rotating with radius r_l. The rotating reference frame $\mathfrak{F}_h$, termed the Hill frame, rotates once per orbit with respect to the inertial frame $\mathfrak{F}_i$. The axes of the Hill frame, $\vec{e}_r$, $\vec{e}_\theta$ and $\vec{e}_z$ are defined in the radial, velocity and orbit-normal directions, respectively. Thus the average angular velocity of the reference frame is given by

$$\vec{\omega}_{ih} = \dot{\nu}\vec{e}_z \tag{4.3}$$

where ν, see 4.2, is the true anomaly of the Leader satellite's orbit. The position vector from the Leader to the Follower satellite can be expressed as

$$\begin{aligned} \vec{\rho} &= \vec{r}_f - \vec{r}_l & (4.4)\\ &= x\vec{e}_r + y\vec{e}_\theta + z\vec{e}_z & (4.5) \end{aligned}$$

where x, y and z are the components of $\vec{\rho}$ in the Hill frame, see figure 4.1. For later use, the

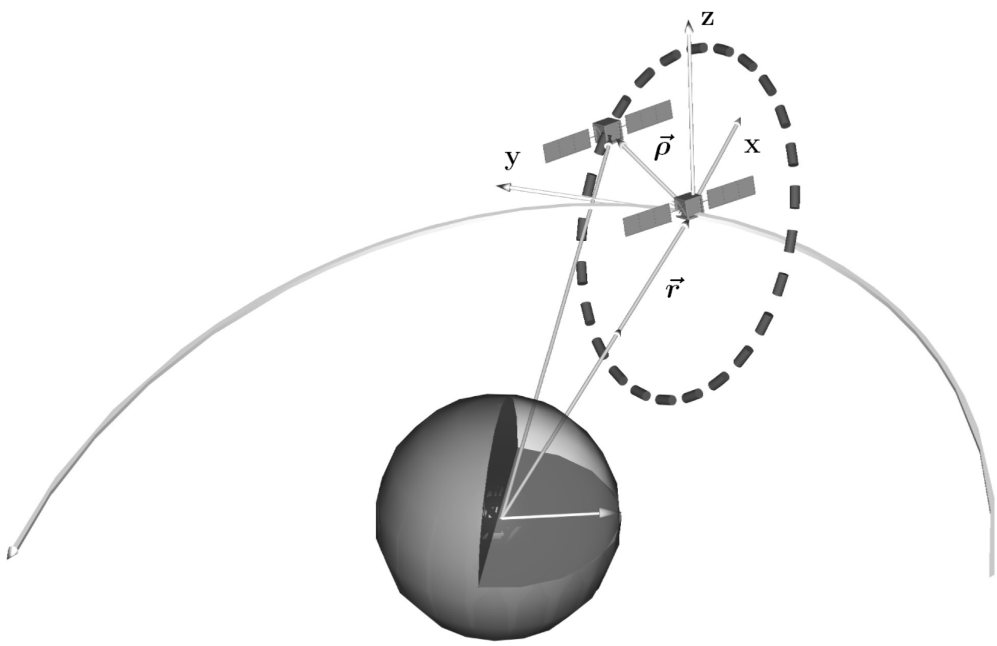

Figure 4.1: The Hill frame

second derivative of ρ is

$$\ddot{\vec{\rho}} = \ddot{x}\vec{e}_r + 2\dot{x}\dot{\vec{e}}_r + x\ddot{\vec{e}}_r + \ddot{y}\vec{e}_\theta + 2\dot{y}\dot{\vec{e}}_\theta + y\ddot{\vec{e}}_\theta + \ddot{z}\vec{e}_z \tag{4.6}$$

Using (A.3), (A.4), (A.5) and (A.6) from appendix A for $\dot{\vec{e}}_r$, $\ddot{\vec{e}}_r$, $\dot{\vec{e}}_\theta$ and $\ddot{\vec{e}}_\theta$, respectively, yields

$$\begin{aligned} \ddot{\vec{\rho}} &= \ddot{x}\vec{e}_r + 2\dot{x}\dot{\nu}\vec{e}_\theta - x\dot{\nu}^2\vec{e}_r + x\ddot{\nu}\vec{e}_\theta + \ddot{y}\vec{e}_\theta - 2\dot{y}\dot{\nu}\vec{e}_r - y\dot{\nu}^2\vec{e}_\theta - y\ddot{\nu}\vec{e}_r \\ &= (\ddot{x} - 2\dot{y}\dot{\nu} - x\dot{\nu}^2 - y\ddot{\nu})\vec{e}_r + (\ddot{y} + 2\dot{x}\dot{\nu} - y\dot{\nu}^2 + x\ddot{\nu})\vec{e}_\theta + \ddot{z}\vec{e}_z \end{aligned} \tag{4.7}$$

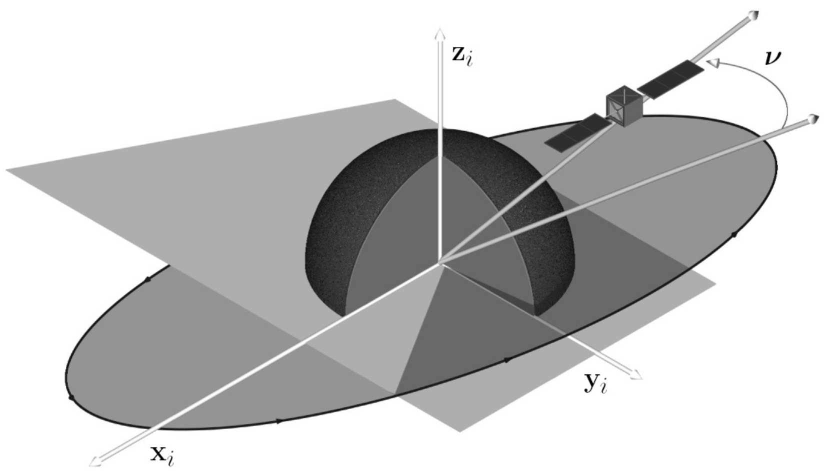

Figure 4.2: The true anomaly is the angle measured from perigee to the spacecraft's position vector, in the direction of the spacecrafts motion

Define the angular momentum per unit mass, i.e. the specific angular momentum as

$$\vec{h} \equiv \frac{\vec{L}}{m} \equiv \frac{\vec{r} \times \vec{p}}{m} = \vec{r} \times \dot{\vec{r}} \tag{4.8}$$

By differentiating, it follows that the specific angular momentum for the Leader satellite is

$$\begin{aligned} \dot{\vec{h}}_l &= \dot{\vec{r}}_l \times \dot{\vec{r}}_l + \vec{r}_l \times \ddot{\vec{r}}_l \\ &= \vec{0} + \vec{r}_l \times \left(-\frac{G(M+m)}{{r_l}^3} \vec{r} \right) \\ &= -\frac{G(M+m)}{{r_l}^3} \vec{r}_l \times \vec{r}_l \\ &= \vec{0} \end{aligned} \tag{4.9}$$

where (4.1) has been used. Therefore $\vec{h}_l$ is conserved, and since $\vec{h}_l$ is perpendicular to the plane defined by the radial and the velocity direction, the motion is confined to a plane spanned by the corresponding vectors, $\vec{e}_r$ and $\vec{e}_\theta$ respectively. Using polar coordinates and (A.3) the following expression is obtained:

$$\begin{aligned} \vec{h}_l &= r_l \vec{e}_r \times (\dot{r}\vec{e}_r + r_l \dot{\vec{e}}_r) \\ &= r_l \vec{e}_r \times (\dot{r}_l \vec{e}_r + r_l \dot{\nu} \vec{e}_\theta) \\ &= {r_l}^2 \dot{\nu} \vec{e}_z \end{aligned} \tag{4.10}$$

Since h_l is constant,

$$h_l = {r_l}^2 \dot{\nu} \tag{4.11}$$

is equivalent to Kepler's third law of motion[1]. Upon taking the derivative of (4.11), the following expression is obtained:

$$\begin{aligned} \dot{h}_l &= 2 r_l \dot{r}_l \dot{\nu} + {r_l}^2 \ddot{\nu} \\ &= r_l (2 \dot{r}_l \dot{\nu} + r_l \ddot{\nu}) \end{aligned} \tag{4.12}$$

[1]See http://scienceworld.wolfram.com/physics/Two-BodyProblem.html, 2005-02-02

Since $\dot{h}_l = 0$ and $r_l \neq 0$ then

$$2\dot{r}_l\dot{\nu} + r_l\ddot{\nu} = 0 \tag{4.13}$$

This provides a constraint on the second derivative of the true anomaly of the Leader satellite's orbit, such that the acceleration equation of the Leader satellite can be written

$$\begin{aligned}\ddot{\vec{r}}_l &= (\ddot{r}_l - r_l\dot{\nu}^2)\vec{e}_r + (2\dot{r}_l\dot{\nu} + r_l\ddot{\nu})\vec{e}_\theta \\ &= (\ddot{r}_l - r_l\dot{\nu}^2)\vec{e}_r\end{aligned} \tag{4.14}$$

where $\ddot{\vec{r}}_l$ was found using the same approach as in finding $\ddot{\vec{\rho}}$ in equation (4.7). Maintaining the assumption that there are no perturbations, (4.1) are compared with (4.14) which gives the following scalar equation for the acceleration of the Leader satellite

$$\ddot{r}_l = (r_l\dot{\nu}^2 - \frac{G(M+m_l)}{{r_l}^2}) \tag{4.15}$$

a second constraint on the motion of the Leader satellite. The second derivative of the vector of the Follower satellite, is, using the same procedure as for deriving equation (4.7),

$$\begin{aligned}\ddot{\vec{r}}_f &= (\ddot{r}_l + \ddot{x} - 2\dot{y}\dot{\nu} - \ddot{\nu}y - \dot{\nu}^2(r_l + x))\vec{e}_r \\ &\quad + (\ddot{y} + 2\dot{\nu}(\dot{r}_l + \dot{x}) + \ddot{\nu}(r_l + x) - \dot{\nu}^2 y)\vec{e}_\theta \\ &\quad + \ddot{z}\vec{e}_z\end{aligned} \tag{4.16}$$

Using (4.1) for the Follower satellite, and (4.15), yields that (4.16) can be written

$$\begin{aligned}\ddot{\vec{r}}_f &= \left(\left(r_l\dot{\nu}^2 - \frac{G(M+m_l)}{{r_l}^2}\right) + \ddot{x} - 2\dot{y}\dot{\nu} - \ddot{\nu}y - \dot{\nu}^2(r_l + x)\right)\vec{e}_r \\ &\quad + (\ddot{y} + 2\dot{\nu}(\dot{r}_l + \dot{x}) + \ddot{\nu}(r_l + x) - \dot{\nu}^2 y)\vec{e}_\theta \\ &\quad + \ddot{z}\vec{e}_z \\ &= \left(\ddot{x} - 2\dot{\nu}\left(\dot{y} - y\frac{\dot{r}_l}{r_l}\right) - x\dot{\nu}^2 - \frac{G(M+m_l)}{{r_l}^2}\right)\vec{e}_r \\ &\quad + \left(\ddot{y} + 2\dot{\nu}\left(\dot{x} - x\frac{\dot{r}_l}{r_l}\right) - y\dot{\nu}^2\right)\vec{e}_\theta \\ &\quad + \ddot{z}\vec{e}_z \\ &= -\frac{G(M+m_f)}{{r_f}^3}\vec{r}_f\end{aligned} \tag{4.17}$$

where the expression for the second derivative of the true anomaly from (4.13) also has been used. This vector expression can be written as three scalar equations

$$\ddot{x} - 2\dot{\nu}\left(\dot{y} - y\frac{\dot{r}_l}{r_l}\right) - x\dot{\nu}^2 - \frac{\mu}{{r_l}^2} = -\frac{\mu}{{r_f}^3}(r_l + x) \tag{4.18a}$$

$$\ddot{y} + 2\dot{\nu}\left(\dot{x} - x\frac{\dot{r}_l}{r_l}\right) - y\dot{\nu}^2 = -\frac{\mu}{{r_f}^3}y \tag{4.18b}$$

$$-\ddot{z} = -\frac{\mu}{{r_f}^3}z \tag{4.18c}$$

where the assumptions $\mu = GM \simeq G(M+m_l)$ and $\mu \simeq G(M+m_f)$, since $M \gg m_l$ and $M \gg m_f$, have been used. These are the full, nonlinear equations of relative motion for a

Follower spacecraft with respect to a Leader spacecraft in an unperturbed orbit.
From any book on basic orbital dynamic, e.g. Sellers (2000), the following relation can be found

$$r = \frac{p}{1 + e\cos\nu} \tag{4.19}$$

where p is the semilatus rectum, defined as

$$p \equiv \frac{h^2}{\mu} \tag{4.20}$$

Now, (4.11) turns into

$$h_l = r_l^2\dot{\nu} = \frac{p^2}{(1 + e\cos\nu)^2}\dot{\nu} \tag{4.21}$$

so that the following relationship is achieved

$$\begin{aligned} \frac{\dot{\nu}^2}{1 + e\cos\nu} &= \frac{h_l\dot{\nu}(1 + e\cos\nu)}{p^2} \\ &= \frac{\mu}{{r_l}^3} \end{aligned} \tag{4.22}$$

In a circular orbit the change-in-radius, $\dot{r}_l$, and the eccentricity terms drop out, and the derivative of the true anomaly, $\dot{\nu}$, can be replaced by the mean motion, n. By also assuming a close formation, such that $r_l \approx r_f$, which can be justified by the following

$$\begin{aligned} r_f &= \sqrt{(r_l + x)^2 + y^2 + z^2} \\ &= r_l\sqrt{1 + \frac{2x}{r_l} + \frac{x^2 + y^2 + z^2}{{r_l}^2}} \\ &\approx r_l\sqrt{1 + \frac{2x}{r_l}} \end{aligned} \tag{4.23}$$

the Hill-Clohessy-Wiltshire equations are obtained

$$\ddot{x} - 2n\dot{y} - 3n^2x = 0 \tag{4.24a}$$
$$\ddot{y} + 2n\dot{x} = 0 \tag{4.24b}$$
$$\ddot{z} + n^2z = 0 \tag{4.24c}$$

These equations form the basis for a lot of research done in the design of tracking controllers in the last half decade. The objective of the control is to herd the satellites into a desired formation after initial deployment, and to pull them back into this formation as soon as they start drifting away. The main reason for them drifting away is the J_2 perturbation, see section 5.1.
In appendix B, the following analytical solution is derived

$$x(t) = \frac{\dot{x}_0}{n}\sin nt - (3x_0 + 2\frac{\dot{y}_0}{n})\cos nt + 4x_0 + 2\frac{\dot{y}_0}{n} \tag{4.25a}$$
$$y(t) = \frac{2\dot{x}_0}{n}\cos nt + (6x_0 + 4\frac{\dot{y}_0}{n})\sin nt - (6nx_0 + 3\dot{y}_0)t - \frac{2\dot{x}_0}{n} + y_0 \tag{4.25b}$$
$$z(t) = \frac{\dot{z}_0}{n}\sin nt + z_0\cos nt \tag{4.25c}$$

Equation (4.25b) includes a secular term, i.e. a term that increases linearly in time. To eliminate the secular drift the following additional constraint is invoked

$$\dot{y}_0 = -2x_0n \tag{4.26}$$

and results in a relative orbit that is displaced from, but has the same energy, and thus the same semimajor axis, as the reference orbit. This leads to the following parametric solution of (4.24a)-(4.24c)

$$x(t) = \frac{\dot{x}_0}{n} \sin nt + x_0 \cos nt \tag{4.27a}$$
$$y(t) = \frac{2\dot{x}_0}{n} \cos nt - 2x_0 \sin nt - \frac{2\dot{x}_0}{n} + y_0 \tag{4.27b}$$
$$z(t) = \frac{\dot{z}_0}{n} \sin nt + z_0 \cos nt \tag{4.27c}$$

4.2 Examples of Satellite Formations

To get a picture of which paths are sustainable with a view to minimization of the fuel consumption, the following examples are considered, based on Yeh & Sparks (2000). Let the initial placement of the Follower satellite be somewhere at radial axis, i.e. $\dot{x_0} = 0$. Then the sine and cosine terms, can be written in terms of the solutions of the HCW-equations in radial- and velocity directions as follows

$$\frac{x}{x_0} = \cos nt \tag{4.28}$$
$$\frac{y - y_0}{-2x_0} = \sin nt \tag{4.29}$$

Taking the square and adding the two equations gives

$$\frac{x^2}{{x_0}^2} + \frac{(y - y_0)^2}{4{x_0}^2} = \cos^2 nt + \sin^2 nt = 1 \tag{4.30}$$

which is the equation for an ellipse centered somewhere at the axis of the velocity direction. Writing the solution of the orbit-normal direction in terms of the other two directions, gives

$$z = -\frac{\dot{z}_0}{2nx_0}(y - y_0) + \frac{z_0}{x_0}x \tag{4.31}$$

The set of equations describing the motion of the Follower-satellite around the Leader-satellite, can also be achieved by letting the initial placement of the Follower-satellite be at the axis of the velocity direction, i.e. $x_0 = 0$. The solutions will now be reduced to

$$x(t) = \frac{\dot{x}_0}{n} \sin nt \tag{4.32}$$
$$y(t) = \frac{2\dot{x}_0}{n} \cos nt - \frac{2\dot{x}_0}{n} + y_0 \tag{4.33}$$

Using the same procedure as above the following equation of an ellipse, centered at the radial direction axis, is achieved for the in-plane motion

$$\frac{x^2}{(\frac{\dot{x}_0}{n})^2} + \frac{(y + \frac{2\dot{x}_0}{n} - y_0)^2}{(\frac{2\dot{x}_0}{n})^2} = 1 \tag{4.34}$$

For the out of plane motion, the equation is

$$z = \frac{\dot{z}_0}{\dot{x}_0}x + \frac{nz_0}{2\dot{x}_0}y + \frac{nz_0}{2\dot{x}_0}(\frac{2\dot{x}_0}{n} - y_0) \tag{4.35}$$

The eccentricity of an ellipse with major axis a and minor axis b is given by

$$e = \sqrt{1 - \frac{b^2}{a^2}} \tag{4.36}$$

which for this case will be

$$e = \sqrt{1 - \frac{{x_0}^2}{4{x_0}^2}} = \frac{\sqrt{3}}{2} \tag{4.37}$$

4.3 Circular Formation

A circular formation is attained by proposing the following constraint

$$x^2 + y^2 + z^2 = k^2 \tag{4.38}$$

where k is the radius of the formation. Using equation (4.30) and (4.31), this can be written

$$\begin{aligned} k^2 = {} & x_0^2(\cos nt)^2 + y_0^2 - 4x_0y_0\sin(nt) + 4x_o^2(\sin(nt))^2 + z_0^2(\cos nt)^2 \\ & + 2z_0\cos nt\frac{\dot{z}_0}{n}\sin nt + \frac{\dot{z}_0^2}{n^2}(\sin nt)^2 \end{aligned} \tag{4.39}$$

The constraint implies that $y_0 = \dot{z}_0 = 0$ and $z_0/x_0 = \pm\sqrt{3}$. This is a circular formation in the plane $z = \pm\sqrt{3}x$, which is at an angle of $\pm 60°$ with the x-axis. This special formation was first described in Sabol, Burns & McLaughlin (1999).

4.4 In-Plane Elliptic Formation

If both $z_0 = 0$ and $\dot{z}_0 = 0$ in (4.31), then the motion is an elliptic motion purely in xy-plane. The eccentricity of the ellipse is $\sqrt{3}/2$ and its major axis is parallel to the y-axis, that is, parallel to the direction of motion of the Leader satellite. Such a formation can be seen in figure 4.3.

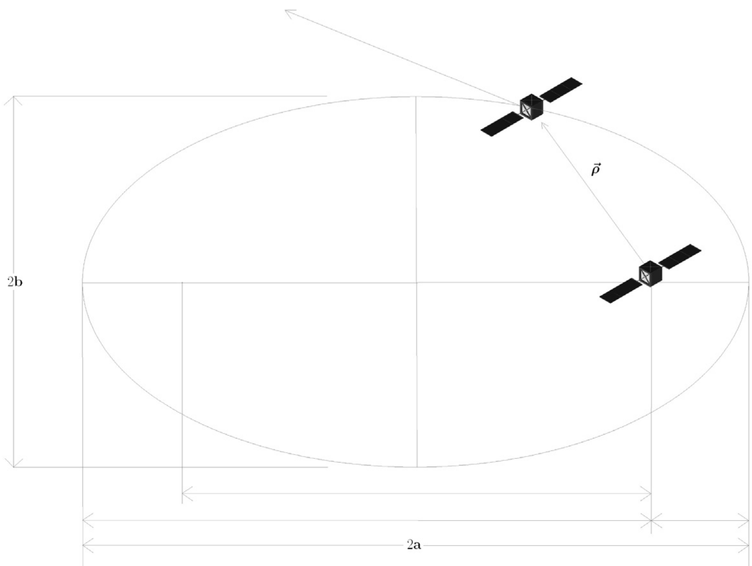

Figure 4.3: The Follower satellite moves in an ellipse relative to the Leader satellite

4.5 Projected Circular Formation

The perhaps most interesting formation, at least for earth pointing devices, is the projected circular formation. That is, the formation appears as circular under the assumption that the viewpoint is on the line connecting the center of Earth to the center of the relative orbit. Extensions to the case of a viewpoint above or below this line is quite straightforward. The formation is achieved from imposing the following constraint

$$y^2 + z^2 = k^2 \tag{4.40}$$

where k is the radius of the projected circle. By using equation (4.30) and (4.31), the initial conditions are $y_0 = \dot{z}_0 = 0$ and $z_0/x_0 = \pm 2$.
It is possible to place as many satellites in a circular apparent orbit with a initial angle separating them, and also as many circular orbits with radial separation, as desired, see Chichka (2001). This would cause a "pinwheel" effect from the planetary surface as the satellites rotate about the center of the formation.

Chapter 5

Perturbing Forces Modeling

A satellite orbiting the Earth is influenced by many perturbing forces and torques. Satellites in all altitudes are highly affected by the gravitational perturbation, caused by the non-symmetric, non-homogenous Earth. For high altitude orbits, the atmospheric drag may be ignored, where as it is a dominating force at low altitudes. Other perturbing effects are caused by solar radiation and solar wind, the magnetic field of the Earth and the gravitational force from the Moon and the Sun. This is shown illustratively in Figure 5.1 from Brown (2002).

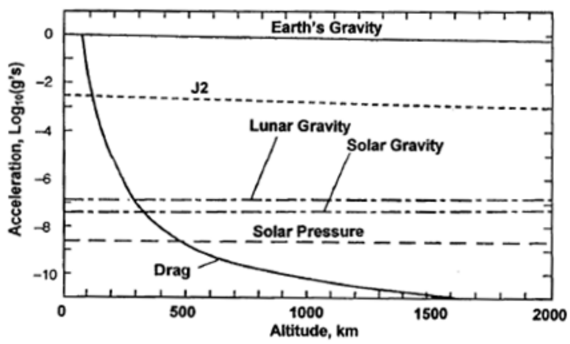

Figure 5.1: The influence of disturbing forces at different altitudes (c.f. Brown (2002))

5.1 J_2 Gravity Perturbation

The Earth is no perfect sphere, and neither is its mass distribution homogeneous. This means that the usual approximation of the gravitational force, based on the assumption that the total mass of the Earth is concentrated in its center,

$$\vec{f} = \frac{\mu m}{r^3}\vec{r} \tag{5.1}$$

where m is the mass of the satellite, situated at $\vec{r}$, $\mu = GM$ and G denotes the universal gravitational constant, is no longer satisfactory. Therefore, following the steps of Montenbruck & Gill (2000), a more realistic model of the gravitational force will be derived.
The model involves the gradient of the gravitational potential, U, as follows

$$\vec{f} = m\nabla U \tag{5.2}$$

where the gravitational potential is generalized to include an arbitrary mass distribution by summing up the contributions from each mass element $\mathrm{d}m = \rho(\vec{s})\mathrm{d}^3\vec{s}$, i.e.

$$U = \mu \int \frac{\rho(\vec{s})\mathrm{d}^3\vec{s}}{|\vec{r} - \vec{s}|} \tag{5.3}$$

The density at some point $\vec{s}$ inside Earth is denoted by $\rho(\vec{s})$. The inverse of the distance may be expanded in a series of Legendre polynomials as

$$\frac{1}{|\vec{r} - \vec{s}|} = \frac{1}{\vec{r}} \sum_{n=0}^{\infty} \left(\frac{s}{r}\right)^n P_n(\cos \gamma_l) \tag{5.4}$$

where

$$P_n(u) = \frac{1}{2^n n!} \frac{\mathrm{d}^n}{\mathrm{d}u^n} (u^2 - 1)^n \tag{5.5}$$

is Rodrigues's formula for the Legendre polynomial of degree n, and γ_l is the angle between $\vec{r}$ and $\vec{s}$ such that

$$\cos \gamma_l = \frac{\vec{r} \cdot \vec{s}}{rs} \tag{5.6}$$

Now, let the point $\vec{r}$ be given by

$$x = r \cos \mu_c \cos l \tag{5.7}$$

$$y = r \cos \mu_c \sin l \tag{5.8}$$

$$z = r \sin \mu_c \tag{5.9}$$

where l is the longitude and μ_c is the geocentric latitude. Let l' and μ_c' be the corresponding values for $\vec{s}$. The spherical harmonic addition theorem, also known as the addition theorem of the Legendre polynomials, states that

$$P_n(\cos \gamma_l) = \sum_{m=0}^{n} (2 - \delta_{0m}) \frac{(n-m)!}{(n+m)!} P_{nm}(\sin \mu_c) P_{nm}(\sin \mu_c') \cos(m(l - l')) \tag{5.10}$$

The associated Legendre polynomial of degree n and order m, is defined, see for example Kreyszig (1999), as

$$P_{nm}(u) = (1 - u^2)^{\frac{m}{2}} \frac{\mathrm{d}^m}{\mathrm{d}u^m} P_n(u) \tag{5.11}$$

The Earth's gravity potential can now be written

$$U = \frac{\mu}{r} \sum_{n=0}^{\infty} \sum_{m=0}^{n} \left(\frac{a}{r}\right)^n P_{nm}(\sin \mu_c)(C_{nm} \cos ml + S_{nm} \sin ml) \tag{5.12}$$

with coefficients

$$C_{nm} = \frac{2 - \delta_{0m}}{m_{Earth}} \frac{(n-m)!}{(n+m)!} \int \left(\frac{s}{a}\right)^n P_{nm}(\sin \mu_c') \cos ml' \rho(\vec{s}) \mathrm{d}^3\vec{s} \tag{5.13}$$

$$S_{nm} = \frac{2 - \delta_{0m}}{m_{Earth}} \frac{(n-m)!}{(n+m)!} \int \left(\frac{s}{a}\right)^n P_{nm}(\sin \mu_c') \sin ml' \rho(\vec{s}) \mathrm{d}^3\vec{s} \tag{5.14}$$

which describe the dependence on the Earth's internal mass distribution. In the literature it is quite common to use the normalized coefficients

$$\overline{C}_{nm} = \sqrt{\frac{(n+m)!}{(2 - \delta_{0m})(2n+1)(n-m)!}} C_{nm} \tag{5.15}$$

$$\overline{S}_{nm} = \sqrt{\frac{(n+m)!}{(2 - \delta_{0m})(2n+1)(n-m)!}} S_{nm} \tag{5.16}$$

C_{nm}	$m = 0$	1	2	3
$n = 0$	1.00			
1	0.00	0.00		
2	$-1.08 \cdot 10^{-3}$	0.00	$1.57 \cdot 10^{-6}$	
3	$2.53 \cdot 10^{-6}$	$2.18 \cdot 10^{-6}$	$3.11 \cdot 10^{-7}$	$1.02 \cdot 10^{-7}$
S_{nm}	$m = 0$	1	2	3
$n = 0$	0.00			
1	0.00	0.00		
2	0.00	0.00	$-9.03 \cdot 10^{-7}$	
3	0.00	$2.68 \cdot 10^{-7}$	$-2.12 \cdot 10^{-7}$	$1.98 \cdot 10^{-7}$

Table 5.1: Geopotential coefficients up to degree and order three

which are much more uniform in magnitude than the unnormalized coefficients. By also using the normalized associated Legendre functions

$$\overline{P}_{nm} = \sqrt{\frac{(2 - \delta_{0m})(2n + 1)(n - m)!}{(n + m)!}} P_{nm} \tag{5.17}$$

the gravitational force can be rewritten as

$$\vec{f} = m\nabla\frac{\mu}{r}\sum_{n=0}^{\infty}\sum_{m=0}^{n}\left(\frac{a}{r}\right)^n \overline{P}_{mn}(\sin\mu_c)(\overline{C}_{nm}\cos(ml) + \overline{S}_{nm}\sin(ml)) \tag{5.18}$$

Approximate values of the Earth's low-order potential coefficients can be found in Table 5.1. In computing the gravity potential at a given point, recursive formulas of the Legendre polynomials can be used. The polynomials of same degree and order, are calculated from

$$P_{mm} = (2m - 1)(1 - u^2)^{\frac{1}{2}} P_{m-1,m-1} \tag{5.19}$$

with $P_{00} = 1$. The remaining values are calculated from

$$P_{m+1,m}(u) = (2m + 1)uP_{mm}(u) \tag{5.20}$$

and from

$$P_{nm}(u) = \frac{1}{n - m}((2n - 1)uP_{n-1,m}(u) - (n + m - 1)P_{n-2,m}(u)) \tag{5.21}$$

for $n > m + 1$. By defining

$$V_{nm} = \left(\frac{a}{r}\right)^{n+1} P_{nm}(\sin\mu_c)\cos ml \tag{5.22}$$

$$W_{nm} = \left(\frac{a}{r}\right)^{n+1} P_{nm}(\sin\mu_c)\sin ml \tag{5.23}$$

it can be shown that the gravity potential may be written as

$$U = \frac{\mu}{a}\sum_{n=0}^{\infty}\sum_{m=0}^{n}(C_{nm}V_{nm} + S_{nm}W_{nm}) \tag{5.24}$$

with

$$V_{mm} = (2m - 1)\left[\frac{xa}{r^2}V_{m-1,m-1} - \frac{ya}{r^2}W_{m-1,m-1}\right] \tag{5.25}$$

$$W_{mm} = (2m - 1)\left[\frac{xa}{r^2}W_{m-1,m-1} + \frac{ya}{r^2}V_{m-1,m-1}\right] \tag{5.26}$$

and

$$V_{nm} = \left(\frac{2n-1}{n-m}\right)\frac{za}{r^2}V_{n-1,m} - \left(\frac{n+m-1}{n-m}\right)\frac{a^2}{r^2}V_{n-2,m} \tag{5.27}$$

$$W_{nm} = \left(\frac{2n-m}{n-m}\right)\frac{za}{r^2}W_{n-1,m} - \left(\frac{n+m-1}{n-m}\right)\frac{a^2}{r^2}W_{n-2,m} \tag{5.28}$$

and $V_{m-1,m}$ and $W_{m-1,m}$ set to zero and $V_{00} = \frac{a}{r}$ and $W_{00} = 0$. The gravitational force may now be calculated using the gradient of U from

$$f_x = m\ddot{x} = m\sum_{n,m}\ddot{x}_{nm} \tag{5.29}$$

$$f_y = m\ddot{y} = m\sum_{n,m}\ddot{y}_{nm} \tag{5.30}$$

$$f_z = m\ddot{z} = m\sum_{n,m}\ddot{z}_{nm} \tag{5.31}$$

with the partial accelerations

$$\begin{aligned}
\ddot{x}_{nm} &\overset{(\mathrm{m=0})}{=} \frac{\mu}{a^2}\Big[-C_{n0}V_{n+1,1}\Big] \\
&\overset{(\mathrm{m>0})}{=} \frac{\mu}{2a^2}\Big[(-C_{nm}V_{n+1,m+1} - S_{nm}W_{n+1,m+1}) \\
&\quad + \frac{(n-m+2)!}{(n-m)!}(C_{nm}V_{n+1,m-1} + S_{nm}W_{n+1,m-1})\Big] \\
\ddot{y}_{nm} &\overset{(\mathrm{m=0})}{=} \frac{\mu}{a^2}\Big[-C_{n0}W_{n+1,1}\Big] \\
&\overset{(\mathrm{m>0})}{=} \frac{\mu}{2a^2}\Big[(-C_{nm}W_{n+1,m+1} + S_{nm}V_{n+1,m+1}) \\
&\quad + \frac{(n-m+2)!}{(n-m)!}(-C_{nm}W_{n+1,m-1} + S_{nm}V_{n+1,m-1})\Big] \\
\ddot{z}_{nm} &\overset{(\mathrm{m\geq0})}{=} \frac{\mu}{a^2}\Big[(n-m+1)(-C_{nm}V_{n+1,m} - S_{nm}W_{n+1,m})\Big]
\end{aligned} \tag{5.32}$$

For simplicity, the mass distribution will be considered symmetric with respect to the axis of rotation. That is, the expansion of the potential contains only zonal terms, C_{n0}, and does not depend on the longitude. Using the recursive equations (5.25),(5.26),(5.27) and (5.28), the gravitational force components are found to be

$$f_x = -\frac{x_e\mu}{r^3}\left[1 + \frac{3J_2a^2}{2r^2} - \frac{15J_2a^2z_e^2}{2r^4}\right] \tag{5.33}$$

$$f_y = -\frac{y_e\mu}{r^3}\left[1 + \frac{3J_2a^2}{2r^2} - \frac{15J_2a^2z_e^2}{2r^4}\right] \tag{5.34}$$

$$f_z = -\frac{z_e\mu}{r^3}\left[1 + \frac{9J_2a^2}{2r^2} - \frac{15J_2a^2z_e^2}{2r^4}\right] \tag{5.35}$$

where the commonly used notation

$$J_n = -C_{n0} \tag{5.36}$$

has been introduced. The gravity vector is therefore given by

$$\mathbf{f}_g^e = \begin{pmatrix} f_x \\ f_y \\ f_z \end{pmatrix} \tag{5.37}$$

in the ECEF-frame. By also taking the accelerations due to J_3 into account, the gravitational force components become

$$f_x = -\frac{x_e \mu}{r^3}\left[1 + \frac{3J_2 a^2}{2r^2} - \frac{15 J_2 a^2 z_e^2}{2r^4} + \frac{15 J_3 a^3 z}{2r^4} - \frac{35 J_3 a^3 z^3}{2r^6}\right] \tag{5.38}$$

$$f_y = -\frac{y_e \mu}{r^3}\left[1 + \frac{3J_2 a^2}{2r^2} - \frac{15 J_2 a^2 z_e^2}{2r^4} + \frac{15 J_3 a^3 z}{2r^4} - \frac{35 J_3 a^3 z^3}{2r^6}\right] \tag{5.39}$$

$$f_z = -\frac{z_e \mu}{r^3}\left[1 + \frac{9J_2 a^2}{2r^2} - \frac{15 J_2 a^2 z_e^2}{2r^4} + \frac{30 J_3 a^3 z}{2r^4} - \frac{35 J_3 a^3 z^3}{2r^6} - \frac{3}{10 r^2 z}\right] \tag{5.40}$$

For higher degree computations, see for example Vallado (2001). It should be noted that the geopotential coefficients C_{nm} and S_{nm} can not be calculated from equations (5.13) and (5.14), but are determined indirectly through *satellite tracking*, *surface gravimetry* and *altimeter data*. The reader are referred to Montenbruck & Gill (2000) for an explanation of these concepts. In Hsu (1996) a comparison of the J_2 gravitational model with other models are made. According to Hsu (1998) the J_2 gravitational model is not good enough for high accuracy applications. A better and more complex model is implemented in the *Aerospace Blockset* toolbox in Simulink, but with the drawback that the satellites position must be given relative to the surface of Earth.

5.2 Gravitational Torque

The gravitational field is not uniform in space, so due to the variations in the specific gravitational force, a gravitational torque about the body mass center will occur. The following assumptions from (Hughes 1986), simplifies the expression for the gravitational torque:

1. Only on celestial primary need be considered.
2. This primary possesses a spherically symmetrical mass distribution.
3. The spacecraft is small compared to its distance from the mass center of the primary.
4. The spacecraft consists of a single body.

Using 1.), 2.) and 4.) above, the total gravitational torque can be expressed as

$$\vec{m}_g = -\mu \int_{\mathfrak{B}} \frac{\vec{t} \times \vec{r}_t}{r_t^3}\, \mathrm{d}m \tag{5.41}$$

where $\vec{t}$ is the location of the mass element $\mathrm{d}m$ relative to the center of mass of the satellite, and $\vec{r}_t = \vec{r} + \vec{t}$ is the location of the mass element $\mathrm{d}m$ relative to the center of Earth. The universal gravitational constant times the mass of Earth is denoted by $\mu = GM$. By using assumption 3), i.e. $t/r \ll 1$ and a binomial expansion, we get that

$$r_t^{-3} = r^{-3}\left[1 - \frac{3(\vec{t}\cdot\vec{r})}{r^2} + O\left(\frac{t^2}{r^2}\right)\right] \tag{5.42}$$

By leaving the higher order terms out and setting $\int_{\mathfrak{B}} \vec{t}\,\mathrm{d}m = 0$, the torque is given by

$$
\begin{aligned}
\vec{m}_g &= -\mu \int_{\mathfrak{B}} \frac{\vec{t} \times \vec{r}_t}{r^3} \left[1 - \frac{3(\vec{t} \cdot \vec{r})}{r^2}\right] \mathrm{d}m \\
&= -\mu \int_{\mathfrak{B}} \frac{\vec{t} \times (\vec{r} + \vec{t})}{r^3} \left[1 - \frac{3(\vec{t} \cdot \vec{r})}{r^2}\right] \mathrm{d}m \\
&= -\mu \int_{\mathfrak{B}} \frac{\vec{t} \times \vec{r}}{r^3} \left[1 - \frac{3(\vec{t} \cdot \vec{r})}{r^2}\right] \mathrm{d}m \\
&= \left(\frac{\mu}{r^3}\right) \vec{r} \times \int_{\mathfrak{B}} \vec{t}\mathrm{d}m - \left(\frac{3\mu}{r^5}\right) \vec{r} \times \int_{\mathfrak{B}} \vec{t}\vec{t}\,\mathrm{d}m \cdot \vec{r} \\
&= -\left(\frac{3\mu}{r^5}\right) \vec{r} \times \int_{\mathfrak{B}} \vec{t}\vec{t}\,\mathrm{d}m \cdot \vec{r}
\end{aligned} \tag{5.43}
$$

The expression $\int_{\mathfrak{B}} \vec{t}\vec{t}\,\mathrm{d}m$ of 5.43 is a part of the expression for the inertia dyadic $\vec{I}$, that is

$$
\vec{I} = \int_{\mathfrak{B}} (t^2 \vec{1} - \vec{t}\vec{t})\,\mathrm{d}m \tag{5.44}
$$

where $\vec{1}$ represents the unity dyadic. By using the vectrix notation from section 3.2, and that $\vec{I} = \boldsymbol{\mathfrak{F}}_b^T \mathbf{I} \boldsymbol{\mathfrak{F}}_b$, the gravitational torque in the body frame $\mathfrak{F}_b$ becomes

$$
\begin{aligned}
\mathbf{m}_g^b &= \boldsymbol{\mathfrak{F}}_b \cdot \vec{m}_g \\
&= \frac{3\mu}{r^5} \boldsymbol{\mathfrak{F}}_b \cdot \vec{r} \times \boldsymbol{\mathfrak{F}}_b^T \mathbf{I} \boldsymbol{\mathfrak{F}}_b \cdot \vec{r}
\end{aligned} \tag{5.45}
$$

Now, by defining $\vec{r} = \boldsymbol{\mathfrak{F}}_b^T \mathbf{p}^b = (\mathbf{p}^b)^T$, where p is chosen so as to coincide with the notation in section 7.2, the torque can be written

$$
\begin{aligned}
\mathbf{m}_g^b &= \frac{3\mu}{r^5} \boldsymbol{\mathfrak{F}}_b^T \cdot (\mathbf{p}^b)^T \boldsymbol{\mathfrak{F}}_b \times \boldsymbol{\mathfrak{F}}_b^T \mathbf{I} \boldsymbol{\mathfrak{F}}_b \cdot \boldsymbol{\mathfrak{F}}_b^T \mathbf{p}^b \\
&= \frac{3\mu}{r^5} \boldsymbol{\mathfrak{F}}_b^T \cdot (\mathbf{p}^b)^T \boldsymbol{\mathfrak{F}}_b \times \boldsymbol{\mathfrak{F}}_b^T \mathbf{I} \mathbf{p}^b
\end{aligned} \tag{5.46}
$$

It has been used that $\boldsymbol{\mathfrak{F}}_b \cdot \boldsymbol{\mathfrak{F}}_b^T$. It can be shown, see Hughes (1986), that $\mathbf{p}_b^T \boldsymbol{\mathfrak{F}}_b \times \boldsymbol{\mathfrak{F}}_b^T \mathbf{I} \mathbf{p}^b = \boldsymbol{\mathfrak{F}}_b^T (\mathbf{p}^b)^T \mathbf{I} \mathbf{p}^b$, such that

$$
\begin{aligned}
\mathbf{m}_g^b &= \frac{3\mu}{r^5} \boldsymbol{\mathfrak{F}}_b \cdot \boldsymbol{\mathfrak{F}}_b^T (\mathbf{p}^b)^T \mathbf{I} \mathbf{p}^b \\
&= \frac{3\mu}{r^5} \mathbf{S}(\mathbf{R}_i^b \mathbf{p}^i) \mathbf{I} \mathbf{R}_i^b \mathbf{p}^i
\end{aligned} \tag{5.47}
$$

Since

$$
\frac{\mu}{r^2} = \frac{|\mathbf{f}_g|}{m} \tag{5.48}
$$

the gravitational torque is given as

$$
\mathbf{m}_g^b = \left(\frac{3|\mathbf{f}_g|}{r^3 m}\right) \mathbf{S}(\mathbf{R}_i^b \mathbf{p}^i) \mathbf{I} \mathbf{R}_i^b \mathbf{p}^i \tag{5.49}
$$

where $\mathbf{f}_g$ is given by (5.37).

5.3 Atmospheric Drag

Atmospheric drag is caused by the momentum transfer from particles in the atmosphere, onto the satellite. There are two different principles for describing this molecular momentum transfer to a physical surface, namely *specular* reflection and *diffuse* reflection. By specular reflection the impinging particles have an elastic impact with the surface, and bounces off with no change in energy and at an angle equal to the angle of incidence. Diffuse reflection, on the other hand, occurs when the atmospheric particles penetrate the satellite surface, interact with the body molecules, and are finally re-emitted in a random manner, see Montenbruck & Gill (2000). Both these types of momentum transfer to the surface appears at various degrees. In the following, a mathematical model of the atmospheric drag is derived, as in Hughes (1986), under the assumptions that

1. The momentum of molecules arriving at the surface is totally lost to the surface, i.e. diffuse reflection.

2. The mean thermal motion of the atmosphere is much smaller than the speed of the spacecraft through the atmosphere.

3. Momentum transfer from molecules leaving the surface is negligible.

4. For spinning vehicles, the relative motion between surface elements is much smaller than the speed of the mass center.

Let the velocity of the local atmosphere relative to a surface element $\mathrm{d}A$ be denoted by $\vec{v}_r$ and let $\vec{n}_A$ be a unit vector pointing inward normal to the surface at $\mathrm{d}A$. The area projected normal to the direction of $\vec{v}_r$ is then $\mathrm{d}A\cos\alpha$, where

$$\cos\alpha \triangleq \frac{\vec{v}_r}{v_r}\cdot\vec{n}_A \tag{5.50}$$

and α is the *angle of attack*. The force imparted to the surface element $\mathrm{d}A$, is the flux through $\mathrm{d}A\cos\alpha$, which is

$$\mathrm{d}\vec{f}_d = \rho_a v_r \cos\alpha \vec{v}_r \mathrm{d}A \tag{5.51}$$

for $\cos\alpha \geq 0$, and 0 otherwise since $\mathrm{d}A$ will then not be directed against the flow. By integrating over the vehicle surface, the total force and torque is given as

$$\vec{f}_d = \oiint H(\cos\alpha)\rho_a v_r \cos\alpha \mathrm{d}A\vec{v}_r \tag{5.52}$$

and

$$\vec{m}_d = \oiint H(\cos\alpha)\rho_a v_r \cos\alpha \vec{t}\mathrm{d}A \times \vec{v}_r \tag{5.53}$$

respectively. Here, $H(x)$ is the Heaviside function, i.e.

$$H = \begin{cases} 1 & \text{for} \quad x \geq 0 \\ 0 & \text{for} \quad x < 0 \end{cases} \tag{5.54}$$

and $\vec{t}$ is the location of $\mathrm{d}A$ relative to the center of mass. In table 5.3, the atmospheric density, ρ_a for different altitudes are found, just as in Wertz & Larson (1999). In terms of conventional aerodynamic, equation (5.52) can be stated as

$$\vec{f}_d = \frac{1}{2}\rho_a v_r C_d A \vec{v}_r \tag{5.55}$$

Alt (km)	**Minimum** $(\mathbf{kg/m^3})$	**Mean** $(\mathbf{kg/m^3})$	**Maximum** $(\mathbf{kg/m^3})$
0	1.2	1.2	1.2
100	$4.61 \cdot 10^{-7}$	$4.79 \cdot 10^{-7}$	$5.10 \cdot 10^{-7}$
200	$1.78 \cdot 10^{-10}$	$2.53 \cdot 10^{-10}$	$3.52 \cdot 10^{-10}$
300	$8.19 \cdot 10^{-12}$	$1.95 \cdot 10^{-11}$	$3.96 \cdot 10^{-11}$
400	$7.32 \cdot 10^{-13}$	$2.72 \cdot 10^{-12}$	$7.55 \cdot 10^{-12}$
500	$8.98 \cdot 10^{-14}$	$4.89 \cdot 10^{-13}$	$1.80 \cdot 10^{12}$
600	$1.68 \cdot 10^{-14}$	$1.04 \cdot 10^{-13}$	$4.89 \cdot 10^{-13}$
700	$5.74 \cdot 10^{-15}$	$2.72 \cdot 10^{-14}$	$1.47 \cdot 10^{-13}$
800	$2.96 \cdot 10^{-15}$	$9.63 \cdot 10^{-15}$	$4.39 \cdot 10^{-14}$
900	$1.80 \cdot 10^{-15}$	$4.66 \cdot 10^{-15}$	$1.91 \cdot 10^{-14}$
1000	$1.17 \cdot 10^{-15}$	$2.79 \cdot 10^{-15}$	$8.84 \cdot 10^{-15}$

Table 5.2: Atmospheric Density

where the drag coefficient C_d is a dimensionless quantity that describes the interaction of the atmosphere with the surface material of the satellite. In table 5.3 the ballistic coefficients, B_C for several low Earth orbit satellites are given, which relates to the drag coefficient as follows

$$B_C = \frac{m}{C_d A} \tag{5.56}$$

For a non-spinning satellite, the aerodynamic torque can be written as

$$\vec{m}_d = \vec{r}_p \times \vec{f}_d \tag{5.57}$$

where $\vec{r}_p$ is the vector from center of mass to the center of pressure.

5.4 Solar Radiation and Solar Wind

According to Sidi (2002), the *Solar radiation* comprises all the electromagnetic waves radiated by the sun with wavelengths ranging from X-rays to radio waves, where as the *solar wind* mainly consists of ionized nuclei and electrons. The radiation pressure is best explained in terms of the corpuscular nature of radiation, i.e. that the photons possesses a momentum flux which results in an pressure on the radiated area. The mean solar energy flux of the solar radiation is proportional to the inverse square of the distance from the sun, and leads to the following force acting on the satellite, see Montenbruck & Gill (2000)

$$\vec{f}_r = -P \cos\beta A \left[(1-\varepsilon)\vec{e} + 2\varepsilon \cos\beta \vec{n}\right] \tag{5.58}$$

where $P \approx 4.56 \cdot 10^{-6}\mathrm{Nm}^{-2}$ is the solar radiation pressure, $\vec{n}$ is the normal vector of the surface A. The vector $\vec{e}$ points in the direction of the Sun, and is inclined at an angle β relative to $\vec{n}$. In (5.58), the distance between the Sun and the satellite are assumed to be constant. This is not true due to the eccentricity of the Earth's orbit, but the annual variation in the solar radiation pressure have a minor impact on the force acting on the satellite, and can therefore be neglected.

The solar wind momentum flux is smaller than that of the solar radiation, by a factor of 100 to 1000, according to Sidi (2002), and will therefore not be modeled.

[1]With solar panels

Satellite	Mass (kg)	Shape	Max. XA (m^2)	Min. XA (m^2)	XA Drag Coef.	Min. XA Drag Coef.	Max. Ballistic Coef. (kg/m^2)	Min. Ballistic Coef. (kg/m^2)	Type of Mission
Oscar-1	5	box	0.075	0.0584	4	2	42.8	16.7	Comm.
Intercos.-16	550	cylind.	2.7	3.16	2.67	2.1	82.9	76.3	Scientific
Viking	277	octag.	2.25	0.833	4	2.6	128	30.8	Scientific
Explorer-11	37	octag.	0.18	0.07	2.83	2.6	203	72.6	Astronomy
Explorer-17	188.2	sphere	0.621	0.621	2	2	152	152	Scientific
Sp. Teles.	11,000	cylin.[1]	112	14.3	3.33	4	192	29.5	Astronomy
OSO-7	634	9-sided	1.05	0.5	3.67	2.9	437	165	Solar Physics
OSO-8	1,063	cylind.[1]	5.99	1.81	3.76	4	147	47.2	Solar Physics
Pegasus-3	10,500	cylind.[1]	264	14.5	3.3	4	181	12.1	Scientific
Landsat-1	891	cylind.[1]	10.4	1.81	3.4	4	123	25.2	Rem. Sens.
ERS-1	2,160	box[1]	45.1	4	4	4	135	12.0	Rem. Sens.
LDEF-1	9,695	12-face	39	14.3	2.67	4	169	93.1	Environment
HEAO-2	3,150	hexag.	13.9	4.52	2.83	4	174	80.1	Astronomy
Vanguard-2	9.39	sphere	0.2	0.2	2	2	23.5	23.5	Scientific
SkyLab	76,136	cylind.[1]	462	46.4	3.5	4	410	47.1	Scientific
Escho-1	75.3	sphere	731	731	2	2	0.515	0.515	Comm.

Table 5.3: Typical Ballistic Coefficients for Low-Earth Orbit Satellites

5.5 Other Perturbing Forces and Torques

For models of other perturbing forces, the reader is referred to Montenbruck & Gill (2000) or Vallado (2001), where as perturbing torques are treated extensively in Hughes (1986) and Kristiansen (2000).

Chapter 6

Modeling: Relative Position and Attitude

In this chapter a nonlinear model for the motion of the Follower satellite relative to the Leader satellite will be derived. It will be obtain in the same way as the linear model from chapter 4, but is now generalized to also include forcing terms due to disturbances, e.g. aerodynamic forces, a third gravitating body, solar radiation, magnetic fields etc.

6.1 Relative Position

Equation (4.1) is generalized to include forcing terms, F_{dl}, F_{df} ϵ $\mathbb{R}^3$, due to disturbances, and actual control input vectors u_l, u_f ϵ $\mathbb{R}^3$, so that

$$\ddot{\vec{r}}_l = -\frac{G(M+m)}{{r_l}^3}\vec{r}_l - \frac{\vec{F}_{dl}}{m_l} + \frac{u_l}{m_l} \tag{6.1}$$

$$\ddot{\vec{r}}_f = -\frac{G(M+m)}{r_f^3}\vec{r}_f - \frac{\vec{F}_{df}}{m\ _f} + \frac{u_f}{m_f} \tag{6.2}$$

where r_l and r_f are the the position of the Leader and the Follower, respectively. By subtracting (6.1) from (6.2), the following equation describing the position of the Follower spacecraft relative to the Leader spacecraft is obtained

$$m_f\ddot{\vec{\rho}} + m_f\mu\left(\frac{\vec{r}_l+\vec{\rho}}{(r_l+\rho)^3} - \frac{\vec{r}_l}{{r_l}^3}\right) + \frac{m_f}{m_l}\vec{u}_l + \vec{F}_{df} - \frac{m_f}{m_l}\vec{F}_{dl} = \vec{u}_f \tag{6.3}$$

Now, by using equation (4.6), the nonlinear position dynamics of the Follower spacecraft relative to the Leader spacecraft can be arranged to

$$\mathbf{M}\ddot{\boldsymbol{\rho}} + \mathbf{C}(\dot{\nu}, m_f)\dot{\boldsymbol{\rho}} + \mathbf{n}(\boldsymbol{\rho}, \dot{\nu}, \ddot{\nu}, r_l) + \frac{m_f}{m_l}\mathbf{u}_l + \mathbf{F}_d = \mathbf{u}_f \tag{6.4}$$

similar to the one found in (Yan, Yang, Kapila & de Queiroz 2000). Here

$$\boldsymbol{\rho} = \begin{bmatrix} x(t) \\ y(t) \\ z(t) \end{bmatrix} \tag{6.5}$$

is the relative position vector,

$$\mathbf{M} = \begin{pmatrix} m_f & 0 & 0 \\ 0 & m_f & 0 \\ 0 & 0 & m_f \end{pmatrix} \tag{6.6}$$

is the mass matrix,

$$\mathbf{C}(\dot{\nu}, m_f) = 2m_f\dot{\nu}\begin{bmatrix} 0 & -1 & 0 \\ 1 & 0 & 0 \\ 0 & 0 & 0 \end{bmatrix} \tag{6.7}$$

is the Coriolis-like matrix and

$$\mathbf{n}(\boldsymbol{\rho}, \dot{\nu}, \ddot{\nu}, r_l) = m_f\begin{bmatrix} \mu(\frac{r_l+x}{{r_f}^3} - \frac{1}{{r_l}^2}) - (\dot{\nu}^2 x + \ddot{\nu}y) \\ \mu(\frac{y}{{r_f}^3}) - (y\dot{\nu}^2 - \ddot{\nu}x) \\ \mu(\frac{z}{{r_f}^3}) \end{bmatrix} \tag{6.8}$$

is a nonlinear term. The composite disturbance force, $\mathbf{F}_d$ is given by

$$\mathbf{F_d} = \mathbf{F_{df}} - \frac{m_f}{m_l}\mathbf{F_{dl}} \tag{6.9}$$

Notice that (6.4) represents the same equations as equations (4.18a)-(4.18c), except that now also the forcing terms are also considered. Using this set of equations, adaptive output feedback tracking controllers were developed in Yan et al. (2000), Wong, Kapila & Sparks (2001) and Wong & Kapila (2003).
The fact that the equations of motion can be stated in the way of (6.4) implies that a lot of the control methods developed for other kind of mechanical agents, e.g. robot manipulators and ocean vehicles, can also be used for formation of satellites.

6.2 Relative Attitude Dynamics and Kinematics

In the following, the relative attitude dynamics and kinematics will be derived, based on Pan & Kapila (2001). Let the reference frames $\mathfrak{F}_l$ and $\mathfrak{F}_f$ be bodyframes of the Leader- and the Follower satellite, respectively. Let $\vec{h}_l$ denote the angular momentum of the Leader spacecraft. The Euler's Second Axioms state that

$$\frac{{}^i\mathrm{d}}{\mathrm{d}t}\vec{h}_l = \vec{m}_l \quad \vec{h}_l = \vec{I}\cdot\vec{\omega_{il}} \tag{6.10}$$

where $\vec{m}_l$ are the moments acting on the body's center of mass, $\vec{\omega}_{il}$ is the angular velocity of frame $\mathfrak{F}_l$ relative to the inertial frame $\mathfrak{F}_i$, and $\vec{I}$ is the inertia dyadic about the body's center of gravity. Using the rule for differentiating of vectors,

$$\frac{{}^i\mathrm{d}}{\mathrm{d}t}(\vec{I}\cdot\vec{\omega_{il}}) = \frac{{}^l\mathrm{d}}{\mathrm{d}t}(\vec{I}\cdot\vec{\omega_{il}}) + \vec{\omega}_{il}\times(\vec{I}\cdot\vec{\omega_{il}}) \tag{6.11}$$

and $\frac{{}^i\mathrm{d}}{\mathrm{d}t}\vec{h}_l = \vec{m}_l$, the rotational motion of the Leader satellite can be written as

$$\vec{I}\cdot\frac{{}^l\mathrm{d}}{\mathrm{d}t}\vec{\omega}_{il} + \vec{\omega}_{il}\times(\vec{I}\cdot\vec{\omega}_{il}) = \vec{m}_l \tag{6.12}$$

It has been used that $\vec{I}$ is constant in $\mathfrak{F}_l$. On coordinate form, the equation becomes

$$\mathbf{I}^l\dot{\boldsymbol{\omega}}^l_{il} + \mathbf{S}(\boldsymbol{\omega}^l_{il})\mathbf{I}^l\boldsymbol{\omega}^l_{il} = \mathbf{m}^l \tag{6.13}$$

The kinematics of the Leader satellite, can according to Egeland & Gravdahl (2002) be described by

$$\dot{\mathbf{q}}_l = \begin{bmatrix} \dot{\eta}_l \\ \dot{\boldsymbol{\varepsilon}}_l \end{bmatrix} = \frac{1}{2}\begin{bmatrix} -\boldsymbol{\varepsilon}_l^T \\ \eta_l\mathbf{I}_{3\times3} + \mathbf{S}(\boldsymbol{\varepsilon}_l) \end{bmatrix}\boldsymbol{\omega}^l_{il} \tag{6.14}$$

The attitude dynamics and kinematics for the Follower satellite are analogously found to be

$$\mathbf{I}^f\dot{\boldsymbol{\omega}}_{if}^f + \mathbf{S}(\boldsymbol{\omega}_{if}^f)\mathbf{I}^f\boldsymbol{\omega}_{if}^f = \mathbf{m}^f \tag{6.15}$$

and

$$\dot{\mathbf{q}}_f = \begin{bmatrix} \dot{\eta}_f \\ \dot{\boldsymbol{\varepsilon}}_f \end{bmatrix} = \frac{1}{2}\begin{bmatrix} -\boldsymbol{\varepsilon}_f^T \\ \eta_l\mathbf{I}_{3\times3} + \mathbf{S}(\boldsymbol{\varepsilon_f}) \end{bmatrix}\boldsymbol{\omega}_{if}^f \tag{6.16}$$

The attitude kinematics of the Follower satellite relative to the Leader satellite can be described by using the quaternion product, see (3.27), as

$$\mathbf{q}_r = \mathbf{q}_l^{-1} \otimes \mathbf{q}_f = \begin{bmatrix} \dot{\eta}_r \\ \dot{\boldsymbol{\varepsilon}}_r \end{bmatrix} = \begin{bmatrix} \eta_l\eta_f + \boldsymbol{\varepsilon}_l^T\boldsymbol{\varepsilon}_f \\ \eta_l\boldsymbol{\varepsilon}_f - \eta_f\boldsymbol{\varepsilon}_l - \mathbf{S}(\boldsymbol{\varepsilon}_l)\boldsymbol{\varepsilon}_f \end{bmatrix} \tag{6.17}$$

The relative angular velocity of the Leader and the Follower is $\vec{\omega}_{lf} = \vec{\omega}_{if} - \vec{\omega}_{il}$, and can be expressed in the Follower reference frame as

$$\boldsymbol{\omega}_{lf}^f = \boldsymbol{\omega}_{if}^f - \mathbf{R}_l^f\boldsymbol{\omega}_{il}^l \tag{6.18}$$

The time derivative will then be

$$\begin{aligned} \dot{\boldsymbol{\omega}}_{lf}^f &= \dot{\boldsymbol{\omega}}_{if}^f - \dot{\mathbf{R}}_l^f\boldsymbol{\omega}_{il}^l - \mathbf{R}_l^f\dot{\boldsymbol{\omega}}_{il}^l \\ &= \dot{\boldsymbol{\omega}}_{if}^f - \mathbf{S}(\boldsymbol{\omega}_{fl}^f)\mathbf{R}_l^f\boldsymbol{\omega}_{il}^l - \mathbf{R}_l^f\dot{\boldsymbol{\omega}}_{il}^l \end{aligned} \tag{6.19}$$

where equation (3.16) has been used. Inserting equation (6.18) for the expression $\mathbf{R}_l^f\boldsymbol{\omega}_{il}^l$, gives

$$\dot{\boldsymbol{\omega}}_{lf}^f = \dot{\boldsymbol{\omega}}_{if}^f - \mathbf{S}(\boldsymbol{\omega}_{fl}^f)(\boldsymbol{\omega}_{if}^f - \boldsymbol{\omega}_{lf}^f) - \mathbf{R}_l^f\dot{\boldsymbol{\omega}}_{il}^l \tag{6.20}$$

By using equation (3.19), that is $\boldsymbol{\omega}_{lf}^f = -\boldsymbol{\omega}_{fl}^f$, and the fact that $\mathbf{S}(\boldsymbol{\omega}_{fl}^f)\boldsymbol{\omega}_{fl}^f = \mathbf{0}$, the time derivative of the angular velocity can be written

$$\begin{aligned} \dot{\boldsymbol{\omega}}_{lf}^f &= \dot{\boldsymbol{\omega}}_{if}^f - \mathbf{S}(\boldsymbol{\omega}_{fl}^f)\boldsymbol{\omega}_{if}^f - \mathbf{R}_l^f\dot{\boldsymbol{\omega}}_{il}^l \\ &= \dot{\boldsymbol{\omega}}_{if}^f - \mathbf{S}(\boldsymbol{\omega}_{if}^f)\boldsymbol{\omega}_{lf}^f - \mathbf{R}_l^f\dot{\boldsymbol{\omega}}_{il}^l \end{aligned} \tag{6.21}$$

Multiplying this equation by the inertia matrix of the Follower spacecraft yields

$$\mathbf{I}^f\dot{\boldsymbol{\omega}}_{lf}^f = \mathbf{I}^f\dot{\boldsymbol{\omega}}_{if}^f - \mathbf{I}^f\mathbf{S}(\boldsymbol{\omega}_{if}^f)\boldsymbol{\omega}_{lf}^f - \mathbf{I}^f\mathbf{R}_l^f\dot{\boldsymbol{\omega}}_{il}^l \tag{6.22}$$

By using (6.13) and (6.15) and (6.18) in the last equation, the following relative attitude dynamics is obtained

$$\begin{aligned} \mathbf{I}^f\dot{\boldsymbol{\omega}}_{lf}^f &= -\mathbf{S}(\boldsymbol{\omega}_{if}^f)\mathbf{I}^f\boldsymbol{\omega}_{if}^f - \mathbf{I}^f\mathbf{S}(\boldsymbol{\omega}_{if}^f)\boldsymbol{\omega}_{lf}^f - \mathbf{I}^f\mathbf{R}_l^f(\mathbf{I}^l)^{-1}(-\mathbf{S}(\boldsymbol{\omega}_{il}^l)\mathbf{I}^l\boldsymbol{\omega}_{il}^l + \mathbf{m}^l) + \mathbf{m}^f \\ &= -\mathbf{S}(\boldsymbol{\omega}_{lf}^f + \mathbf{R}_l^f\boldsymbol{\omega}_{il}^l)\mathbf{I}^f(\boldsymbol{\omega}_{lf}^f + \mathbf{R}_l^f\boldsymbol{\omega}_{il}^l) - \mathbf{I}^f\mathbf{S}(\mathbf{R}_l^f\boldsymbol{\omega}_{il}^l)\boldsymbol{\omega}_{lf}^f \\ &\quad - \mathbf{I}^f\mathbf{R}_l^f(\mathbf{I}^l)^{-1}(-\mathbf{S}(\boldsymbol{\omega}_{il}^l)\mathbf{I}^l\boldsymbol{\omega}_{il}^l + \mathbf{m}^l) + \mathbf{m}^f \end{aligned} \tag{6.23}$$

In addition the Follower spacecraft relative attitude kinematics is given by

$$\dot{\mathbf{q}}_r = \begin{bmatrix} \dot{\eta}_r \\ \dot{\boldsymbol{\varepsilon}}_r \end{bmatrix} = \frac{1}{2}\begin{bmatrix} -\boldsymbol{\varepsilon}_r^T \\ -\eta_r\mathbf{I}_{3\times3} + \mathbf{S}(\boldsymbol{\varepsilon}_r) \end{bmatrix}\boldsymbol{\omega}_{lf}^f \tag{6.24}$$

Next, let $\vec{\omega}_{dl}$ denote the desired angular velocity of the Follower spacecraft relative to the Leader spacecraft. The desired kinematics will then be

$$\dot{\mathbf{q}}_d = \begin{bmatrix} \dot{\eta}_d \\ \dot{\boldsymbol{\varepsilon}}_d \end{bmatrix} = \frac{1}{2}\begin{bmatrix} -\boldsymbol{\varepsilon}_d^T \\ \eta_d\mathbf{I}_{3\times3} + \mathbf{S}(\boldsymbol{\varepsilon}_d) \end{bmatrix}\boldsymbol{\omega}_{dl}^d \tag{6.25}$$

where $\boldsymbol{\omega}_{dl}^d$ denotes the coordinate form of $\vec{\omega}_{dl}$, decomposed in the desired, Follower spacecraft body-fixed reference frame, $\mathfrak{F}_d$. From the above equation it should be noted that

$$\begin{aligned}\boldsymbol{\omega}_{dl}^d &= 2\begin{bmatrix} -\boldsymbol{\varepsilon}_d^T \\ \eta_d\mathbf{I}_{3\times3} + \mathbf{S}(\boldsymbol{\varepsilon}_d)\end{bmatrix}^T \dot{\mathbf{q}}_d \\ &= 2(\eta_d\dot{\boldsymbol{\varepsilon}}_d - \dot{\eta}_d\boldsymbol{\varepsilon}_d - \mathbf{S}(\boldsymbol{\varepsilon}_d)\dot{\boldsymbol{\varepsilon}}_d)\end{aligned} \tag{6.26}$$

and consequently

$$\begin{aligned}\dot{\boldsymbol{\omega}}_{ld}^d &= 2(\dot{\eta}_d\dot{\boldsymbol{\varepsilon}}_d + \eta_d\ddot{\boldsymbol{\varepsilon}}_d - \dot{\eta}_d\dot{\boldsymbol{\varepsilon}}_d - \ddot{\eta}_d\boldsymbol{\varepsilon}_d - \mathbf{S}(\dot{\boldsymbol{\varepsilon}}_d)\dot{\boldsymbol{\varepsilon}}_d - \mathbf{S}(\boldsymbol{\varepsilon}_d)\ddot{\boldsymbol{\varepsilon}}_d) \\ &= 2(\eta_d\ddot{\boldsymbol{\varepsilon}}_d - \ddot{\eta}_d\boldsymbol{\varepsilon}_d - \mathbf{S}(\boldsymbol{\varepsilon}_d)\ddot{\boldsymbol{\varepsilon}}_d)\end{aligned} \tag{6.27}$$

Then, if η_d,$\boldsymbol{\varepsilon}_d$ and their first two time derivative are all bounded functions of time, it follows that $\boldsymbol{\omega}_{ld}^d$ and $\dot{\boldsymbol{\omega}}_{ld}^d$ also will be bounded.
The open loop error dynamics of the attitude motion of the Follower spacecraft relative to the Leader can be found as follows. Let $\tilde{\mathbf{q}}$ denote the unit quaternion characterizing the mismatch between the actual orientation of the Follower spacecraft relative to the Leader spacecraft and the desired orientation of the Follower spacecraft relative to the Leader

$$\tilde{\mathbf{q}} = \mathbf{q}_d^* \otimes \mathbf{q}_r \tag{6.28}$$

Let the angular velocity of the the frame $\mathfrak{F}_f$ relative to $\mathfrak{F}_d$ be defined by $\vec{\omega}_{df} = \vec{\omega}_{if} - \vec{\omega}_{ld}$. Notice also that $\vec{\omega}_{df} = \vec{\omega}_{lf} - \vec{\omega}_{ld}$, which expressed in the Follower spacecraft body-fixed reference frame becomes

$$\boldsymbol{\omega}_{df}^f = \boldsymbol{\omega}_{lf}^f - \mathbf{R}_d^f\boldsymbol{\omega}_{ld}^d \tag{6.29}$$

where $\mathbf{R}_d^f = \mathbf{R}_l^f\mathbf{R}_d^l$. Its time derivative will then be

$$\begin{aligned}\dot{\boldsymbol{\omega}}_{df}^f &= \dot{\boldsymbol{\omega}}_{lf}^f - \dot{\mathbf{R}}_d^f\boldsymbol{\omega}_{ld}^d - \mathbf{R}_d^f\dot{\boldsymbol{\omega}}_{ld}^d \\ &= \dot{\boldsymbol{\omega}}_{lf}^f - \mathbf{S}(\boldsymbol{\omega}_{fd}^f)\mathbf{R}_d^f\boldsymbol{\omega}_{ld}^d - \mathbf{R}_d^f\dot{\boldsymbol{\omega}}_{ld}^d \\ &= \dot{\boldsymbol{\omega}}_{lf}^f + \mathbf{S}(\boldsymbol{\omega}_{df}^f)(\boldsymbol{\omega}_{lf}^f - \boldsymbol{\omega}_{df}^f) - \mathbf{R}_d^f\dot{\boldsymbol{\omega}}_{ld}^d\end{aligned} \tag{6.30}$$

Multiplying this expression with $\mathbf{I}_f^f$ on both sides yields

$$\mathbf{I}_f^f\dot{\boldsymbol{\omega}}_{df}^f = \mathbf{I}_f^f\dot{\boldsymbol{\omega}}_{lf}^f + \mathbf{I}_f^f\mathbf{S}(\boldsymbol{\omega}_{if}^f)(\boldsymbol{\omega}_{lf}^f - \boldsymbol{\omega}_{df}^f) - \mathbf{I}_f^f\mathbf{R}_d^f\dot{\boldsymbol{\omega}}_{ld}^d \tag{6.31}$$

The open-loop tracking error dynamics of the Follower spacecraft relative to the desired attitude reference frame can now be stated

$$\begin{aligned}\mathbf{I}_f^f\dot{\boldsymbol{\omega}}_{df}^f = &-\mathbf{S}(\boldsymbol{\omega}_{lf}^f + \mathbf{R}_l^f\boldsymbol{\omega}_{il}^l)\mathbf{I}^f(\boldsymbol{\omega}_{lf}^f + \mathbf{R}_l^f\boldsymbol{\omega}_{il}^l) - \mathbf{I}^f\mathbf{S}(\mathbf{R}_l^f\boldsymbol{\omega}_{il}^l)\boldsymbol{\omega}_{lf}^f \\ &- \mathbf{I}^f\mathbf{R}_l^f(\mathbf{I}^l)^{-1}(-\mathbf{S}(\boldsymbol{\omega}_{il}^l)\mathbf{I}^l\boldsymbol{\omega}_{il}^l + \mathbf{m}^l) + \mathbf{m}^f \\ &+ \mathbf{I}_f^f\mathbf{S}(\boldsymbol{\omega}_{if}^f)(\boldsymbol{\omega}_{lf}^f - \boldsymbol{\omega}_{df}^f) - \mathbf{I}_f^f\mathbf{R}_d^f\dot{\boldsymbol{\omega}}_{ld}^d\end{aligned} \tag{6.32}$$

using (6.23) and, which by using (6.29) and (6.18), can be written

$$\begin{aligned}\mathbf{I}_f^f\dot{\boldsymbol{\omega}}_{df}^f = &-\mathbf{S}(\boldsymbol{\omega}_{df}^f + \mathbf{R}_d^f\boldsymbol{\omega}_{lf}^d + \mathbf{R}_l^f\boldsymbol{\omega}_{il}^l)\mathbf{I}_f^f(\boldsymbol{\omega}_{df}^f + \mathbf{R}_d^f\boldsymbol{\omega}_{lf}^d + \mathbf{R}_l^f\boldsymbol{\omega}_{il}^l) \\ &- \mathbf{I}_f^f\mathbf{S}(\mathbf{R}_l^f\boldsymbol{\omega}_{il}^l)(\boldsymbol{\omega}_{df}^f + \mathbf{R}_d^f\boldsymbol{\omega}_{ld}^d) \\ &- \mathbf{I}_f^f\mathbf{R}_l^f(\mathbf{I}_l^l)^{-1}(-\mathbf{S}(\boldsymbol{\omega}_{il}^l)\mathbf{I}_l^l\boldsymbol{\omega}_{il}^l + \mathbf{m}_l^l) + \mathbf{m}_f^f \\ &+ \mathbf{I}_f^f\mathbf{S}(\boldsymbol{\omega}_{df}^f + \mathbf{R}_d^f\boldsymbol{\omega}_{ld}^d + \mathbf{R}_l^f\boldsymbol{\omega}_{il}^l) - \mathbf{I}_f^f\mathbf{R}_d^f\dot{\boldsymbol{\omega}}_{ld}^d\end{aligned} \tag{6.33}$$

The open loop tracking error kinematics is given by

$$\dot{\mathbf{q}}_e = \begin{bmatrix} \dot{\eta}_e \\ \dot{\boldsymbol{\varepsilon}}_e \end{bmatrix} = \frac{1}{2} \begin{bmatrix} -\boldsymbol{\varepsilon}_e^T \\ -\eta_e \mathbf{I}_{3\times3} + \mathbf{S}(\boldsymbol{\varepsilon}_e) \end{bmatrix} \boldsymbol{\omega}_{df}^f \tag{6.34}$$

Finally, the tracking control objective can then be stated as

$$\lim_{t\to\infty} \boldsymbol{\varepsilon}_e, \boldsymbol{\omega}_{df}^f = \mathbf{0} \tag{6.35}$$

Chapter 7

Modeling: Rigid Body

In this chapter the satellites will be modeled using the vectorial rigid body differential equations. These equations are well known from the robotics and from the modeling of ocean vehicles.

7.1 Kinematics

The kinematics is given by the quaternion differential equations of section 3.4 and restated here as

$$\dot{\mathbf{q}} = \mathbf{T}(\mathbf{q})\boldsymbol{\omega}_{ib}^{b} \tag{7.1}$$

where

$$\mathbf{T}(\mathbf{q}) = \frac{1}{2}\begin{bmatrix} -\varepsilon_1 & -\varepsilon_2 & -\varepsilon_3 \\ \eta & -\varepsilon_3 & \varepsilon_2 \\ \varepsilon_3 & \eta & -\varepsilon_1 \\ -\varepsilon_2 & \varepsilon_1 & \eta \end{bmatrix} \tag{7.2}$$

7.2 Dynamics

The rigid-body dynamics of a satellite can be expressed in several different ways, as shown in Ploen, Hadaegh & Scharf (2004). The equations given here, is a representation of the equations of motion of a rigid body about an arbitrary point fixed to the body in terms of body-fixed rates of change. It is the same representation as given in Fossen (2002). The translational motion is given by

$$m[\dot{\mathbf{v}}_o^b + \dot{\boldsymbol{\omega}}_{ib}^b \times \mathbf{r}_g^b + \boldsymbol{\omega}_{ib}^b \times \mathbf{v}_o^b + \boldsymbol{\omega}_{ib}^b \times (\boldsymbol{\omega}_{ib}^b \times \mathbf{r}_g^b)] = \mathbf{f}_o^b \tag{7.3}$$

whereas the rotational motion is given by

$$\mathbf{I}_o^b\dot{\boldsymbol{\omega}}_{ib}^b + \boldsymbol{\omega}_{ib}^b + m\mathbf{r}_g^b \times (\dot{\mathbf{v}}_o^b + \boldsymbol{\omega}_{ib}^b \times \mathbf{v}_o^b) = \mathbf{m}_o^b \tag{7.4}$$

where

$\mathbf{v}_o^b$	$=$	$[X\,Y\,Z]^T$	-force decomposed in $\mathfrak{F}_b$-frame
$\mathbf{m}_o^b$	$=$	$[K\,M\,N]^T$	-moment decomposed in $\mathfrak{F}_b$-frame
$\mathbf{v}_o^b$	$=$	$[u\,v\,w]^T$	-linear velocity decomposed in $\mathfrak{F}_b$-frame
$\boldsymbol{\omega}_{ib}^b$	$=$	$[p\,q\,r]^T$	-angular velocity of the $\mathfrak{F}_b$-frame relative to the $\mathfrak{F}_i$-frame
$\mathbf{r}_c^b$	$=$	$[x_c\,y_c\,z_c]^T$	-vector from a point P to CG decomposed in the $\mathfrak{F}_b$-frame

By letting the origin of the body-fixed coordinate system coincide with the center of gravity, CG, $\mathbf{r}_g^b = [0\,0\,0]^T$, these expressions reduces to

$$m(\dot{\mathbf{v}}_c^b + \mathbf{S}(\boldsymbol{\omega}_{ib}^b)\mathbf{v}_{\mathbf{c}}^{\mathbf{b}}) = \mathbf{f}_c^b \tag{7.5}$$

for the translational motion and to

$$\mathbf{I}_c^b \dot{\boldsymbol{\omega}}_{ib}^b + \mathbf{S}(\boldsymbol{\omega}_{ib}^b)\mathbf{I}_c^b \boldsymbol{\omega}_{ib}^b = \mathbf{m}_c^b \tag{7.6}$$

for the rotational dynamics. As shown in Fossen (2002) the rigid-body dynamics can be expressed in a vectorial setting as

$$\mathbf{M}\dot{\boldsymbol{\nu}} + \mathbf{C}(\boldsymbol{\nu})\boldsymbol{\nu} = \boldsymbol{\tau} \tag{7.7}$$

with $\boldsymbol{\nu} = [(\mathbf{v}_c^b)^T \quad (\boldsymbol{\omega}_{ib}^b)^T]^T$ being the generalized velocity vector and $\boldsymbol{\tau} = [(\mathbf{f}_c^b)^T \quad (\mathbf{m}_c^b)^T]^T$ being the generalized vector of external forces and moments, all decomposed in $\mathfrak{F}_b$. Notice that $\mathbf{M}$ and $\mathbf{C}$ have the following advantageous properties:

Property 7.1. (Rigid-Body System Inertia Matrix M)
The representation of the system inertia matrix $\mathbf{M}$ *is unique and satisfies:*

$$\mathbf{M} = \mathbf{M}^T > 0, \quad \dot{\mathbf{M}} = \mathbf{0}_{6\times 6}$$

Property 7.2. (Rigid-Body Coriolis and Centripetal Matrix C)
The rigid-body Coriolis and centripetal matrix $\mathbf{C}(\boldsymbol{\nu})$ *can always be represented such that* $\mathbf{C}(\boldsymbol{\nu})$ *is skew-symmetric-i.e.:*

$$\mathbf{C}(\boldsymbol{\nu}) = -\mathbf{C}^T(\boldsymbol{\nu}), \quad \forall \boldsymbol{\nu} \epsilon \mathbb{R}^6$$

The proofs can be found in Sagatun & Fossen (1991). These properties are valid for an arbitrary choice of origin, and an example of such a skew-symmetric representation of the rigid-body Coriolis and centripetal matrix, is

$$\mathbf{C}(\boldsymbol{\nu}) = \begin{bmatrix} \mathbf{0}_{3\times 3} & -m\mathbf{S}(\boldsymbol{\nu}_1) - m\mathbf{S}(\mathbf{S}(\boldsymbol{\nu}_2)\mathbf{r}_g^b) \\ -m\mathbf{S}(\boldsymbol{\nu}_1) - m\mathbf{S}(\mathbf{S}(\boldsymbol{\nu}_2)\mathbf{r}_g^b) & m\mathbf{S}(\mathbf{S}(\boldsymbol{\nu}_1)\mathbf{r}_g^b) - \mathbf{S}(\mathbf{I}_o^b\boldsymbol{\nu}_2) \end{bmatrix} \tag{7.8}$$

where $\boldsymbol{\nu}_1 = [u, v, w]^T$ and $\boldsymbol{\nu}_2 = [p, q, r]^T$. By letting the origin coincide with the center of gravity, this representations simplifies to

$$\mathbf{C}(\boldsymbol{\nu}) = \begin{bmatrix} \mathbf{0}_{3\times 3} & -m\mathbf{S}(\boldsymbol{\nu}_1) \\ -m\mathbf{S}(\boldsymbol{\nu}_1) & -\mathbf{S}(\mathbf{I}_c^b\boldsymbol{\nu}_2) \end{bmatrix} \tag{7.9}$$

Other useful skew-symmetric representations can be found in Fossen & Fjellstad (1995). Another important property is

Property 7.3. (Linearity of C in its Argument)
The rigid-body Coriolis and centripetal matrix is linear in its argument, i.e.:

$$\mathbf{C}(\alpha_1\mathbf{a} + \alpha_2\mathbf{b}) = \alpha_1\mathbf{C}(\mathbf{a}) + \alpha_2\mathbf{C}(\mathbf{b})$$

Now the total 6 DOF model can be stated

$$\dot{\boldsymbol{\eta}} = \mathbf{J}(\mathbf{q})\boldsymbol{\nu} \tag{7.10a}$$

$$\mathbf{M}\dot{\boldsymbol{\nu}} + \mathbf{C}(\boldsymbol{\nu})\boldsymbol{\nu} + \mathbf{D}(\boldsymbol{\nu})\boldsymbol{\nu} + \mathbf{g}(\mathbf{q}) = \boldsymbol{\tau} \tag{7.10b}$$

with $\boldsymbol{\eta} = [(\mathbf{p}^i)^T \quad \mathbf{q}^T]^T$,

$$\mathbf{J}(\mathbf{q}) = \begin{pmatrix} \mathbf{R}_b^i & \mathbf{0}_{3\times 3} \\ \mathbf{0}_{4\times 3} & \mathbf{T}(\mathbf{q}) \end{pmatrix} \tag{7.11}$$

The aerodynamic damping matrix $\mathbf{D}$ can be defined, using a similar notation as for the hydrodynamic damping matrix for ocean vehicles, see Fossen (2002), as

$$\mathbf{D}(\boldsymbol{\nu}) = \begin{pmatrix} \boldsymbol{\nu}^T\mathbf{D}_1\boldsymbol{\nu} \\ \boldsymbol{\nu}^T\mathbf{D}_2\boldsymbol{\nu} \\ \boldsymbol{\nu}^T\mathbf{D}_3\boldsymbol{\nu} \\ \boldsymbol{\nu}^T\mathbf{D}_4\boldsymbol{\nu} \\ \boldsymbol{\nu}^T\mathbf{D}_5\boldsymbol{\nu} \\ \boldsymbol{\nu}^T\mathbf{D}_6\boldsymbol{\nu} \end{pmatrix} \tag{7.12}$$

Here, $\mathbf{D}_i$ are 6×6 matrices that depend on the atmospheric density ρ_a, the drag coefficient C_d and the area projected A, see section 5.3. Aerodynamic damping satisfy the following important property:

Property 7.4. (Aerodynamic Damping Matrix $\mathbf{D}(\boldsymbol{\nu})$)
For a rigid-body moving through the atmosphere, the aerodynamic damping matrix will be real and strictly positive, i.e.

$$\mathbf{D}(\boldsymbol{\nu}) > 0, \forall \boldsymbol{\nu} \epsilon \mathbb{R}^6$$

The gravity vector $\mathbf{g}$ is defined as

$$\mathbf{g} = \begin{bmatrix} \mathbf{f}_g^b \\ \mathbf{m}_g^b \end{bmatrix} \tag{7.13}$$

where $\mathbf{f}_g$ and $\mathbf{m}_g$ are defined in section 5.1 and 5.2, respectively.

7.3 Gyrostat Dynamics

The dynamics of the gyrostat has been derived using Hughes (1986), Tsiostras, Shen & Hall (2001) and in particular Goeree & Chatel (1999). The total angular momentum of a gyrostat about CG, $\mathbf{h}_c^i$, is the sum of the angular momentum of the core and the angular momentum of the reaction wheels

$$\mathbf{h}_c^i = \mathbf{R}_b^i[\mathbf{I}_c\boldsymbol{\omega}_{ib}^b + \mathbf{h}_w^b] \tag{7.14}$$

where $\mathbf{I}_c$ is total moment of inertia of the satellite, $\mathbf{h}_w^b$ is the angular momentum of the reaction wheels and $\boldsymbol{\omega}_{ib}^b$ is the angular velocity of the body frame $\mathfrak{F}_b$, relative to the inertial frame $\mathfrak{F}_i$, expressed in body frame coordinates. Let $I_{w,k}$ be moment of inertia about the spin axis $\mathbf{t}_k^b$ of reaction wheel k, and $\Omega_k + (\mathbf{t}_k^b)^T\boldsymbol{\omega}_{ib}^b$ the total angular velocity. Then the angular momentum of reaction wheel k can be written as

$$\mathbf{h}_{w,k}^b = [\mathbf{t}_k I_k(\Omega_k + \mathbf{t}_k^T\boldsymbol{\omega}_{ib}^b)] \tag{7.15}$$

The total angular momentum of the reaction wheels is the sum of the individual momentums, and can be expressed in matrix form as

$$\mathbf{h}_w^b = \mathbf{T}_w\mathbf{I}_w(\boldsymbol{\Omega} + \mathbf{T}_w^T\boldsymbol{\omega}_{ib}^b) \tag{7.16}$$

where the following vector and matrices have been defined

$$\boldsymbol{\Omega} = [\Omega_1\,\Omega_2\,\Omega_3\,\Omega_4]^T \tag{7.17}$$
$$\mathbf{I}_w = I_w\mathbf{1}_{4\times 4} \tag{7.18}$$
$$\mathbf{T}_w = [\mathbf{t}_1\,\mathbf{t}_2\,\mathbf{t}_3\,\mathbf{t}_4] \tag{7.19}$$

Type	Thrust Range (mN)	Specific Impulse (sec)	Thruster Efficiency (%)	Thrust Duration	Typical Propellants	Kinetic Power per Unit Thrust (W/mN)
Resistojet	200-300	200-350	65-90	Months	NH_3, N_2H_4, H_2	0.5-6
Arcjet	200-1000	400-1000	30-50	Months	H_2, N_2, N_2H_4, NH_3	2-3
Ion engine	0.01-200	1500-5000	60-80	Months	Xe, Kr, Ar	10-70
PPT[1]	0.05-10	600-2000	10	Years	Teflon	10-50
MPD[2]	0.001-2000	2000-5000	30-50	Weeks	Ar, Xe, H_2, Li	100
Hall thruster	0.01-2000	1500-2000	30-50	Months	Xe, Ar	100

Table 7.1: Typical performance parameters for electrical propulsion systems

Euler's second axiom states that

$$\dot{\mathbf{h}}_c^i = \mathbf{m}_c^i \tag{7.20}$$

such that the moment exerted from the reaction wheels becomes

$$\begin{aligned} \mathbf{m}_w^b &= \mathbf{S}(\boldsymbol{\omega}_{ib}^b)\mathbf{h}_w^b + \dot{\mathbf{h}}_w^b \\ &= [\mathbf{S}(\boldsymbol{\omega}_{ib}^b)(\mathbf{T}_w\mathbf{I}_w(\boldsymbol{\Omega} + \mathbf{T}_w^T\boldsymbol{\omega}_{ib}^b)) + \mathbf{T}_w\mathbf{I}_w(\dot{\boldsymbol{\Omega}} + \mathbf{T}_w^T\dot{\boldsymbol{\omega}}_{ib}^b)] \end{aligned} \tag{7.21}$$

where $\dot{\mathbf{R}}_b^i = \mathbf{R}_b^i\mathbf{S}(\boldsymbol{\omega}_{ib}^b)$ has been used. Due to the principle of conservation of energy, the torque rotating the reaction wheels will produce a torque of the same magnitude on the satellite, but in the opposite direction.

7.4 Propulsion system

Electric propulsion systems will be used for orbital control of the satellites. According to Sutton & Biblarz (2001) it is common to distinguish between these three fundamental types

1. *Electrothermal.* Propellant is heated electrically and expanded thermodynamically; ie., the gas is accelerated to supersonic speeds through a nozzle, and in the chemical rocket.

2. *Electrostatic.* Acceleration is achieved by the interaction of electrostatic fields on non-neutral or charged propellant particles such as atomic ions, droplets, or colloids.

3. *Electromagnetic.* Acceleration is achieved by the interaction of electric and magnetic fields within a plasma. Moderately dense plasmas are high-temperature or nonequilibrium gases, electrically neutral and reasonably good conductors of electricity.

Table 7.4 from Sutton & Biblarz (2001) shows the typical performance parameters of various types of electrical propulsion systems.

[1] Solid pulsed plasma
[2] Magnetoplasma dynamic

Chapter 8

Controllers and Observers

Throughout the literature, the research done on the Hill-Clohessy-Wiltshire equations is quite extensive. Therefore, no controller or observer will be designed here, based on those equations. Instead the reader is referred to Scharf et al. (2004) to get a overview over the work already done.
In this chapter a state feedback linearizing controller and a passivity based controller for the relative position case are derived. The passivity based controller is then extended to also incorporate an observer.
At last a controller and an observer for the synchronization of two satellites modeled as rigid bodies are proposed.

8.1 Relative Position Control by State Feedback Linearization

In this section a state feedback linearizing controller will be derived, based on the model of section 6.1. Of simplicity reasons, let the Leader satellite and the Follower satellite have the same attitude, i.e. the components $u_{l,x}, u_{l,y}, u_{l,z}$ and $u_{f,x}, u_{f,y}, u_{f,z}$ of the control-forces $\mathbf{u_l}$ and $\mathbf{u_f}$ are assumed to work in the radial, velocity and out-of-plane direction, respectively. The disturbance forces are not taken into account, neither is the control forces from the Leader satellite. Now, using

$$\boldsymbol{\rho} = \begin{bmatrix} x_1 \\ x_3 \\ x_5 \end{bmatrix}, \dot{\boldsymbol{\rho}} \begin{bmatrix} x_2 \\ x_4 \\ x_5 \end{bmatrix} \tag{8.1}$$

the system can be written on state-space form as

$$\dot{\mathbf{x}} = \mathbf{f}(\mathbf{x}) + \sum_{i=1}^{m} \mathbf{g}_i(\mathbf{x}) u_i = \mathbf{f}(\mathbf{x}) + G(\mathbf{x})\mathbf{u} \tag{8.2}$$

$$y_i = h_i(\mathbf{x}) \tag{8.3}$$

which in this case will be

$$\dot{\mathbf{x}} = \begin{bmatrix} x_2 \\ \frac{1}{m_f}\left(2\dot{\nu}x_4 - \mu(\frac{r_l + x_1}{{r_f}^3} - \frac{1}{{r_l}^2}) + (\dot{\nu}^2 x_1 + \ddot{\nu}x_3)\right) \\ x_4 \\ \frac{1}{m_f}\left(-2\dot{\nu}x_2 - \mu(\frac{x_3}{{r_f}^3}) - (\dot{\nu}^2 x_3 - \ddot{\nu}x_1)\right) \\ x_6 \\ \frac{1}{m_f}\left(-\mu\frac{x_5}{{r_f}^3}\right) \end{bmatrix} + \begin{bmatrix} 0 \\ \frac{1}{m_f} \\ 0 \\ 0 \\ 0 \\ 0 \end{bmatrix} u_x + \begin{bmatrix} 0 \\ 0 \\ 0 \\ \frac{1}{m_f} \\ 0 \\ 0 \end{bmatrix} u_y + \begin{bmatrix} 0 \\ 0 \\ 0 \\ 0 \\ 0 \\ \frac{1}{m_f} \end{bmatrix} u_z \tag{8.4}$$

and

$$\mathbf{y} = \mathbf{x} \tag{8.5}$$

where it is assumed that all states can be measured, i.e. the relative distance and velocity between the Leader and the Follower satellite can be measured, and decomposed in the x-,y- and z-direction. By differentiating the output until the input appears explicit, the following equation is attained

$$\begin{bmatrix} \overset{(r_1)}{y_1} \\ \vdots \\ \overset{(r_m)}{y_m} \end{bmatrix} = \begin{bmatrix} L_f^{r_1} h_1(\mathbf{x}) \\ \vdots \\ L_f^{r_m} h_m(\mathbf{x}) \end{bmatrix} + \begin{bmatrix} L_{g_1} L_f^{r_1-1} h_1(\mathbf{x}) & \cdots & L_{g_m} L_f^{r_1-1} h_1(\mathbf{x}) \\ \vdots & \ddots & \vdots \\ L_{g_1} L_f^{r_m-1} h_m(\mathbf{x}) & \cdots & L_{g_m} L_f^{r_m-1} h_m(\mathbf{x}) \end{bmatrix} \begin{bmatrix} u_1 \\ \vdots \\ u_m \end{bmatrix} \tag{8.6}$$

With the output

$$\mathbf{y} = \begin{bmatrix} x_1 \\ x_3 \\ x_5 \end{bmatrix} \tag{8.7}$$

the first vector on the right side will be

$$\alpha(\mathbf{x}) = \begin{bmatrix} \frac{1}{m_f}\left(2\dot{\nu}x_4 - \mu(\frac{r_l + x_1}{{r_f}^3} - \frac{1}{{r_l}^2}) + (\dot{\nu}^2 x_1 + \ddot{\nu}x_3)\right) \\ \frac{1}{m_f}\left(-2\dot{\nu}x_2 - \mu(\frac{x_3}{{r_f}^3}) - (\dot{\nu}^2 x_3 - \ddot{\nu}x_1)\right) \\ \frac{1}{m_f}\left(-\mu\frac{x_5}{{r_f}^3}\right) \end{bmatrix} \tag{8.8}$$

where as the matrix becomes

$$\beta(\mathbf{x}) = \begin{bmatrix} \frac{1}{m_f} & 0 & 0 \\ 0 & \frac{1}{m_f} & 0 \\ 0 & 0 & \frac{1}{m_f} \end{bmatrix} \tag{8.9}$$

Since the total relative degree, with the output stated above is

$$\sum_{i=1}^{m} r_i = n \tag{8.10}$$

the nonlinear system (8.3) is transformable into a linear controllable system in Brunovsky controller form, by a nonsingular state feedback transformation, which consists of a nonsingular state feedback

$$\mathbf{u} = \{\beta(\mathbf{x})\}^{-1}[-\alpha(\mathbf{x}) + \mathbf{v}] \tag{8.11}$$

and a diffeomorphism

$$\mathbf{z} = T(\mathbf{x}) \tag{8.12}$$

The new input $\mathbf{v}$ is chosen such that

$$\lim_{t\to\infty} \mathbf{y}(t) \overset{!}{=} \mathbf{y_r}(t) \tag{8.13}$$

where $\mathbf{y_r}$ is the reference-trajectory, or with error $\mathbf{e}(t) = \mathbf{y}(t) - \mathbf{y_r}(t)$, the elements of $\mathbf{e}$ must satisfy

$$\overset{(r)}{e} + p_{r-1}\overset{(r-1)}{e} + \cdots + p_1\dot{e} + p_0 \overset{!}{=} 0 \tag{8.14}$$

Here, p_i are chosen from poleplacement, and must satisfy

$$\lambda^n + p_{n-1}\lambda^{n-1} + \cdots + p_1\lambda + p_0 \overset{!}{=} \prod_{i=1}^{n}(\lambda - \lambda_i) \tag{8.15}$$

Theorem 8.1. *The state feedback linearizing tracking controller*

$$\mathbf{u} = \{\beta(\mathbf{x})\}^{-1}[-\alpha(\mathbf{x}) + \mathbf{v}]$$

with $\mathbf{v}$, α *and* $\beta((x))$ *as given above, is globally exponentially stable.*

Proof. Since all nonlinearities are canceled out and the poles of the linear system are placed in the left half plane, globally exponentially stability follows. □

For an analytical proof of this kind of multiple input, multiple output linearizing controller, see Isidori (1995)

8.2 Relative Position Control Based on the Passivity Concept

In the following a controller for the model of section 6.1 will be derived, based on the Lyapunov concept. Notice that equation (6.4) is quite similar to the nonlinear dynamic equation for a multiple-link robot. Passivity result for such a robot is presented in Berghuis (1993), and is attained for a satellite in formation in a similar way here. The matrix $\mathbf{C}$ is skew-symmetric and obviously is also $\dot{\mathbf{M}} - \mathbf{C}$ skew-symmetric, since here $\mathbf{M}$ is assumed to be constant. Let $\dot{\boldsymbol{\rho}}_r \equiv \dot{\boldsymbol{\rho}}_d - \boldsymbol{\Lambda}\mathbf{e}$, where $\boldsymbol{\rho}_d$ is the desired reference trajectory, $\mathbf{e} \equiv \boldsymbol{\rho} - \boldsymbol{\rho}_d$ is the position error, and $\boldsymbol{\Lambda}$ is a symmetric, positive definite matrix. Define

$$\mathbf{s} \equiv \dot{\boldsymbol{\rho}} - \dot{\boldsymbol{\rho}}_r = \dot{\mathbf{e}} + \boldsymbol{\Lambda}\mathbf{e} \tag{8.16}$$

a so-called sliding variable. Let the control law be

$$\mathbf{u}_f = \mathbf{M}\ddot{\boldsymbol{\rho}}_r + \mathbf{C}\dot{\boldsymbol{\rho}}_r + \mathbf{n} - \mathbf{K}_p\mathbf{e} + \mathbf{v} \tag{8.17a}$$

$$\mathbf{v} = -\mathbf{K}_d\mathbf{s} \tag{8.17b}$$

where $\mathbf{K}_p$ and $\mathbf{K}_d$ are positive definite symmetric matrices. By inserting $\mathbf{u}_f$ into (6.4) the following equation is attained

$$\mathbf{M}\dot{\mathbf{s}} + \mathbf{C}\mathbf{s} + \mathbf{K}_p\mathbf{e} + \mathbf{K}_d\mathbf{s} = \mathbf{0} \tag{8.18}$$

Here, $\mathbf{F}_d$ and $\mathbf{u}_f$ in (6.4), are not taken into consideration.

Theorem 8.2. *The tracking controller*

$$\begin{aligned}
\mathbf{u}_f &= \mathbf{M}\ddot{\boldsymbol{\rho}}_r + \mathbf{C}\dot{\boldsymbol{\rho}}_r + \mathbf{n} - \mathbf{K}_p\mathbf{e} - \mathbf{K}_d\mathbf{s} \\
\dot{\boldsymbol{\rho}}_r &= \dot{\boldsymbol{\rho}}_d - \boldsymbol{\Lambda}\mathbf{e} \\
\mathbf{e} &= \boldsymbol{\rho} - \boldsymbol{\rho}_d \\
\mathbf{s} &= \dot{\boldsymbol{\rho}} - \dot{\boldsymbol{\rho}}_r
\end{aligned}$$

with $\mathbf{K}_p$,$\mathbf{K}_d$ *and* $\boldsymbol{\Lambda}$ *being symmetric, positive definite matrices, is globally exponentially stable.*

Proof. As storage function candidate

$$V = \frac{1}{2}\mathbf{s}^T\mathbf{M}\mathbf{s} + \frac{1}{2}\mathbf{e}^{\mathbf{T}}\mathbf{K}_p\mathbf{e} \tag{8.19}$$

is chosen, which formally defines a Lyapunov function candidate. Besides being positive definite, it is radially unbounded, and its derivative satisfies

$$
\begin{aligned}
\dot{V} &= \mathbf{s}^T\mathbf{M}\dot{\mathbf{s}} + \dot{\mathbf{e}}^T\mathbf{K}_p\mathbf{e} \\
&= \mathbf{s}^{\mathbf{T}}(-\mathbf{C}\mathbf{s} - \mathbf{K}_p\mathbf{e} - \mathbf{K}_d\mathbf{s}) + \dot{\mathbf{e}}^T\mathbf{K}_p\mathbf{e} \\
&= -\mathbf{s}^T\mathbf{K}_d\mathbf{s} - (\mathbf{s} - \dot{\mathbf{e}})^T\mathbf{K}_p\mathbf{e} \\
&= -\mathbf{s}^T\mathbf{K}_d\mathbf{s} - (\dot{\mathbf{e}} + \mathbf{\Lambda}\mathbf{e} - \dot{\mathbf{e}})^T\mathbf{K}_p\mathbf{e} \\
&= -\mathbf{s}^T\mathbf{K}_d\mathbf{s} - \mathbf{e}^T\mathbf{\Lambda}\mathbf{K}_p\mathbf{e}
\end{aligned}
\tag{8.20}
$$

Hence the system is passive with input $\mathbf{v} = -\mathbf{K}_d\mathbf{s}$ and output $\mathbf{s}$, with V as the storage function. From Lyapunov's direct method, the closed-loop system is globally exponentially stable. □

8.3 Relative Position Control by Combined Controller-Observer Design

In the case where only position measurements are available, an observer has to be designed to give the appropriate estimates of the velocity. According to Berghuis & Nijmeijer (1993) a combined controller-observer design has the advantage of a simpler structure, compared to that of separate controller and observer design. As seen in section 8.2, $\ddot{\boldsymbol{\rho}}$ cannot be realized without velocity measurement. Therefore, following the steps of Berghuis & Nijmeijer (1993), the vector $\dot{\boldsymbol{\rho}}_r$ from that section is redefined to be

$$\dot{\boldsymbol{\rho}}_r \equiv \dot{\boldsymbol{\rho}}_d - \mathbf{\Lambda}_1(\hat{\boldsymbol{\rho}} - \boldsymbol{\rho}_d) \tag{8.21}$$

where $\mathbf{\Lambda}_1$ is symmetric and positive definite. Consequently

$$\mathbf{s}_1 = \dot{\boldsymbol{\rho}} - \dot{\boldsymbol{\rho}}_r \equiv \dot{\mathbf{e}} + \mathbf{\Lambda}_1(\mathbf{e} - \tilde{\boldsymbol{\rho}}) \tag{8.22}$$

Furthermore, define

$$\dot{\boldsymbol{\rho}}_0 \equiv \dot{\hat{\boldsymbol{\rho}}} - \mathbf{\Lambda}_2\tilde{\boldsymbol{\rho}} \tag{8.23}$$

where $\mathbf{\Lambda}_2$ is diagonal and positive definite. In addition, let

$$\mathbf{s}_2 = \dot{\boldsymbol{\rho}} - \dot{\boldsymbol{\rho}}_0 \equiv \dot{\tilde{\boldsymbol{\rho}}} + \mathbf{\Lambda}_2\tilde{\boldsymbol{\rho}} \tag{8.24}$$

The control law is chosen as

$$\mathbf{u}_f = \mathbf{M}\ddot{\boldsymbol{\rho}}_r + \mathbf{C}\dot{\boldsymbol{\rho}}_r + \mathbf{n} - \mathbf{K}_d(\mathbf{s}_1 - \mathbf{s}_2) - \mathbf{K}_p\mathbf{e} \tag{8.25}$$

where $\mathbf{K}_p$ and $\mathbf{K}_d$ are symmetric, positive definite matrices, and $\mathbf{s}_1 - \mathbf{s}_2$ is found to be

$$\mathbf{s}_1 - \mathbf{s}_2 = (\dot{\hat{\boldsymbol{\rho}}} - \dot{\boldsymbol{\rho}}_d) + \mathbf{\Lambda}_1(\mathbf{e} - \tilde{\boldsymbol{\rho}}) - \mathbf{\Lambda}_2\tilde{\boldsymbol{\rho}} \tag{8.26}$$

from combining equation (8.22) and (8.24). The reason for introducing $\mathbf{s}_2$ in the first place is that $\mathbf{s}_1$ cannot be realized, whereas the difference $\mathbf{s}_1 - \mathbf{s}_2$ is a function of known signals. By combining equation (6.4) and (8.25), the tracking error dynamics becomes

$$\mathbf{M}\dot{\mathbf{s}}_1 + \mathbf{C}\mathbf{s}_1 = -\mathbf{K}_d(\mathbf{s}_1 - \mathbf{s}_2) - \mathbf{K}_p\mathbf{e} \tag{8.27}$$

As in section 8.2, $\mathbf{F}_d$ and $\mathbf{u}_f$ in (6.4), are not taken into consideration. The observer is chosen as

$$\dot{\hat{\boldsymbol{\rho}}} = \mathbf{z} + \mathbf{L}_d\tilde{\boldsymbol{\rho}} \tag{8.28a}$$

$$\dot{\mathbf{z}} = \ddot{\boldsymbol{\rho}}_r + \mathbf{M}^{-1}(\mathbf{L}_{p1}\tilde{\boldsymbol{\rho}} - \mathbf{K}_p\mathbf{e}) + \mathbf{L}_{p2}\tilde{\boldsymbol{\rho}} \tag{8.28b}$$

with $\mathbf{L}_d$, $\mathbf{L}_{p1}$ and $\mathbf{L}_{p2}$ are constant, diagonal and positive definite matrices. Furthermore, $\mathbf{L}_d$ and $\mathbf{L}_{p2}$ are chosen to be

$$\mathbf{L}_d = l_d \mathbf{1}_{3\times3} + \mathbf{\Lambda}_2 \tag{8.29a}$$

$$\mathbf{L}_{p2} = l_d \mathbf{\Lambda}_2 \tag{8.29b}$$

where $l_d > 0$. Inserting equation (8.28a) into (8.28b) and using (8.22) and (8.24) gives the observer error dynamics

$$\mathbf{M}(\dot{\mathbf{s}}_2 + l_d \mathbf{s}_2) + \mathbf{L}_{p1}\tilde{\boldsymbol{\rho}} = \mathbf{M}\dot{\boldsymbol{s}}_1 + \mathbf{K}_p \mathbf{e} \tag{8.30}$$

By inserting the tracking error dynamics, i.e. equation (8.27), the observer error dynamics can be rewritten as

$$\mathbf{M}\dot{\mathbf{s}}_2 + \mathbf{C}\mathbf{s}_2 + (l_d\mathbf{M} - \mathbf{K}_d)\mathbf{s}_2 + \mathbf{L}_{p1}\tilde{\boldsymbol{\rho}} = -\mathbf{K}_d\mathbf{s}_1 + \mathbf{C}(\mathbf{s}_2 - \mathbf{s}_1) \tag{8.31}$$

In the robotics, the matrix $\mathbf{C}$ can be represented in terms of the Cristoffel symbols. This is not the case here, and the stability analysis will be slightly different. First, assume the following:

Assumption 8.1
The matrix $\mathbf{C}(\dot{\nu}, m_f)$ is bounded with respect to $\dot{\nu}$ and m_f, so

$$\mathbf{C}_m \leq \|\mathbf{C}(\dot{\nu}, m_f)\| \leq \mathbf{C}_M \tag{8.32}$$

This is a fair assumption since the physical values of m_f and $\dot{\nu}$ are obviously bounded. Let a storage function candidate be given as

$$V = \frac{1}{2}\mathbf{s}_1^T\mathbf{M}\mathbf{s}_1 + \frac{1}{2}\mathbf{e}^T\mathbf{K}_p\mathbf{e} + \frac{1}{2}\mathbf{s}_2^T\mathbf{M}\mathbf{s}_2^T + \frac{1}{2}\tilde{\boldsymbol{\rho}}^T\mathbf{L}_{p1}\tilde{\boldsymbol{\rho}} \tag{8.33}$$

The time derivative of the storage function is found to be

$$\begin{aligned}
\dot{V} &= \mathbf{s}_1^T\mathbf{M}\dot{\mathbf{s}}_1 + \mathbf{e}^T\mathbf{K}_p\dot{\mathbf{e}} + \mathbf{s}_2^T\mathbf{M}\dot{\mathbf{s}}_2 + \tilde{\boldsymbol{\rho}}^T\mathbf{L}_{p1}\dot{\tilde{\boldsymbol{\rho}}} \\
&= \mathbf{s}_1^T(-\mathbf{C}\mathbf{s}_1 - \mathbf{K}_d(\mathbf{s}_1 - \mathbf{s}_2) - \mathbf{K}_p\mathbf{e}) + \mathbf{e}^T\mathbf{K}_p\dot{\mathbf{e}} \\
&\quad + \mathbf{s}_2^T(-\mathbf{C}\mathbf{s}_2 - l_d\mathbf{M}\mathbf{s}_2 + \mathbf{K}_d\mathbf{s}_2 - \mathbf{L}_{p1}\tilde{\boldsymbol{\rho}} - \mathbf{K}_d\mathbf{s}_1 + \mathbf{C}(\mathbf{s}_2 - \mathbf{s}_1)) + \tilde{\boldsymbol{\rho}}^T\mathbf{L}_{p1}\dot{\tilde{\boldsymbol{\rho}}} \\
&= -\mathbf{s}_1^T\mathbf{K}_d\mathbf{s}_1 + \mathbf{s}_2^T\mathbf{K}_d\mathbf{s}_2 - \mathbf{s}_2^T l_d\mathbf{M}\mathbf{s}_2 + \mathbf{e}^T\mathbf{K}_p(\dot{\mathbf{e}} - \mathbf{s}_1^T) + \boldsymbol{\rho}^T\mathbf{L}_{p1}(\dot{\tilde{\boldsymbol{\rho}}} - \mathbf{s}_2) + \mathbf{s}_2^T\mathbf{C}(\mathbf{s}_s - \mathbf{s}_1) \\
&= -\mathbf{s}_1^T\mathbf{K}_d\mathbf{s}_1 + \mathbf{s}_2^T\mathbf{K}_d\mathbf{s}_2 - \mathbf{s}_2^T l_d\mathbf{M}\mathbf{s}_2 - \mathbf{e}^T\mathbf{K}_p\mathbf{\Lambda}_1\mathbf{e} + \mathbf{e}^T\mathbf{K}_p\tilde{\boldsymbol{\rho}} - \boldsymbol{\rho}^T\mathbf{L}_{p1}\mathbf{\Lambda}_2\tilde{\boldsymbol{\rho}} - \mathbf{s}_2^T\mathbf{C}\mathbf{s}_1
\end{aligned} \tag{8.34}$$

by using equation (8.27), (8.31), (8.22) and (8.24). Now, let $\mathbf{\Lambda}_1 = \mathbf{\Lambda}_2 = \mathbf{\Lambda}$ and $\mathbf{K}_p = \mathbf{L}_{p1}$. Then

$$-\mathbf{e}^T\mathbf{\Lambda}_1\mathbf{K}_p\mathbf{e} + \tilde{\boldsymbol{\rho}}^T\mathbf{\Lambda}_1\mathbf{K}_p\mathbf{e} - \tilde{\boldsymbol{\rho}}^T\mathbf{\Lambda}_2\mathbf{L}_{p1}\tilde{\boldsymbol{\rho}} \leq -\frac{1}{2}\mathbf{e}^T\mathbf{\Lambda}\mathbf{K}_p\mathbf{e} - \frac{1}{2}\tilde{\boldsymbol{\rho}}^T\mathbf{\Lambda}\mathbf{K}_p\tilde{\boldsymbol{\rho}} \tag{8.35}$$

and

$$\begin{aligned}
-\mathbf{s}_2^T\mathbf{C}\mathbf{s}_1 &\leq \mathbf{C}_M\mathbf{s}_2^T\mathbf{s}_1 \\
&\leq \mathbf{C}_M(\frac{\lambda}{2}\mathbf{s}_2^T\mathbf{s}_2 + \frac{1}{2\lambda}\mathbf{s}_1^T\mathbf{s}_1) \quad \forall\lambda
\end{aligned} \tag{8.36}$$

For any matrix $\mathbf{A} = \mathbf{A}^T > 0$, let $\mathbf{A}_m$ and $\mathbf{A}_M$ denote the minimum and maximum eigenvalue of $\mathbf{A}$, respectively. Then the time derivative of the storage function can be upper bounded by

$$\begin{aligned}
\dot{V} \leq &-(\mathbf{K}_{d,m} - \frac{1}{2\lambda}\mathbf{C}_M)\|\mathbf{s}_1\|^2 \\
&- (l_d\mathbf{M}_m - \mathbf{K}_{d,M} - \frac{\lambda}{2}\mathbf{C}_M)\|\mathbf{s}_2\|^2 \\
&- \frac{1}{2}\mathbf{K}_{p,m}\mathbf{\Lambda}_M^{-1}\|\mathbf{\Lambda}\tilde{\boldsymbol{\rho}}\|^2 - \frac{1}{2}\mathbf{K}_{p,m}\mathbf{\Lambda}_M^{-1}\|\mathbf{\Lambda}\mathbf{e}\|^2
\end{aligned} \tag{8.37}$$

and the following theorem can be stated:

Theorem 8.3. *The closed-loop system, with controller*

$$\begin{aligned}
\mathbf{u}_f &= \mathbf{M}\ddot{\boldsymbol{\rho}}_r + \mathbf{C}\dot{\boldsymbol{\rho}}_r + \mathbf{n} - \mathbf{K}_d(\dot{\boldsymbol{\rho}}_0 - \dot{\boldsymbol{\rho}}_r) - \mathbf{K}_p\mathbf{e} \\
\dot{\boldsymbol{\rho}}_r &= \dot{\boldsymbol{\rho}}_d - \boldsymbol{\Lambda}(\hat{\boldsymbol{\rho}} - \boldsymbol{\rho}_d) \\
\dot{\boldsymbol{\rho}}_0 &= \dot{\hat{\boldsymbol{\rho}}} - \boldsymbol{\Lambda}(\boldsymbol{\rho} - \hat{\boldsymbol{\rho}})
\end{aligned}$$

and observer

$$\begin{aligned}
\dot{\hat{\boldsymbol{\rho}}} &= \mathbf{z} + \mathbf{L}_d(\boldsymbol{\rho} - \hat{\boldsymbol{\rho}}) \\
\dot{\mathbf{z}} &= \ddot{\boldsymbol{\rho}}_r + \mathbf{L}_{p2}(\boldsymbol{\rho} - \boldsymbol{r\hat{ho}}) + \mathbf{M}^{-1}\mathbf{K}_p(\boldsymbol{\rho}_d - \hat{\boldsymbol{\rho}})
\end{aligned}$$

is locally exponentially stable under the following conditions

$$\mathbf{K}_{d,m} > \frac{1}{2\lambda}\mathbf{C}_M \tag{8.38a}$$

$$l_d > \mathbf{M}_m^{-1}(\mathbf{K}_{d,m} + \frac{\lambda}{2}\mathbf{C}_M) \tag{8.38b}$$

Proof. Take the storage function, V, given above as a Lyapunov function. This function satisfies

$$\frac{1}{2}P_m\|\mathbf{x}\|^2 \leq V \leq \frac{1}{2}P_M\|\mathbf{x}\|^2 \tag{8.39}$$

with $\mathbf{x}^T = [\mathbf{s}_1^T\ (\boldsymbol{\Lambda}\mathbf{e})^T\ \mathbf{s}_2^T\ (\boldsymbol{\Lambda}\tilde{\boldsymbol{\rho}})^T]$,

$$\delta = \min\left\{\frac{l_d\mathbf{M}_m - \mathbf{K}_{d,M}}{\mathbf{C}_M} - \frac{1}{2}, \frac{\mathbf{K}_{k,m}}{\mathbf{C}_M} - \frac{1}{2}\right\} \tag{8.40}$$

and

$$P_m = \min\{\mathbf{M}_m, \boldsymbol{\Lambda}_M^{-2}\mathbf{K}_{p,m}\} \tag{8.41a}$$

$$P_M = \max\{\mathbf{M}_M, \boldsymbol{\Lambda}_m^{-2}\mathbf{K}_{p,M}\} \tag{8.41b}$$

Under the conditions (8.38a) and (8.38b), there exists a constant κ such that

$$\dot{V} \leq -\kappa\|\mathbf{x}\|^2 \tag{8.42}$$

and local, exponential stability follows. □

8.4 Syncronization

Now turn to the second case, where each satellite is modeled with the rigid body equations of motion. In Nijmeijer & Rodriguez-Angeles (2003) a distinction is made between *internal synchronization* and *external synchronization*. Internal synchronization refers to an interaction of all elements in the system, and can in the context of formation flying satellites be related to the Cyclic Structure, (see section 1.2). External synchronization on the other hand, refers to the case where one object in the system is dominant, and its motion can be considered as independent of the motion of the others. The Leader/Follower architecture is therefore an external synchronization problem.
The control of the Leader satellite is a tracking problem, that is, the control objective is to

follow a predefined reference trajectory. The trajectory is given by the desired position, $\mathbf{p}^i_{d,l}$, the desired attitude, $\mathbf{q}_{d,l}$, and the desired velocities and their time derivatives

$$\mathbf{v}^l_{d,l} = \mathbf{R}^l_i \dot{\mathbf{p}}^i_{d,l} \tag{8.43a}$$
$$\dot{\mathbf{v}}^l_{d,l} = \mathbf{R}^l_i \ddot{\mathbf{p}}^i_{d,l} - \mathbf{S}(\boldsymbol{\omega}^l_{il})\mathbf{R}^l_i \dot{\mathbf{p}}^i_{d,l} \tag{8.43b}$$
$$\boldsymbol{\omega}^l_{d,l} = \mathbf{R}^l_i \boldsymbol{\omega}^i_{d,l} \tag{8.43c}$$
$$\dot{\boldsymbol{\omega}}^l_{d,l} = \mathbf{R}^l_i \ddot{\boldsymbol{\omega}}^i_{d,l} - \mathbf{S}(\boldsymbol{\omega}^l_{il})\mathbf{R}^l_i \dot{\boldsymbol{\omega}}^i_{d,l} \tag{8.43d}$$

The control of the Follower satellite, on the other hand, is a synchronization problem. A reference trajectory for the Follower satellite will therefore also depend on the states of the Leader satellite. For many applications of formations of satellites the objective will be to point measuring instruments in the same direction. Let therefore the reference trajectory for the Follower satellite be the measured attitude of the Leader satellite, i.e.

$$\mathbf{q}_{d,f} = \mathbf{q}_l \tag{8.44a}$$
$$\boldsymbol{\omega}^f_{d,f} = \mathbf{R}^f_l \boldsymbol{\omega}^l_{il} \tag{8.44b}$$
$$\dot{\boldsymbol{\omega}}^f_{d,f} = \mathbf{R}^f_l \mathbf{S}(\boldsymbol{\omega}^l_{fl})\boldsymbol{\omega}^l_{il} + \mathbf{R}^f_l \dot{\boldsymbol{\omega}}^l_{il} \tag{8.44c}$$

As mentioned in the introduction each satellite should be designated its own orbit, so as not to spend fuel unnecessarily. Let the position of such a orbit for the follower satellite be defined with $\mathbf{p}^i_p$. Then the actual desired trajectory for the position of the follower satellite is given by

$$\mathbf{p}^i_{d,f} = \mathbf{p}^i_p - \mathbf{p}^i_{d,l} + \mathbf{p}^i_l \tag{8.45a}$$
$$\mathbf{v}^f_d = \mathbf{R}^f_i \dot{\mathbf{p}}^i_p + \mathbf{R}^f_l(\mathbf{v}^l - \mathbf{v}^l_{d,l}) \tag{8.45b}$$
$$\dot{\mathbf{v}}^f_d = \mathbf{R}^f_i \ddot{\mathbf{p}}^i_p - \mathbf{S}(\boldsymbol{\omega}^f_{if})\mathbf{R}^f_i \dot{\mathbf{p}}^i_p + \mathbf{R}^f_l \mathbf{S}(\boldsymbol{\omega}^l_{fl})(\mathbf{v}^l - \mathbf{v}^l_{d,l}) + \mathbf{R}^f_l(\dot{\mathbf{v}}^l - \dot{\mathbf{v}}^l_{d,l}) \tag{8.45c}$$

8.5 Controller Design for Synchronization in 6 DOF

It can be shown, see Egeland & Gravdahl (2002), that composite rotations can be expressed in terms of unit quaternions

$$\mathbf{R}(\mathbf{q}_1)\mathbf{R}(\mathbf{q}_2) = \mathbf{R}(\mathbf{q}_1 \otimes \mathbf{q}_2) \tag{8.46}$$

The deviation between two rotation matrices is described by the two alternative error matrices

$$\tilde{\mathbf{R}}_1 = \mathbf{R}^T_d \mathbf{R} \tag{8.47a}$$
$$\tilde{\mathbf{R}}_2 = \mathbf{R}_d \mathbf{R}^T \tag{8.47b}$$

where $\tilde{\mathbf{R}}_1$ is the rotation matrix from the desired frame $\mathfrak{F}_d$ to the body frame $\mathfrak{F}_b$, and $\tilde{\mathbf{R}}_2$ is the rotation matrix from the body frame to the desired frame. Combining (8.47a) and (3.25) results in

$$\tilde{\mathbf{R}}_1 = \mathbf{R}(\tilde{\mathbf{q}}) \tag{8.48}$$

where $\tilde{\mathbf{q}} = \mathbf{q}^*_d \otimes \mathbf{q}$.
Perfect tracking in terms of quaternions parametrization is obtained for

$$\mathbf{q} = \pm\mathbf{q}_d \tag{8.49}$$

which implies that

$$\tilde{\mathbf{q}} = \begin{bmatrix} \pm 1 \\ \mathbf{0} \end{bmatrix} \tag{8.50}$$

The rotation error matrices, $\tilde{\mathbf{R}}_1$ and $\tilde{\mathbf{R}}_2$ are related through a similarity transformation $\tilde{\mathbf{R}}_2 = \mathbf{R}\tilde{\mathbf{R}}_1\mathbf{R}^T = \mathbf{R}\tilde{\mathbf{R}}_1\mathbf{R}^{-1}$, and hence they have both the same eigenvalues, that is

$$\mathrm{eig}(\tilde{\mathbf{R}}_1), \mathrm{eig}(\tilde{\mathbf{R}}_2)\epsilon\{1, 2\tilde{\eta}^2 - 1 \pm i2\tilde{\eta}\sqrt{1-\tilde{\eta}^2}\} \tag{8.51}$$

Notice that $\tilde{\mathbf{R}}_1$ and $\tilde{\mathbf{R}}_2$ are strictly positive for $\tilde{\eta}^2 > \frac{1}{2}$. The controller stated in this section is the one found in Fjellstad & Fossen (1994) and Fjellstad (1994). It was originally derived for the control of underwater vehicles, which attitude representation neither can contain singularities. The control law is given in the body frame, $\mathfrak{F}_b$, as

$$\boldsymbol{\tau} = \mathbf{M}\dot{\boldsymbol{\nu}}_r + \mathbf{C}(\boldsymbol{\nu})\boldsymbol{\nu}_r + \mathbf{D}(\boldsymbol{\nu})\boldsymbol{\nu}_r + \mathbf{g} - \mathbf{K}_d\mathbf{s} \tag{8.52}$$

The virtual velocity reference vector

$$\boldsymbol{\nu}_r \triangleq \boldsymbol{\nu}_d - \boldsymbol{\Lambda}\mathbf{e} \tag{8.53}$$

is assumed to be continuously differentiable. This calls for some further definitions:

$$\boldsymbol{\nu}_d \triangleq \begin{bmatrix} \mathbf{v}_d \\ \boldsymbol{\omega}_d \end{bmatrix} \tag{8.54}$$

$$\boldsymbol{\Lambda} \triangleq \begin{bmatrix} \mathbf{K}_p & \mathbf{0}_{3\times3} \\ \mathbf{0}_{3\times3} & -2c\frac{\partial W}{\partial \tilde{\eta}}\mathbf{1}_{3\times3} \end{bmatrix} \tag{8.55}$$

$$\mathbf{e} \triangleq \begin{bmatrix} \tilde{\mathbf{p}}^i \\ \tilde{\boldsymbol{\varepsilon}} \end{bmatrix} \tag{8.56}$$

$$\tilde{\mathbf{p}}^i \triangleq \mathbf{p}^i - \mathbf{p}^i_d \tag{8.57}$$

The scalar function $W(\tilde{\eta})$ satisfies the Lipschitz condition on the interval $\tilde{\eta}\epsilon[-1, 1]$. Moreover, it is non-negative on the same interval an vanishes only at $\tilde{\eta} = -1$ and/or $\tilde{\eta} = 1$.
Now, the following theorem is stated

Theorem 8.4. *The controller*

$$\boldsymbol{\tau} = \mathbf{M}\dot{\boldsymbol{\nu}}_r + \mathbf{C}(\boldsymbol{\nu})\boldsymbol{\nu}_r + \mathbf{D}(\boldsymbol{\nu})\boldsymbol{\nu}_r + \mathbf{g} - \mathbf{K}_d\mathbf{s}$$

is globally uniformly asymptotically stable

The proof, found in Fjellstad & Fossen (1994), is given here for the sake of completeness.

Proof. Let the virtual body-fixed velocity error vector $\mathbf{s}$ is defined as

$$\mathbf{s} \triangleq \boldsymbol{\nu} - \boldsymbol{\nu}_r \tag{8.58}$$

The error dynamics, achieved from substituting (8.52) into(7.10b), is

$$\mathbf{M}\dot{\mathbf{s}} + \mathbf{C}(\boldsymbol{\nu})\mathbf{s} + \mathbf{D}(\boldsymbol{\nu})\mathbf{s} = -\mathbf{K}_d\mathbf{s} \tag{8.59}$$

By using the positive definite Lyapunov function

$$V = \frac{1}{2}\mathbf{s}^T\mathbf{M}\mathbf{s} > 0, \quad \forall \mathbf{s} \neq \mathbf{0} \tag{8.60}$$

which is decrescent and satisfy

$$\lambda_{min}(\mathbf{M})\|\mathbf{s}\|^2 \leq 2V \leq \lambda_{max}(\mathbf{M})\|\mathbf{s}\|^2 \tag{8.61}$$

global uniform asymptotical stability of the equilibrium point $\mathbf{s} = \mathbf{0}$ can be guaranteed, since

$$\begin{aligned}
\dot{V} &= \mathbf{s}^T\mathbf{M}\dot{\mathbf{s}} && (8.62)\\
&= \mathbf{s}^T(-\mathbf{C}(\boldsymbol{\nu})\mathbf{s} - \mathbf{D}(\boldsymbol{\nu})\mathbf{s} - \mathbf{K}_d\mathbf{s}) && (8.63)\\
&= -\mathbf{s}^T[\mathbf{K}_d + \mathbf{D}(\boldsymbol{\nu})]\mathbf{s} && (8.64)\\
&\leq -[\lambda_{min}(\mathbf{K}_d) + \lambda_{min}(\mathbf{D}(\boldsymbol{\nu}))]\|\mathbf{s}\|^2 && (8.65)
\end{aligned}$$

This is due to application of Lyapunov's direct method for non-autonomous systems, see Khalil (2002). □

By combining (8.58) with (8.53), the dynamics at $\mathbf{s} = \mathbf{0}$, becomes

$$\begin{bmatrix} \tilde{\mathbf{v}}^b \\ \tilde{\boldsymbol{\omega}}^b_{ib} \end{bmatrix} = \begin{bmatrix} \mathbf{K}_p & \mathbf{0}_{3\times3} \\ \mathbf{0}_{3\times3} & -2c\frac{\partial W}{\partial \tilde{\eta}}\mathbf{1}_{3\times3} \end{bmatrix} \begin{bmatrix} \tilde{\mathbf{p}}^i \\ \tilde{\boldsymbol{\varepsilon}} \end{bmatrix} \tag{8.66}$$

The following candidate for K_p is chosen

$$\mathbf{K}_p = \lambda_1 \mathbf{R}^b_i(\mathbf{q}_d) \tag{8.67}$$

Since $\dot{\tilde{\mathbf{p}}}^i = \mathbf{R}^i_b(\mathbf{q})\tilde{\mathbf{v}}^b$, using (8.66) and (8.67),

$$\begin{aligned}
\dot{\tilde{\mathbf{p}}}^i &= \lambda_1 \mathbf{R}^i_b(\mathbf{q})\mathbf{R}^b_i(\mathbf{q}_d)\tilde{\mathbf{p}}^i \\
&= \lambda_3 \mathbf{R}^i_b(\tilde{\mathbf{q}})\tilde{\mathbf{p}}^i
\end{aligned} \tag{8.68}$$

where equation (8.46) has been used in the last line. Since $\mathbf{R}^i_b(\tilde{\mathbf{q}})$ is strictly positive for $\tilde{\eta}^2 > \frac{1}{2}$, see equation (8.51), $\tilde{\mathbf{p}}^i$ converges to zero for $\lambda_1 > 0$. To prove convergence of $\tilde{\boldsymbol{\omega}}^b_{ib}$ to zero, the attitude error differential equation is considered, namely

$$\dot{\tilde{\mathbf{q}}} = \begin{bmatrix} -\tilde{\boldsymbol{\varepsilon}}^T \\ \tilde{\eta}\mathbf{1}_{3\times3} + \mathbf{S}(\tilde{\varepsilon}) \end{bmatrix} \tilde{\boldsymbol{\omega}}^b_{ib} \tag{8.69}$$

As seen, $\dot{\tilde{\eta}} = -\frac{1}{2}\tilde{\boldsymbol{\varepsilon}}^T\tilde{\boldsymbol{\omega}}^b_{ib}$, which will be used in the time differentiation of the Lyapunov function candidate, $W(\tilde{\eta})$, as follows

$$\begin{aligned}
\dot{W}(\tilde{\eta}) &= \frac{\partial W}{\partial \tilde{\eta}}\dot{\tilde{\eta}} \\
&= -\frac{1}{2}\frac{\partial W}{\partial \tilde{\eta}}\tilde{\boldsymbol{\varepsilon}}^T\tilde{\boldsymbol{\omega}}^b_{ib} \\
&= -c(\frac{\partial W}{\partial \tilde{\eta}})^2\tilde{\boldsymbol{\varepsilon}}^T\tilde{\boldsymbol{\varepsilon}}
\end{aligned} \tag{8.70}$$

which is negative $\forall \frac{\partial W}{\partial \tilde{\eta}} \neq 0, \tilde{\boldsymbol{\varepsilon}} \neq \mathbf{0}$. In Fjellstad & Fossen (1994) many suggestions for $W(\tilde{\eta})$ are stated. One of them is

$$W(\tilde{\eta}) = 1 - |\tilde{\eta}| \tag{8.71}$$

which leads to

$$\frac{\partial W}{\partial \tilde{\eta}} = \mathrm{sgn}(\tilde{\eta}) \tag{8.72}$$

where the signum function is defined as

$$\mathrm{sgn}(x) = \begin{cases} -1 & x < 0 \\ 1 & x \geq 0 \end{cases} \tag{8.73}$$

The signum function is non-zero by definition to avoid an extra (unstable) equilibrium point at $\tilde{\eta} = 0$. This leads to

$$-c\tilde{\boldsymbol{\varepsilon}}^T\tilde{\boldsymbol{\varepsilon}} \tag{8.74}$$

and consequently, $\tilde{\boldsymbol{\varepsilon}} \to \mathbf{0}$ and $\tilde{\eta} \to \pm 1$. From (8.66), it follows that $\tilde{\boldsymbol{\omega}}_{ib}^b \to \mathbf{0}$. This definition of $W(\tilde{\eta})$ leads strictly speaking to a $\boldsymbol{\nu}_r$ which is not continuously differentiable. This is solved by either defining

$$\frac{\mathrm{d}}{\mathrm{d}t}\mathrm{sgn}(x) \equiv 0 \tag{8.75}$$

or for example redefine $W(\tilde{\eta})$ to

$$W(\tilde{\eta}) = 1 - \frac{2}{\pi}\arctan(\alpha\tilde{\eta}) \tag{8.76}$$

which converges to the original $W(\tilde{\eta})$ for large α.
It should be noted that the control law presented in this section quite easily can be extended to an adaptive version, to account for parameter uncertainties in the dynamical model. This is shown in Fjellstad & Fossen (1994), based on the results for attitude control of satellites in Egeland & Godhavn (1994).

8.6 Observer Design for Synchronization in 6 DOF

The controller design from the previous section, assumed that the angular and translational velocity could be measured. If this is not the case, a velocity observer has to be implemented. In Salcudean (1991), the following globally convergent velocity observer for rigid body motion is derived

$$\dot{\hat{\mathbf{h}}}^i = \mathbf{R}_b^i[\mathbf{m}^b + \frac{1}{2}k_p(\mathbf{I}^b)^{-1}\tilde{\boldsymbol{\varepsilon}}\,\mathrm{sgn}(\tilde{\eta})] \tag{8.77}$$

$$\dot{\hat{\mathbf{q}}} = \frac{1}{2}\mathbf{T}_q(\hat{\mathbf{q}})(\hat{\boldsymbol{\omega}}_{ib}^b + k_v(\mathbf{I}^i)^{-1}\tilde{\boldsymbol{\varepsilon}}\,\mathrm{sgn}(\tilde{\eta}) \tag{8.78}$$

This observer is quite extensively used throughout the literature. With minor changes, it is used in Fjellstad (1994) for estimating the angular velocity of underwater vehicles, where as in Bondhus, Pettersen & Gravdahl (2005) the same observer is used for Leader/Follower synchronization of satellite attitude.
Now, using the fact that $\mathbf{I}^i = \mathbf{R}_b^i\mathbf{I}^b\mathbf{R}_i^b$ and $\boldsymbol{\omega}_{ib}^i = \mathbf{R}_b^i\boldsymbol{\omega}_{ib}^b$ the left-hand side of equation (8.77) can be written

$$\begin{aligned}\dot{\hat{\mathbf{h}}}^i &= \frac{\mathrm{d}}{\mathrm{d}t}(\mathbf{R}_b^i\mathbf{I}^b\mathbf{R}_i^b\mathbf{R}_b^i\hat{\boldsymbol{\omega}}_{ib}^b) \\ &= \dot{\mathbf{R}}_b^i\mathbf{I}^b\hat{\boldsymbol{\omega}}_{ib}^b + \mathbf{R}_b^i\mathbf{I}^b\dot{\hat{\boldsymbol{\omega}}}_{ib}^b \\ &= \mathbf{R}_b^i\mathbf{S}(\hat{\boldsymbol{\omega}}_{ib}^b)\mathbf{I}^b\hat{\boldsymbol{\omega}}_{ib}^b + \mathbf{R}_b^i\mathbf{I}^b\dot{\hat{\boldsymbol{\omega}}}_{ib}^b \\ &= \mathbf{R}_b^i(\mathbf{S}(\hat{\boldsymbol{\omega}}_{ib}^b)\mathbf{I}^b\hat{\boldsymbol{\omega}}_{ib}^b + \mathbf{I}^b\dot{\hat{\boldsymbol{\omega}}}_{ib}^b)\end{aligned} \tag{8.79}$$

It has been used that $\dot{\mathbf{R}}_b^i = \mathbf{R}_b^i\mathbf{S}(\boldsymbol{\omega}_{ib}^b)$ and $\hat{\boldsymbol{\omega}}_{ib}^b \simeq \boldsymbol{\omega}_{ib}^b$ and $\mathbf{R}_b^i\mathbf{R}_i^b = \mathbf{1}$. Hence the attitude observer dynamics and kinematics becomes

$$\mathbf{I}^b\dot{\hat{\boldsymbol{\omega}}}_{ib}^b + \mathbf{S}(\hat{\boldsymbol{\omega}}_{ib}^b)\mathbf{I}^b\hat{\boldsymbol{\omega}}_{ib}^b = \mathbf{m}^b + \frac{1}{2}k_p(\mathbf{I}^b)^{-1}\tilde{\boldsymbol{\varepsilon}}\,\mathrm{sgn}(\tilde{\eta}) \tag{8.80}$$

and

$$\dot{\hat{\mathbf{q}}} = \frac{1}{2}\mathbf{T}_q(\hat{\mathbf{q}})(\hat{\boldsymbol{\omega}}_{ib}^b + k_v(\mathbf{R}_b^i(\mathbf{I}^b)^{-1}\mathbf{R}_i^b\tilde{\boldsymbol{\varepsilon}}\,\mathrm{sgn}(\tilde{\eta}) \tag{8.81}$$

by using $(\mathbf{R}_b^i)^{-1} = \mathbf{R}_i^b$. This is really just a copy of equation (7.6) and an injection term. Since the observer is changed from the one given in Salcudean (1991), the stability analysis given there, is no longer valid. By also copying the translational dynamics and kinematics in the same way, the total 6 DOF observer dynamics becomes.

$$\mathbf{M}\dot{\hat{\boldsymbol{\nu}}} + \mathbf{C}(\hat{\boldsymbol{\nu}})\hat{\boldsymbol{\nu}} + \mathbf{g}(\mathbf{q}) = \boldsymbol{\tau} + \mathbf{k}_1 \tag{8.82}$$

with

$$\mathbf{k}_1 = \begin{bmatrix} \frac{1}{2}k_p(\mathbf{I}^b)^{-1}\tilde{\boldsymbol{\varepsilon}}\,\mathrm{sgn}(\tilde{\eta}) \\ \mathbf{K}_q(\mathbf{p}^i - \hat{\mathbf{p}}^i) \end{bmatrix} \tag{8.83}$$

As stated above, the rotational observer kinematics is

$$\dot{\hat{\mathbf{q}}} = \frac{1}{2}\mathbf{T}_q(\hat{\mathbf{q}})(\hat{\boldsymbol{\omega}}_{ib}^b + k_v(\mathbf{R}_b^i(\mathbf{I}^b)^{-1}\mathbf{R}_i^b\tilde{\boldsymbol{\varepsilon}}\,\mathrm{sgn}(\tilde{\eta}) \tag{8.84}$$

and finally the translational observer kinematics

$$\dot{\hat{\mathbf{p}}}^i = \mathbf{R}_b^i\mathbf{v}^b + \mathbf{K}_q(\mathbf{p}^i - \hat{\mathbf{p}}^i) \tag{8.85}$$

The main reason for using this particular observer, is that these equations also give an estimate of the acceleration, which can be forwarded to the controller of the Follower satellite.

Chapter 9

Simulations

The simulations are performed using Matlab and Simulink, together with the Marine GNC Toolbox[1]. The Leader satellite is in all cases assumed to orbit the Earth at a circular orbit of 600 km altitude. The orbit have an inclination, see figure 9.1, of 90 degrees, i.e. the orbit is polar. Perfect measurement of both position and attitude is assumed.

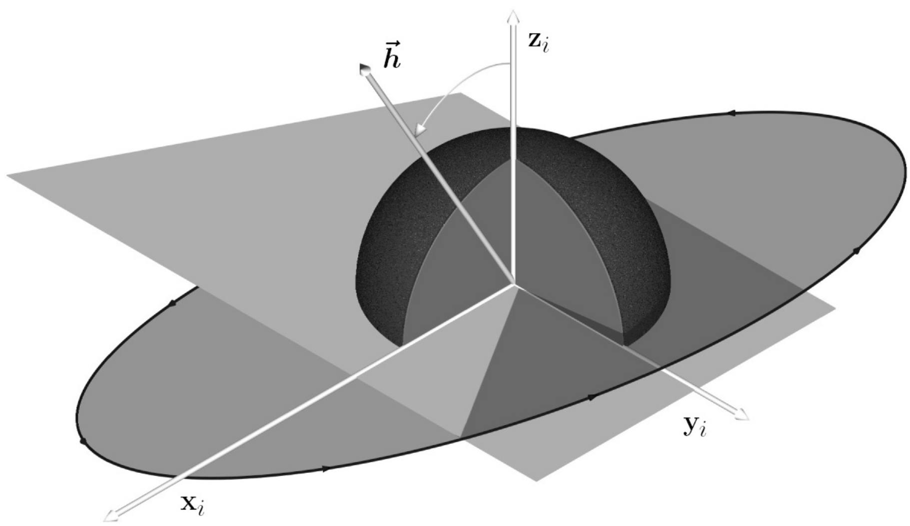

Figure 9.1: The inclination is the angle from the z_i vector to the angular momentum vector $\vec{h}$

9.1 Position Control by State Feedback Linearization

In this section the simulation results of the satellites relative motion using the controller of section 8.1 are presented. The orientation of the two satellites is not taken into consideration, which can be justified by the fact that the attitude dynamics are much faster than the position dynamics. For simplicity reasons the thruster forces are assumed to work in the directions of the Hill-frame. Maximum thrust force is set to 5 Newton. The Follower satellite is furthermore only assumed to be influenced by the gravitational forces, including the J_2-perturbations. Other

[1] **NTNU-MSS, Marine Systems Simulator (2005).**
Norwegian University of Science and Technology, Trondheim, Norway.
Available at <www.cesos.ntnu.no/mss>

Mass	$m = 70kg$
Moment of Inertia	$I = \begin{bmatrix} 4 & 0 & 0 \\ 0 & 4 & 0 \\ 0 & 0 & 3 \end{bmatrix}$
Altitude	600 km
Orbit	Circular, Polar

Table 9.1: Satellite data

perturbing forces have hardly any impact on satellites at 600 km attitude. The Follower satellite is controlled, so as to make up an in-plane elliptic formation, as described in section 4.4. The reference trajectory is found from equation (4.28) and (4.29), and their time derivatives.
Adequate performance was reached by placing the poles of each of the decoupled linear systems at $\lambda_1 = 0.05$ and $\lambda_2 = 600$. The initial conditions for the Follower satellite were chosen to be $\boldsymbol{\rho}(\mathbf{0}) = \mathbf{0}$, and $\dot{\boldsymbol{\rho}}(\mathbf{0}) = \mathbf{0}$, i.e. it started at the same position and with the same velocity as the Leader satellite. Figure 9.2(a) and 9.2(b) shows how the Follower satellite reaches the desired position and velocity after approximately 70 seconds. In figure 9.2(c) the actuating forces needed to bring the satellite into the desired position are plotted, where as in figure 9.2(d) the relative position between the satellites throughout one orbit is shown.

The exponential stability and the fact that well-established linear design techniques can be

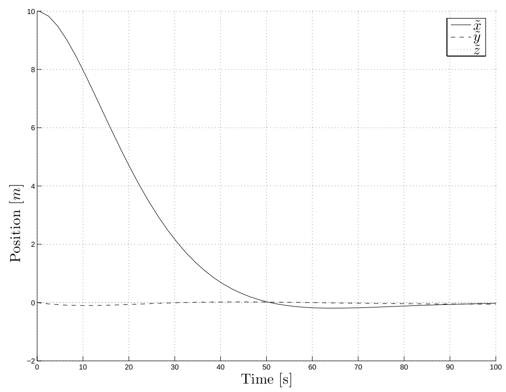

(a) Tracking position error for the Follower satellite

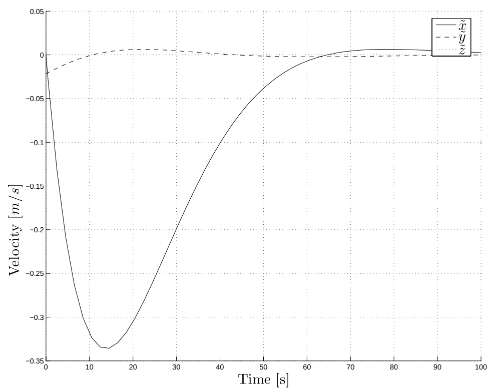

(b) Tracking velocity error for the Follower satellite

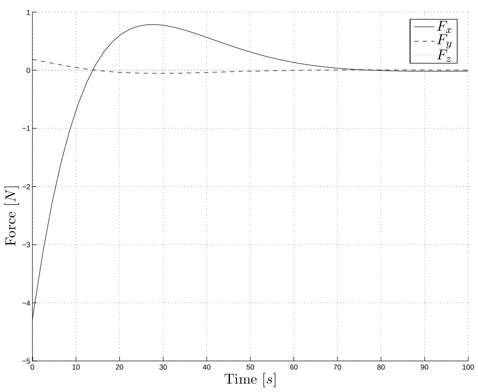

(c) Forces necessary to bring the Follower satellite into desired orbit

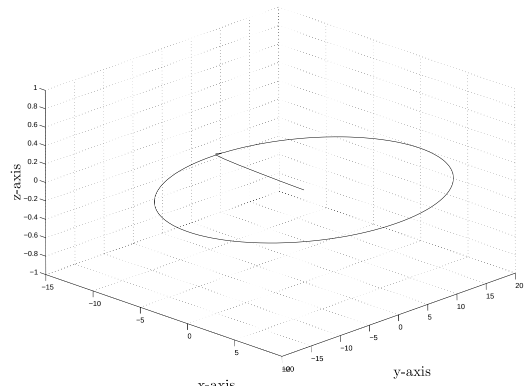

(d) 3D plot of Follower satellites position relative to Leader satellite

Parameter	Value
$\mathbf{\Lambda}_1$	$\mathbf{1}_{3\times 3}$
$\mathbf{\Lambda}_2$	$\mathbf{1}_{3\times 3}$
$\mathbf{K}_p$	$\begin{bmatrix} 10 & 5 & 5 \\ 5 & 10 & 5 \\ 5 & 5 & 10 \end{bmatrix}$
$\mathbf{K}_d$	$\begin{bmatrix} 3 & 1.5 & 1.5 \\ 1.5 & 3 & 1.5 \\ 1.5 & 1.5 & 3 \end{bmatrix}$
l_d	1
$\mathbf{L}_{p1}$	$\mathbf{L}_{p2}$
$\mathbf{L}_{p2}$	$l_d\mathbf{\Lambda}_2$
$\mathbf{L}_d$	$l_d\mathbf{1}_{3\times 3} + \mathbf{\Lambda}_2$

Table 9.2: Controller and observer parameters for the combined controller-observer design

used, are the main advantages with state-feedback linearization. But even though the plots indicate good performance, state feedback linearizing controllers has a number of limitations that are important to keep in mind.
First, the full state of the satellite has to be measured. This can be solved using a nonlinear observer, but stability analysis of a combination of a stable state feedback controller and a stable observer is not straight forward, due to the lack of a general separation principle. Note that this is not just a limitation for state feedback linearizing controllers, but applies to nonlinear systems in general.
Secondly, according to Slotine & Li (1991), in the presence of parameter uncertainties or unmodeled dynamics, no robustness is guaranteed. State feedback linearizing controllers are especially sensitive, since they rely on an exact model of the system.
Finally, by state-feedback linearization, the advantage of stabilizing terms are not taken, since all nonlinearities are canceled. Hence the control efforts are even greater than they have to be.

9.2 Position Control by Combined Controller-Observer Design

Using the combined controller-observer design of section 8.3, the motion of the Follower satellite relative to the Leader is simulated. The assumptions, initial conditions and reference trajectories are the same as in the previous section. In addition the observer is given the somewhat arbitrary initial conditions $\hat{\boldsymbol{\rho}}(\mathbf{0}) = [3 \quad 2 \quad 5]^T$ and $\mathbf{z}(\mathbf{0}) = [1 \quad 4 \quad 2]^T$. The controller and estimator parameters are shown in table 9.2.

Figure 9.2(e) and 9.2(f) shows that the tracking position and velocity errors are within reasonable values after 50 seconds. The estimation position and velocity errors are plotted in figure 9.2(g) and 9.2(h), respectively. Figure 9.2(i) shows the actuator forces needed to bring the Follower satellite into desired orbit, where as a 3D model of the follower satellites motion relative to the leader is depicted in figure 9.2(j).

One of the advantages of passivity-based control is its robustness. If the model possesses the same passivity properties, regardless of the numerical values of the physical parameters, and a controller is designed so that stability relies on the passivity properties only, then the closed loop will be stable whatever the values of the physical parameters. As opposed to the state feedback linearizing controller, a passivity based controller takes advantage of stabilizing terms. More about advantages and disadvantages can be found in Khalil (2002).

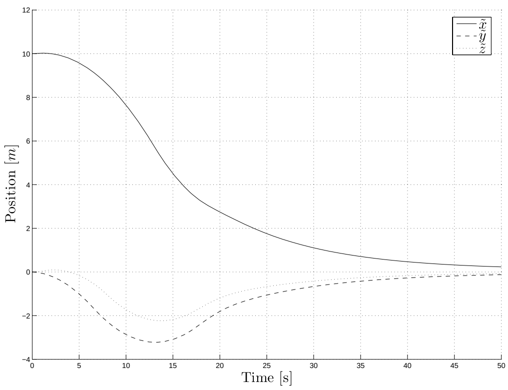

(e) Tracking position error for the Follower satellite

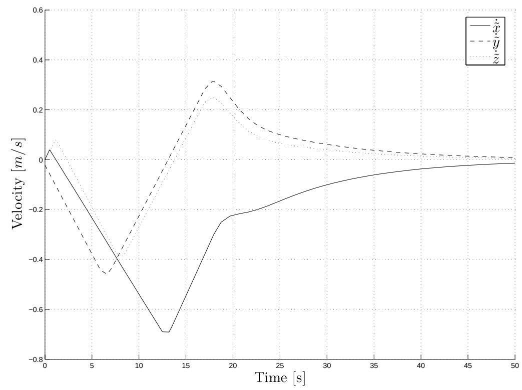

(f) Tracking velocity error for the Follower satellite

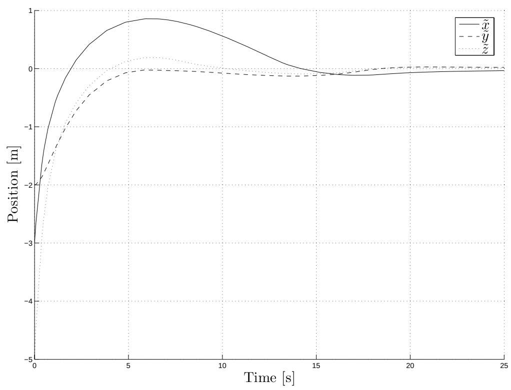

(g) Estimation position error for the Follower satellite

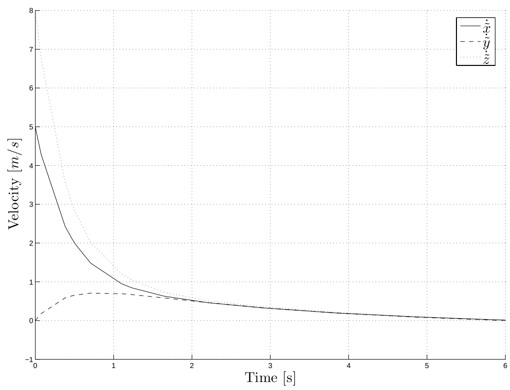

(h) Estimation velocity error for the Follower satellite

9.3 Synchronization of Position and Attitude

In this section the controller from section 8.5, together with the observer from section 8.6 are used in the synchronization of two satellites. The reference trajectory for both satellites is a polar orbit in the same orbital plane, but with the Follower satellite 10 meters behind the Leader satellite. These trajectories are generated using equation (8.43), (8.44) and (8.45). The same controller and observer parameters are used for both satellites, and are summarized in table 9.3. The thruster forces and gyro moments are saturated to 10 Newton and 10 Newtonmeter, respectively.

The satellites were given an initial displacement in position from the reference trajectory, but no displacement in attitude. Figure 9.2(k), 9.2(l), 9.2(m) and 9.2(n) show the tracking and estimation error for the Leader satellite in position and attitude. Notice that the attitude error is given in Euler angles by using a quaternion- to Euler angles transformation algorithm, see Fossen (2002). The input forces needed to control the Leader satellite are shown in figure 9.2(o). Figure 9.2(p), 9.2(q), 9.2(r) and 9.2(s) show the tracking and estimation error for the Follower satellite in position and attitude, where as figure 9.2(t) shows the input forces needed to control the Follower satellite. In the case where an initial displacement in orientation was given, the satellites were unable to follow the reference trajectory, even with velocity feedback. This was most likely due to an implementation error.

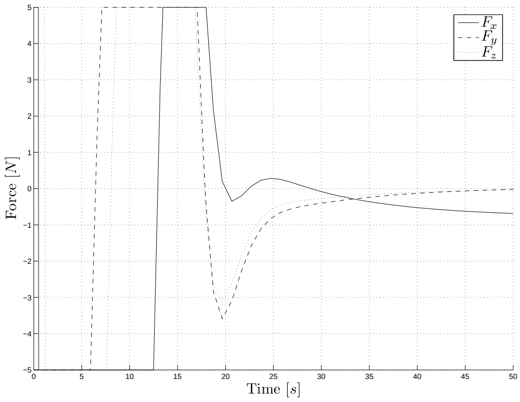

(i) Forces needed to bring the Follower satellite into desired orbit

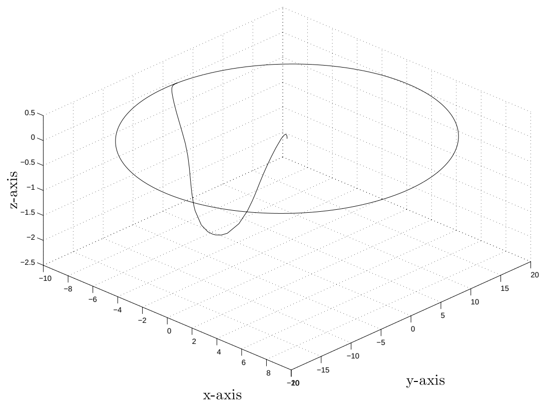

(j) 3D plot of Follower satellites position relative to Leader satellite

Parameter	Value
λ_1	1
c	1
$\mathbf{K}_d$	$\mathrm{diag}\{200 \cdot \mathbf{1}_{3\times3}, 10 \cdot \mathbf{1}_{3\times3}\}$
λ_2	5
$\mathbf{K}_p$	$[100 \cdot \mathbf{1}_{3\times3}]$
λ_3	20
λ_4	20
$\mathbf{K}_q$	$\mathrm{diag}\{1500, 300, 500, \frac{1}{2}\lambda_4 \mathbf{1}_{3\times3}\}$

Table 9.3: Controller and observer parameters for synchronization of satellites

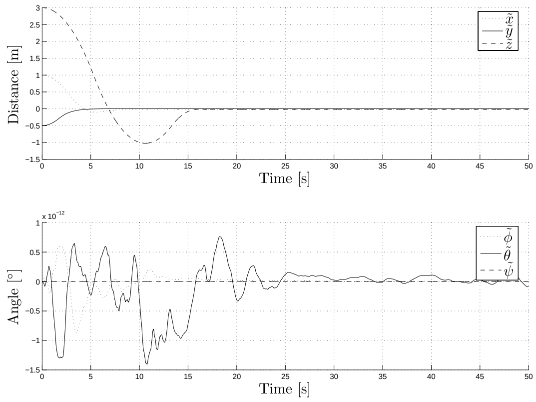

(k) Tracking position and attitude error for the Leader satellite

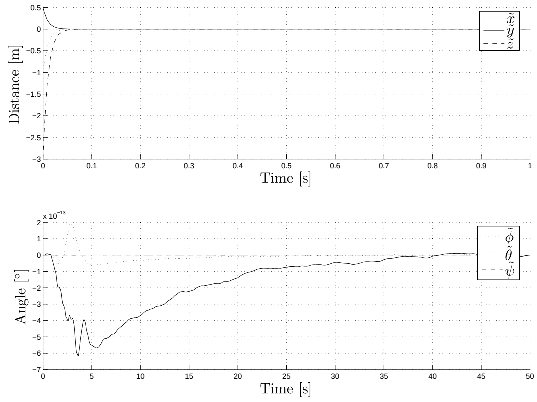

(l) Estimation position and attitude error for the Leader satellite

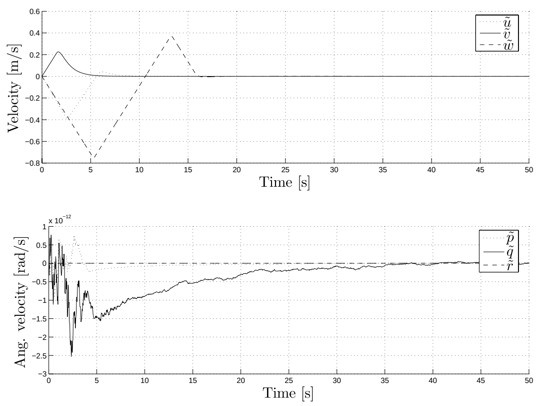

(m) Tracking velocity error for the Leader satellite

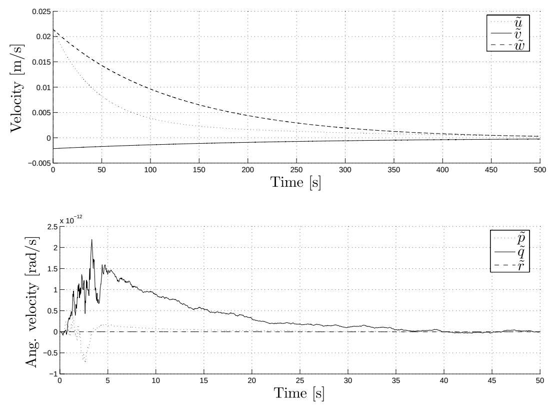

(n) Estimation velocity error for the Leader satellite

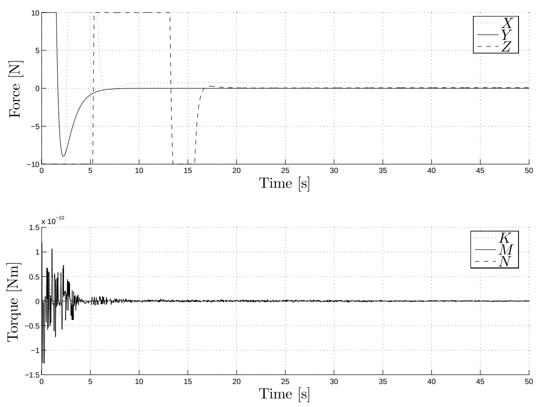

(o) Control forces and torques necessary to bring the Leader satellite to its reference trajectory

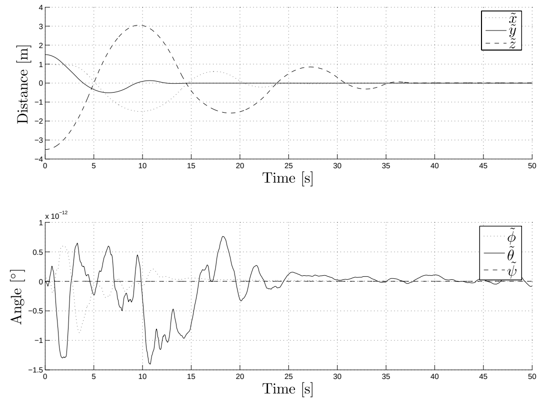

(p) Tracking position and attitude error for the Follower satellite

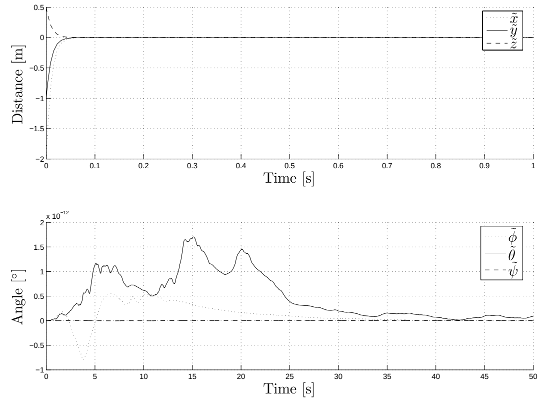

(q) Estimation position and attitude error for the Follower satellite

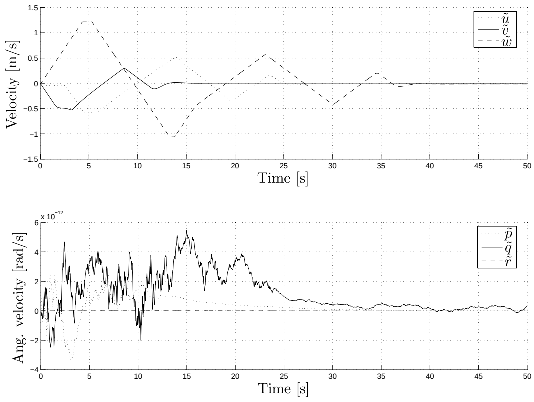

(r) Tracking velocity error for the Follower satellite

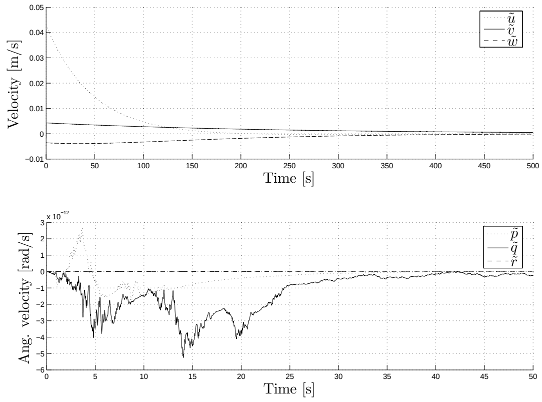

(s) Estimation velocity error for the Follower satellite

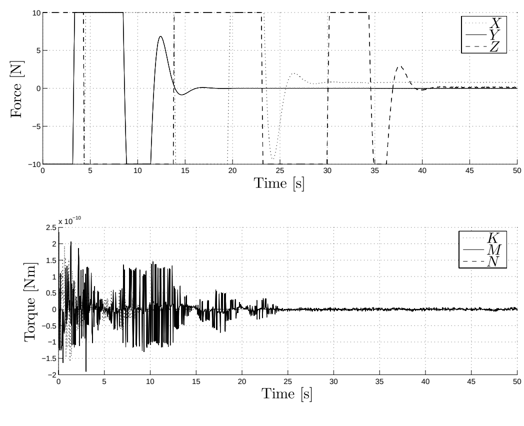

(t) Control forces and torques necessary to bring the Follower satellite to its reference trajectory

Chapter 10

Concluding Remarks and Recommendations

10.1 Conclusion

In this thesis the linear equations for the relative position of satellites, called the Hill-Clohessy-Wiltshire equations, have been presented. They have been used in the development of fuel efficient reference orbits, suitable for formations flying of satellites.
The linear relative model has been extended to a nonlinear version, where also the forcing terms from actuators and disturbance forces have been incorporated. In a similar manner a model for the relative attitude has been derived.
For the nonlinear relative equations of motion, both a state feedback linearizing controller and a passivity based controller, were developed. The passivity based controller was extended to a combined observer-controller scheme, by taking advantage of such schemes already developed for robot manipulators. In this way velocity measurements were no longer needed. Simulations were performed to illustrate the behavior of the different controllers.
A different approach was then taken in the modeling of the formation. Each satellite was modeled using the 6DOF rigid body equations of motions, which are well known from the modeling and control of robot manipulators and ocean vehicles. In this way not only a more complete model for the behavior of the satellites was achieved, but it also opens a toolbox of controllers and observers already developed in other fields of study.
Using synchronization theory and a controller developed for underwater vehicles, formations were simulated.

10.2 Recommendations

For future work based on this thesis, the following recommendations are given

- The complete 6 DOF model for the relative position and attitude could be implemented. Further should controllers and observers for the relative attitude be designed.
- The controller proposed for synchronization of satellites should be re-implemented. Incorporating an observer, and perform stability analysis of the total system. Relevant articles for combined controller-observer schemes in 6 DOF using quaternions for describing the attitude are Caccavale, Natale & Villani (2003), Antonelli, Caccavale & Chiaverini (2004), Antonelli, Caccavale, Chiaverini & Villani (1998) and Caccavale, Natale & Villani (1999).
- Incorporate the models for the actuators.

- The accuracy of using the GPS for position measurements should be investigated. Perhaps incorporate and investigate other sensors, such as star trackers, magnetometers and inertial measuring units.

Appendix A

Polar Coordinates

The unit-vectors in polar coordinates are given by

$$\vec{e}_r = \cos\theta\vec{e}_x + \sin\theta\vec{e}_y \tag{A.1}$$

$$\vec{e}_\theta = -\sin\theta\vec{e}_x + \cos\theta\vec{e}_y \tag{A.2}$$

The time derivative of (A.1) is

$$\begin{aligned}\dot{\vec{e}}_r &= -\dot{\theta}\sin\theta\vec{e}_x + \dot{\theta}\cos\theta\vec{e}_y \\ &= \dot{\theta}\vec{e}_\theta\end{aligned} \tag{A.3}$$

where (A.2) have been used. Taking the second time derivative of the same equation gives

$$\begin{aligned}\ddot{\vec{e}}_r &= -(\dot{\theta}^2\cos\theta + \ddot{\theta}\sin\theta)\vec{e}_x + (-\dot{\theta}^2\sin\theta + \ddot{\theta}\cos\theta)\vec{e}_y \\ &= -\dot{\theta}^2(\cos\theta\vec{e}_x + \sin\theta\vec{e}_y) + \ddot{\theta}(-\sin\theta\vec{e}_x + \cos\theta\vec{e}_y) \\ &= -\dot{\theta}^2\vec{e}_r + \ddot{\theta}\vec{e}_\theta\end{aligned} \tag{A.4}$$

where both (A.1) and (A.2) have been used. The time derivative of (A.2) is given by

$$\begin{aligned}\dot{\vec{e}}_\theta &= -\dot{\theta}\cos\theta\vec{e}_x - \dot{\theta}\sin\theta\vec{e}_y \\ &= -\dot{\theta}\vec{e}_r\end{aligned} \tag{A.5}$$

where (A.1) has been used. Its second time derivative is

$$\begin{aligned}\ddot{\vec{e}}_\theta &= (\dot{\theta}^2\sin\theta - \ddot{\theta}\cos\theta)\vec{e}_x - (\dot{\theta}^2\cos\theta + \ddot{\theta}\sin\theta)\vec{e}_y \\ &= -\dot{\theta}^2(-\sin\theta\vec{e}_x + \cos\theta\vec{e}_y) - \ddot{\theta}(\cos\theta\vec{e}_x + \sin\theta\vec{e}_y) \\ &= -\dot{\theta}^2\vec{e}_\theta - \ddot{\theta}\vec{e}_r\end{aligned} \tag{A.6}$$

where both (A.1) and (A.2) have been used.

Appendix B

Analytical Solution of the Unperturbed HCW Equations

The Laplace-transformed of unperturbed HCW equations can be written

$$s^2X - sx_0 - \dot{x}_0 - 2nsY + 2ny_0 - 3n^2X = 0 \tag{B.1}$$

$$s^2Y - sy_0 - \dot{y}_0 + 2nsX - 2nx_0 = 0 \tag{B.2}$$

$$s^2Z - sz_0 - \dot{z}_0 + n^2Z = 0 \tag{B.3}$$

where $X = \mathscr{L}\{x\}$, $Y = \mathscr{L}\{y\}$ and $Z = \mathscr{L}\{z\}$, i.e. the Laplace transformed of x, y and z respectively. Inserting (B.2) into (B.1) gives

$$X = \frac{sx_0}{s^2+n^2} + \frac{\dot{x}_0}{s^2+n^2} + \frac{2n\dot{y}_0}{s(s^2-n^2)} + \frac{4n^2x_0}{s(s^2+n^2)} \tag{B.4}$$

Inserting this result for X in (B.2) gives

$$Y = \frac{y_0}{s} + \frac{\dot{y}_0}{s^2} - \frac{2nx_0}{s^2+n^2} + \frac{2n\dot{x}_0}{s(s^2+n^2)} - \frac{4n^2\dot{y}_0}{s^2(s^2+n^2)} - \frac{8n^3x_0}{s^2(s^2+n^2)} + \frac{2nx_0}{s^2} \tag{B.5}$$

Equation (B.3) can be written

$$Z = \frac{sz_0}{s^2+n^2} + \frac{\dot{z}_0}{s^2+n^2} \tag{B.6}$$

The inverse Laplace transformed of each term for these three equations give

$$x = x_0\cos nt + \frac{\dot{x}_0}{n}\sin nt + \frac{2\dot{y}_0}{n}(1-\cos nt) + 4x_0(1-\cos nt) \tag{B.7}$$

$$\begin{aligned} y = {} & y_0 + \dot{y}_0 t - 2x_0\sin nt + \frac{2\dot{x}_0}{n}(1-\cos nt) \\ & - 4\dot{y}_0(t - \frac{1}{n}\sin nt) - 8nx_0(t - \frac{1}{n}\sin nt) + 2nx_0t \end{aligned} \tag{B.8}$$

$$z = z_0\cos nt + \frac{\dot{z}_0}{n}\sin nt \tag{B.9}$$

which finally can be written

$$x = \frac{\dot{x}_0}{n}\sin nt - (3x_0 + \frac{2\dot{y}_0}{n})\cos nt + 4x_0 + \frac{2\dot{y}_0}{n} \tag{B.10}$$

$$y = \frac{2\dot{x}_0}{n}\cos nt + (6x_0 + 4\frac{\dot{y}_0}{n})\sin nt - (6nx_0 + 3y_0)t - \frac{2\dot{x}_0}{n} + y_0 \tag{B.11}$$

$$z = z_0\cos nt + \frac{\dot{z}_0}{n}\sin nt \tag{B.12}$$

Appendix C

Lie-derivatives in Mathematica

The *Lie derivative* of a function $\lambda(\mathbf{x})$ along a vector field $\mathbf{f}(\mathbf{x})$ is, as in Isidori (1995)

$$L_f\lambda(\mathbf{x}) = \frac{\partial\lambda(\mathbf{x})}{\partial\mathbf{x}}\mathbf{f}(\mathbf{x}) = \langle d\lambda(\mathbf{x}), \mathbf{f}(\mathbf{x})\rangle, \quad \mathrm{d}\lambda = \left[\frac{\partial\lambda}{\partial x_1}, \frac{\partial\lambda}{\partial x_2}, \ldots, \frac{\partial\lambda}{\partial x_n}\right] \tag{C.1}$$

$$L_f^k\lambda(\mathbf{x}) = \frac{\partial L_f^{k-1}\lambda(\mathbf{x})}{\partial\mathbf{x}}\mathbf{f}(\mathbf{x}), \quad L_f^0\lambda(\mathbf{x}) = \lambda(\mathbf{x}) \tag{C.2}$$

where the recursive formula for the last equation can be written in Mathematica as

```
Lie[\[Lambda]_List, x_List, f_List, 0] := \[Lambda]
Lie[\[Lambda]_,x_,f_,k_] :=
Flatten[Outer[D,Lie[\[Lambda],x,f,k-1],x].f]
```

The *Lie product* (or *bracket*) of $\mathbf{f}$ and $\mathbf{g}$ is

$$[\mathbf{f}, \mathbf{g}] = \frac{\partial\mathbf{g}}{\partial\mathbf{x}}\mathbf{f}(\mathbf{x}) - \frac{\partial\mathbf{f}}{\partial\mathbf{x}}\mathbf{g}(\mathbf{x}) = \mathrm{ad}_f\mathbf{g}(\mathbf{x}) \tag{C.3}$$

$$\mathrm{ad}_f^k = [\mathbf{f}, \mathrm{ad}_f^{k-1}\mathbf{g}](\mathbf{x}), \quad \mathrm{ad}_f^0\mathbf{g}(\mathbf{x}) = \mathbf{g}(\mathbf{x}) \tag{C.4}$$

and the recursive formula can be written in Mathematica as

```
LieKla[f_List,g_List,x_List,0] := g
LieKla[f_List,g_List,x_List,k_Integer] :=
Flatten[Outer[D,LieKla[f,g,x,k-1],x].f-Outer[D,f,x].LieKla[f,g,x,k-1]]
```

Appendix D

Submitted Abstract and Conference Presentation

D.1 Space Technology Education Conference, Aalborg, Denmark

Coordinated control of satellites: the relative position case

Esten Ingar Grøtli

Department of Engineering Cybernetics,
Norwegian University of Science and Technology,
N-7491 Trondheim
Norway

Outline of the talk

- Introduction
- Model
- Controllers and observer
- Simulations
- Conclusion

What is a formation of satellites?

- Definition: ”*Two or more spacecraft that use an active control scheme to maintain the relative positions of the spacecraft.*”

Folta, Newman & Gardner

Why do we want formations of satellites?

- We are familiar with other types of formations...

Why do we want formations of satellites?

- Distribute the functionality of large satellites
- Lowered total cost and risk
- Increased flexibility
- Redundancy

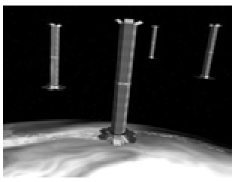

Applications

- Ultra powerful telescopes
- Space-based radar
- Next-generation Internet

HCW Equations

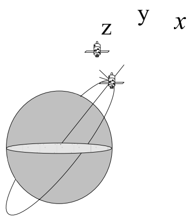

- x – radial direction
- y – velocity direction
- z – completes the right-hand rule

HCW Equations

- The Hill-Clohessy-Wiltshire equations:

$$\begin{aligned} \ddot{x} - 2n\dot{y} - 3n^2x &= 0 \\ \ddot{y} + 2n\dot{x} &= 0 \\ \ddot{z} + n^2z &= 0 \end{aligned}$$

- Analytical solution:

$$\begin{aligned} x(t) &= \frac{\dot{x}_0}{n}\sin nt - (3x_0 + 2\frac{\dot{y}_0}{n})\cos nt + 4x_0 + 2\frac{\dot{y}_0}{n} \\ y(t) &= \frac{2\dot{x}_0}{n}\cos nt + (6x_0 + 4\frac{\dot{y}_0}{n})\sin nt - (6nx_0 + 3\dot{y}_0)t - \frac{2\dot{x}_0}{n} + y_0 \\ z(t) &= \frac{\dot{z}_0}{n}\sin nt + z_0\cos nt \end{aligned}$$

HCW Equations

- "Force free" paths:

$$\frac{x^2}{{x_0}^2} + \frac{(y-y_0)^2}{4{x_0}^2} = 1$$

$$z = -\frac{\dot{z}_0}{2nx_0}(y - y_0) + \frac{z_0}{x_0}x$$

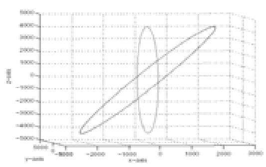

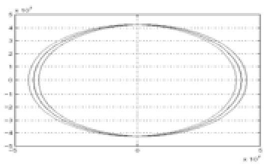

Nonlinear Equations

$$m_f(\ddot{\mathbf{q}} + C(\dot{v})\dot{\mathbf{q}} + \mathbf{n}(\mathbf{q}, \dot{v}, \ddot{v}, r_l) + \frac{1}{m_l}\mathbf{u_l}) + \mathbf{F_d} = \mathbf{u_f}$$

$$\mathbf{q} = \begin{bmatrix} x(t) \\ y(t) \\ z(t) \end{bmatrix} \qquad C(\dot{v}) = 2\dot{v}\begin{bmatrix} 0 & -1 & 0 \\ 1 & 0 & 0 \\ 0 & 0 & 0 \end{bmatrix}$$

$$\mathbf{n}(\mathbf{q}, \dot{v}, \ddot{v}, r_l) = \begin{bmatrix} \mu(\frac{r_l+x}{r_f^3} - \frac{1}{r_l^2}) - (\dot{v}^2x + \ddot{v}y) \\ \mu(\frac{y}{r_f^3}) - (y\dot{v}^2 - \ddot{v}x) \\ \mu(\frac{z}{r_f^3}) \end{bmatrix} \qquad \mathbf{F_d} = \mathbf{F_{df}} - \frac{m_f}{m_l}\mathbf{F_{dl}}$$

Satellite

Disturbance Models

- J2 Gravity Model:

$$\begin{aligned} G_x &= \frac{\partial V}{\partial x_e} = -\frac{x_e\mu_g}{r^3}\left[1 + \frac{3J_2a^2}{2r^2} - \frac{15J_2a^2z_e^2}{2r^4}\right] \\ G_y &= \frac{\partial V}{\partial y_e} = -\frac{y_e\mu_g}{r^3}\left[1 + \frac{3J_2a^2}{2r^2} - \frac{15J_2a^2z_e^2}{2r^4}\right] \\ G_z &= \frac{\partial V}{\partial z_e} = -\frac{z_e\mu_g}{r^3}\left[1 + \frac{9J_2a^2}{2r^2} - \frac{15J_2a^2z_e^2}{2r^4}\right] \end{aligned}$$

- Atmospheric Drag Model:

$$F = \frac{1}{2}\rho V^2 C_D A$$

Guidance, Navigation and Control

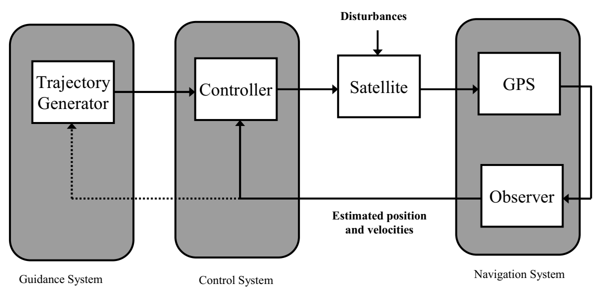

State Feedback Linearization

- State feedback controller

$$\mathbf{u} = \{\beta(\mathbf{x})\}^{-1}[-\boldsymbol{\alpha}(\mathbf{x}) + \mathbf{v}]$$

$$\beta(\mathbf{x}) = \begin{bmatrix} \frac{1}{m_f} & 0 & 0 \\ 0 & \frac{1}{m_f} & 0 \\ 0 & 0 & \frac{1}{m_f} \end{bmatrix}$$

$$\boldsymbol{\alpha}(\mathbf{x}) = \begin{bmatrix} \frac{1}{m_f}\left(2\dot{\nu}x_4 - \mu(\frac{r_l+x_1}{r_f^3} - \frac{1}{r_l^2}) + (\dot{\nu}^2 x_1 + \ddot{\nu}x_3)\right) \\ \frac{1}{m_f}\left(-2\dot{\nu}x_2 - \mu(\frac{x_3}{r_f^3}) - (\dot{\nu}^2 x_3 - \ddot{\nu}x_1)\right) \\ \frac{1}{m_f}\left(-\mu\frac{x_5}{r_f^3}\right) \end{bmatrix}$$

State Feedback Linearization

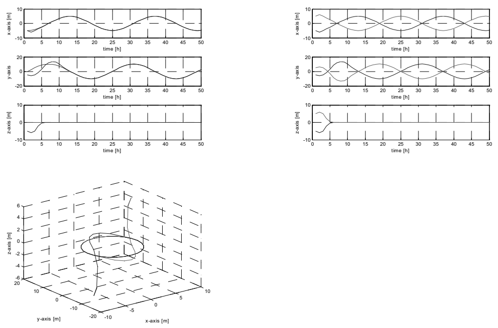

Passivity based controller-observer design

- Passivity based controller with only position measurement available:

$$\mathbf{u_f} = M\ddot{\mathbf{q}}_\mathbf{r} + m_f C\dot{\mathbf{q}}_\mathbf{r} + m_f\mathbf{n} - K_p\mathbf{e} - K_d(\mathbf{s}_1 - \mathbf{s}_2)$$

$$\mathbf{e} \equiv \mathbf{q} - \mathbf{q_d}$$

$$\tilde{\mathbf{q}} = \mathbf{q} - \hat{\mathbf{q}}$$

$$\mathbf{s}_1 - \mathbf{s}_2 = (\dot{\hat{\mathbf{q}}} - \dot{\mathbf{q}}_d) + \Lambda_1(\mathbf{e} - \tilde{\mathbf{q}}) - \Lambda_2\tilde{\mathbf{q}}$$

$$\dot{\mathbf{q}}_r = \dot{\mathbf{q}}_d - \Lambda_1(\hat{\mathbf{q}} - \mathbf{q}_d)$$

Passivity based controller-observer design

- Passivity based observer

$$\dot{\hat{\mathbf{q}}} = \mathbf{z} + L_d\tilde{\mathbf{q}}$$
$$\dot{\mathbf{z}} = \ddot{\mathbf{q}}_r + M^{-1}(L_{p1}\tilde{\mathbf{q}} - K_p\mathbf{e}) + L_{p2}\tilde{\mathbf{q}}$$

Passivity based controller-observer design

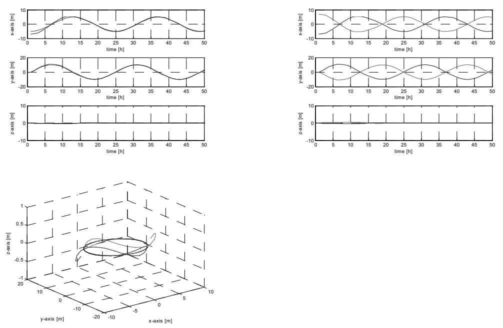

Conclusion

- Generation of appropriate reference trajectories using the Hill-Clohessy-Wiltshire equations
- Nonlinear model
- Disturbance models
- Design and implementation of state-feedback linearizing controller and passivity based controller

D.2 Scandinavian Conference on Simulation and Modeling, Trondheim, Norway

A model of relative position and attitude in a leader-follower spacecraft formation

R. Kristiansen*, E. I. Grøtli**, P. J. Nicklasson* and J. T. Gravdahl**

*Department of Space Technology
Narvik University College, Norway
**Department of Engineering Cybernetics
Norwegian University of Science and Technology, Norway

June 14, 2005

Extended abstract

Flying spacecraft in formations is revolutionizing our way of performing space-based operations, and this new paradigm brings on several advantages in space mission accomplishment and extends the possible application area for such systems. Spacecraft formation flying is a technology that includes two or more spacecraft in a tightly controlled spatial configuration, whose operations are closely synchronized. Earth and deep space surveillance with radio interferometry and Synthetic Aperture Radar (SAR) technology is one area where spacecraft formations can be useful. These systems involve data collection and processing over an aperture where the resolution of the observation is inversely proportional to the baseline lengths. Further exploration of neighboring galaxies in space can only be achieved by indirect observation of astronomical objects, and space based interferometers with baselines of up to ten kilometers have been proposed. However, to successfully utilize spacecraft formations for this purpose, accurate synchronization of both position and attitude of the cooperating spacecraft is vital, which again depends on accurate system models of the formation including external elements that might perturb the flight.

This paper presents a detailed nonlinear mathematical model in six degrees of freedom of relative translation and rotation of two spacecraft in a leader-follower formation. The model of relative position is based on the two-body equations derived from Newton's inverse square law of force, and the position and velocity vectors of the follower spacecraft are represented in a reference frame located in the center of mass of the leader spacecraft, known as the Hill frame. In addition, rotation matrices between the Hill frame and an earth centered inertial reference frame are given. The relative attitude model is based on Euler's momentum equations, and the attitude is represented by unit quaternions and angular velocities.

The model also includes the mathematical expressions for external disturbances originating from gravitational variations, atmospheric drag, solar radiation, and perturbations due to other celestial bodies, known as third body effects. Results from simulations in Matlab are presented to visualize the properties of the model and to show the impact of the different disturbances on the flight path.

References

Antonelli, G., Caccavale, F. & Chiaverini, S. (2004), 'Adaptive tracking control of underwater vehicle-manipulator systems based on the virtual decomposition approach', *IEEE Transactions on Robotics and Automation* .

Antonelli, G., Caccavale, F., Chiaverini, S. & Villani, L. (1998), 'An output feedback algorithm for position and attitude tracking control of underwater vehicles', *Proceedings of the 37th IEEE Conference on Decision & Control* .

Beard, R. & F. Hadaegh, F. (1999), Fuel optimization for unconstrained rotation of spacecraft formations, pp. 259–273.

Berghuis, H. (1993), Model-based Robot Control: from Theory to Practice, PhD thesis, Universiteit Twente.

Berghuis, H. & Nijmeijer, H. (1993), 'A passivity approach to controller-observer design for robots', *IEEE Transactions on Robotics and Automation* .

Bondhus, A. K., Pettersen, K. Y. & Gravdahl, J. T. (2005), 'Leader/follower synchronization of satellite attitude without angular velocity measurements'.

Brown, C. D. (2002), *Elements of Spacecraft Design*, AIAA Education Series.

Caccavale, F., Natale, C. & Villani, L. (1999), 'Task-space tracking control without velocity measurements', *Proceedings of the 1999 IEEE International Conference on Robotics and Automation* .

Caccavale, F., Natale, C. & Villani, L. (2003), 'Output feedback control of mechanical systems with application to spacecraft and robots', *Journal of Guidance, Control, and Dynamics* .

Chichka, D. F. (2001), 'Satellite Clusters with Constant Apparent Distribution', *Journal of Guidance, Control, and Dynamics* **24**, 117–122.

Clohessy, W. H. & Wiltshire, R. S. (1960), 'Terminal guidance system for satellite rendezvous', *Journal of Aerospace Sciences* .

Egeland, O. & Godhavn, J.-M. (1994), 'Passivity-based adaptive attitude control of a rigid spacecraft', *IEEE Transactions on Automatic Control* .

Egeland, O. & Gravdahl, J. T. (2002), *Modeling and Simulation for Automatic Control*, Marine Cybernetics.

Fjellstad, O.-E. (1994), Control of unmanned underwater vehicles in six degrees of freedom: a quaternion feedback apporach, PhD thesis, The Norwegian institute of Technology, University of Trondheim.

Fjellstad, O.-E. & Fossen, T. I. (1994), Singularity-free tracking of unmanned underwater vehicles in 6 dof, *in* 'Proceeding of the 33rd Conference on Decision and Control'.

Folta, D. C., Newman, L. K. & Gardner, T. (1996), 'Foundations of formation flying for mission to planet earth and new millennium', *AIAA-96-3654-Cp, NASA Goddard Space Center* .

Fossen, T. I. (2002), *Marine Control Systems*, Marine Cybernetics.

Fossen, T. I. & Fjellstad, O.-E. (1995), 'Nonlinear modelling of marine vehicles in 6 degrees of freedom', *International Journal of Mathematical Modelling of Systems* .

Goeree, B. & Chatel, G. (1999), 'University of arizona student satellite project: Technical note'.

Hill, G. W. (1878), 'Researches in the lunar theory', *American Journal of Mathematics* **1**, 5–26.

Hsu, D. Y. (1996), 'Comparison of four gravity models', *Position Location and Navigation Symposium* .

Hsu, D. Y. (1998), 'An accurate and efficient approximation to the normal gravity', *Position Location and Navigation Symposium* .

Hughes, P. C. (1986), *Spacecraft Attitude Dynamics*, John Wiley & Sons, Inc.

Inalhan, G., Tillerson, M. & How, J. P. (2002), Relative dynamics and control of spacecraft formations in eccentric orbits, Vol. 25, pp. 48–59.

Isidori, A. (1995), *Nonlinear Control Systems*, Springer-Verlag.

Karlsgaard, C. & Lutze, F. (2001), 'Second-order relative motion equations'.

Khalil, H. K. (2002), *Nonlinear Systems*, Prentice-Hall, Inc.

Kreyszig, E. (1999), *Advanced Engineering Mathematics*, John Wiley & Sons, Inc.

Kristiansen, R. (2000), Attitude controll of mini satellite, Master's thesis, Norwegian University of Science and Technology.

Kyrkjebø, E. (2000), Satellite attitude determination, Master's thesis, Nowegian University of Science and Technology.

Montenbruck, O. & Gill, E. (2000), *Satellite Orbits: Models, Methods, and Applications*, Springer-Verlag.

Naasz, B. J., Karlgaard, C. D. & Hall, C. D. (2002), Application of several control techniques for the ionospheric observation nanosatellite formation, AAS/AIAA Space Flight Mechanics Conference.

Nijmeijer, H. & Rodriguez-Angeles, A. (2003), *Synchronization of Mechanical Systems*, World Scientific Publishing Co. Pte. Ltd.

Pan, H. & Kapila, V. (2001), Adaptive nonlinear control for spacecraft formation flying with coupled translational and attitude dynamics.

Ploen, S. R., Hadaegh, F. Y. & Scharf, D. P. (2004), Rigid body equations of motion for modelling and control of spacecraft formations - part 1: Absolute equations of motion, *in* 'Proceeding of the 2004 American Control Conference'.

Sabol, C., Burns, R. & McLaughlin, C. (1999), Satellite formation flying design and evaluation, AAS/AIAA Space Flight Mechanic Meeting.

Sagatun, S. I. & Fossen, T. I. (1991), 'Lagrangian formulation of underwater vehicles' dynamics', *Proceedings of the IEEE International Conference on Systems, Man and Cybernetics* .

Salcudean, S. (1991), 'A globally convergent angular velocity observer for rigid body motion', *IEEE Transactions on Automatic Control* .

Scharf, D. P., Hadaegh, F. Y. & Ploen, S. R. (2003), A survey of spacecraft fomation flying guidance and control (part I): Guidance, pp. 1733–1739.

Scharf, D. P., Hadaegh, F. Y. & Ploen, S. R. (2004), A survey of spacecraft fomation flying guidance and control (part II): Control, pp. 2976–2985.

Schwartz, J. L. (2004), The Distributed Spacecraft Attitude Control System Simulator: From Design Concept to Decentralized Control, PhD thesis, Virgina State University.

Sellers, J. J. (2000), *Understanding Space. An Introduction to Astronautics*, McGraw-Hill Higher Educations.

Serrani, A. (2003), Robust coordinated control of satellite formations subject to gravity perturbations.

Sidi, M. J. (2002), *Spacecraft Dynamics & Control: A Practical Engineering Approach*, Cambridge University Press.

Slotine, J.-J. E. & Li, W. (1991), *Applied Nonlinear Control*, Prentice Hall.

Sutton, G. P. & Biblarz, O. (2001), *Rocket Propulsion Elements*, John Wiley & Sons, Inc.

Tsiostras, P., Shen, H. & Hall, C. (2001), 'Satellite attitude control and power tracking with energy/momentum wheels', *Journal of Guidance, Control and Dynamics* .

Vallado, D. A. (2001), *Fundamentals of Astrodynamics and Applications*, Microcosm Press and Kluwer Academic Publishers.

Wertz, J. R. & Larson, W. J., eds (1999), *Space Mission Analysis and Design*, Kluwer Academic Publishers.

Wong, H. & Kapila, V. (2003), 'Adaptive learning control-based periodic trajectory tracking for spacecraft formations', *Proceedings of the 42nd IEEE Conference on Decision and Control* .

Wong, H., Kapila, V. & Sparks, A. (2001), 'Adaptive output feedback tracking control of multiple spacecraft', *Proceedings of the American Control Conference* .

Yan, Q., Yang, G., Kapila, V. & de Queiroz, M. S. (2000), Nonlinear dynamics and output feedback control of multiple spacecraft in elliptical orbits, pp. 839–843.

Yeh, H.-H. & Sparks, A. (2000), Geometry and Control of Satellite Formations, Vol. 1, pp. 384–388.